UNIVERSITY OF WARSAW

DOCTORAL THESIS

Stationary perturbations of near-horizon geometries

Author:
Maciej KOLANOWSKI

Supervisors:
Prof. dr hab. Jerzy LEWANDOWSKI
Dr Wojciech KAMIŃSKI

A thesis submitted in fulfillment of the requirements for the degree of Doctor of Philosophy

in the

Chair of Theory of Relativity and Gravity
Institute of Theoretical Physics
Faculty of Physics

March 8, 2023

"When we can't think for ourselves, we can always quote."

Ludwig Wittgenstein

Abstract

This thesis is devoted to the following question: what does the neighborhood of a *generic* extremal horizon look like? We are interested in all possible (stationary) perturbations that may be induced either by a far-away matter distribution or by non-trivial boundary conditions at infinity (in the case of asymptotically AdS spacetimes). Thus, we want to go beyond explicitly known solutions such as Kerr-Newman (AdS). To this end, we consider the behavior of a small perturbation that is supposed to die off at the horizon. Its smallness allows us to linearize appropriate (e.g. Einstein-Maxwell) equations. Our considerations will mainly focus on spacetimes with a negative cosmological constant.

We found out that in four dimensions, *generically* the perturbations are not C^2. As a result, the horizon is replaced by a null singularity. Perhaps counter-intuitively, the larger the black hole, the worse the singularity can get. At the same time, all curvature scalars remain finite and thus analytic continuation of those solutions to the Euclidean signature is smooth. The singularity vanishes when the cosmological constant $\Lambda = 0$. It exists for $\Lambda > 0$ albeit it is no longer so robust. Moreover, in that case, the tidal forces are always integrable through the horizon and thus the effect is not so big.

At finite temperatures, the singularity leaves significant observational imprints. The tidal forces at the horizon, though finite, may be arbitrarily large as $T \to 0$. Moreover, the specific heat is changed by an anomalous term that, for large and cold black holes, dominates over the usual (linear in T) contribution.

In five (and higher) dimensions the singularity for RN AdS becomes even worse and leads to *RG instability* - a small perturbation of the boundary conditions dramatically changing the infrared (it means near-horizon) region. New near-horizon geometries were constructed. However, none of them is RG stable. In dimensions higher than five, the same conclusion also holds without a cosmological constant. Moreover, for toroidal black holes, we have a phase transition. Small ones are stable and only large ones are not. At the phase transition threshold, we expect the resistivity to approach a constant.

As a result, we predict that the boundary theory put on a non-homogeneous background could flow to a different infrared fixed point. Unfortunately, the endpoint of that instability (either in the bulk or on the boundary) is currently unknown. In particular, it is not clear that it is described by only one horizon.

Finally, we show that the higher-curvature corrections generated by UV physics may render even an asymptotically flat extremal Kerr black hole singular. This is an example of a scenario in which quantum effects qualitatively change the system despite the fact that the curvature is very small. The scaling dimensions of RN_4 do not get modified. However, they are shifted in higher dimensions. In particular, quantum corrections render RN_5 RG-unstable provided that the Weak Gravity Conjecture is satisfied. Moreover, we found that this very conjecture implies that Kerr-Newman (AdS) is unstable with respect to stationary perturbations by massive, charged scalar fields.

Acknowledgements

I've been blessed with many wonderful people on my scientific path. This dissertation would not be possible without constant support from my supervisors – prof. Jerzy Lewandowski and dr Wojciech Kamiński. I owe them gratitude for many discussions (especially ones ending with disagreements), ideas, and bits of advice. My life as a researcher started in their group and even though a siren song of physics led me towards slightly different topics, I am still immersed in the inspiring atmosphere they created. Thanks!

That atmosphere would not be possible without other people. I should in particular mention my officemates – Eryk and Maciej – who had to endure my constant babbling or (quite often) a random stream of consciousness I would project on them. They've been a great emotional support during (not-always-easy) PhD times. Also my interactions with Andrzej and Kacper were always rewarding. Even though our research interests have small overlaps, I believe I learned a great bunch of physics of physics from our discussions. Those four are also main enablers of my coffee addiction. Thanks!

Quite often my random walk on the graph of possible topics would lead me to interactions with Jan. For some reason, that usually happened during our common breakfasts. He always kept bugging me about the bigger picture of my research. My attempts to connect this thesis with recent developments in JT gravity are hugely inspired by him. Now, we finally managed to create a bound state and we are trying to understand how sources for Kaluza-Klein modes change Schwarzian calculations for small scaling dimensions. Hopefully, something interesting will come out of it. Thanks!

An adventure that I did not expect to take part in was the PhD Students' Union. I am grateful to my wonderful colleagues – Justyna, Katarzyna, Karolina, Tadek, Kasia, Damian, Damian. Not only they helped me a lot, they were a great support system but I believe they helped a lot of people with their PhDs and allowed me to do that as well. For giving my time in grad school this additional social meaning I'm extremely grateful. Obviously, the largest thanks go to Przemek whose constant care for other people's well-being was really inspirational. My PhD would be depressing without our constant talks and brainstorms. Thanks!

I would also like to thank my friends from non-UW circles: Daria, Kasia, Filip, Przemek, Ola, Martyna. A chance to talk about something else than physics or academia was always highly appreciated. Thanks!

In this regard of course I'm eternally grateful to my wonderful girlfriend Magda. She kept making me do things, broaden my horizons, leave my comfort zone at the same time respecting my boundaries. She was always open to my (let's be honest, more often than not, overly nerdy) suggestions. Most importantly, we are having a great time together. I have no idea how I would finish this Thesis without her support. Thanks!

Large part of the research presented here was initiated during my Fulbright scholarship at the University of California in Santa Barbara. I believe UCSB is one of the awesomest places in the Universe and I'm grateful for their hospitality. I'm indebted to Don Marolf for letting me join his group, for his constant enthusiasm and spending a lot of time discussing physics. I met at UCSB many great people with whom I had very rewarding interactions: Xiaoyi, Zhencheng, Marija, Grant, Sean and Wayne. Thanks!

At UCSB I met Gary with whom most I collaborated on most of this work. He is a very patient, very open person, very keen to listen to new ideas. Despite his great

knowledge of GR, I never felt intimidated. Without that, nothing in this work would be done. Through Gary I met also Jorge. His enthusiasm was infectious and the pace of his work was enviable. I learned so much from them. Thanks!

Last but not least, I would like to thank my family. My siblings, Asia and Jan, were always very hospitable during my visits. We had a lot of fun together and quite a few nights we spent on chatting. I'm most grateful to my parents who birthed me, raised me and were a constant support during all those long years of my education. How they managed to cope with such a smart-ass kid is beyond me. Thank you!

As already mentioned, part of this work was done during my visit at the UCSB funded by the The Polish-U.S. Fulbright Commission. Parts of this work were also funded from Polish budgetary funds for science in 2018-2022 as a research project under the program "Diamentowy Grant" and by the Polish National Science Center (grant number: OPUS 2021/43/B/ST2/02950).

Contents

List of Figures

Pracę tę dedykuję moim rodzicom

Chapter 1

Introduction

1.1 Motivation

Quite likely the most recognizable objects from the modern[1] theoretical physics are black holes. Intuitively, they are spacetime's regions from which even light cannot escape. Thus, I imagine it must have been rather surprising when Hawking showed that they in fact radiate thermally [59]. The topic of this work are extremal black holes, it means such that their Hawking temperature T vanishes[2].

There are many reasons to study extremal black holes. First of all, due to the lack of Hawking radiation, they are believed to have a simpler quantum-mechanical description. In particular, they allow for a better control over the microstates counting [104]. In the same spirit, they are deeply intertwined with a supersymmetry. Moreover, black hole spacetimes in AdS/CFT corresponds to the thermal states on the boundary. Thus, extremal black holes should describe the ground state of the (deformed) CFT. In the language of RG (renormalization group) flow the region near the horizon (one that we shall work with extensively here) encodes information about the infrared. Quite often this near-horizon geometry is characterized by an emergent $O(2,1)$ symmetry that simplifies many calculations.

Also Readers with a more mathematical[3] approach may find the topic interesting. Many important results, even in the classical gravity, are derived assuming that the horizon is not extremal, for example higher-dimensional version of the rigidity theorem [64]. Even an extremal version of (obviously, four-dimensional) 'no hair theorem' was proven relatively recently [28]. Thus, the quest for generalizing many results to the $T = 0$ case is still open and may lead to interesting developments. Even more, we know that in five dimensions there are more exotic horizons, for example black rings. A finite classification of asymptotically flat black holes remains an open problem. One step towards it must consist of classifying all possible extremal horizons.

We may now state the main question behind the Thesis: what does a *generic* extremal black hole look like? To answer that, we will consider small (stationary) perturbations in the near-horizon region of well-known black holes. One may think that they originate from non-trivial boundary conditions (in AdS) or a matter distribution in the galaxies far away. Either way, our analysis is local and does not depend on those details. Hopefully, the answers we obtained are going to be interesting to Readers interested both in physical and mathematical aspects of the story.

[1] Author firmly believes that viewing Laplace as the black holes' father is highly anachronistic.

[2] It does not mean that they do not radiate though but only that the spectrum is not thermal at infinity. In particular, RN black holes may produce particles due to the Schwinger process.

[3] While searching the literature, one should keep in mind that mathematicians prefer to use a name 'degenerate horizon'. This nomenclature from the fact that most $T > 0$ black holes have bifurcated horizons that overlap as $T \to 0$.

1.2 Horizons – a few definitions

It is a good practice to start any discourse by defining terms used throughout it. Since this thesis is devoted to (certain aspects of) horizons, it would be incomplete without a short explanation what we mean by the word 'horizon'. Here we encounter our first difficulty: literature is filled with different approaches to the topic. Before we will commit to one of them, let us present a few (and likely omit a few more) non-equivalent definitions and discuss their respective advantages and drawbacks[4].

The most common association, even outside the scientific community, is probably 'the event horizon' which informally speaking is supposed to be a boundary of a black hole. And in that spirit the black hole is a region in which the gravity is so strong that even light cannot escape it. In the asymptotically flat context[5] be formalized in the following manner:

Definition 1.1. [108] Let (M, g) be a strongly asymptotically predictable (SAP) spacetime. It contains a black hole if $M \not\subset J^-(\mathcal{I}^+)$. Then $B = M \setminus J^-(\mathcal{I}^+)$ is called a black hole region and its boundary is called the (future) event horizon.

Although this notion encompasses a common intuition about black holes, it is not useful in practice. The event horizon is defined teleologically – one needs to know the whole spacetime, up to infinite future to find that surface. It cannot be a priori excluded that the event horizon is growing (say, due to a merger that could happen billions of years from now) even in a little café I am writing these words in. This difficulty is the raison d'être behind this Section and different proposals presented below – we are rather interested in (quasi)local objects. Before that, let us introduce

Definition 1.2. [108] Let T be a compact, two-dimensional , smooth spacelike submanifold such that the expansion of both ingoing and outgoing future directed null geodesics orthogonal to T is everywhere negative. Such T is called a trapped surface.
Given a Cauchy slice Σ, we call it closed sub-region C a trapped region if at ∂C the outgoing expansion is non-positive and we call ∂C a marginally outer trapped surface (MOTS).

Trapped surfaces are extremely important in the mathematical and numerical relativity due to the Penrose theorem [99] and quite often they are a litmus test for the presence of singularities. One can show that all trapped surfaces are hidden behind the event horizon if the spacetime is SAP and null energy-condition is satisfied. Similarly, it was argued that if the gravity theory enjoys a holographic dual, all MOTSs must be hidden behind the horizon [41]. We can now introduce

Definition 1.3. [108] Given a Cauchy slice Σ, let the total trapped region $\mathcal{F}$ be the closure of the union of all trapped regions. We call its boundary $\partial\mathcal{F} = \mathcal{A}_\Sigma$ the apparent horizon on Σ.

Clearly, the apparent horizon is defined using much more local data than the event horizon – one needs to know only initial data for the Einstein equations. On the other hand (as its name could suggest) it depends on the choice of the Cauchy

[4] Most of the notions described below are not going to appear in the Thesis later on. This Section resulted just from the fact the author thought it would be useful to have all those definitions in one place for his own sake and thus can be safely omitted.

[5] Analogous definitions may be given also for different asymptotics.

foliation and thus it is not unique. Let us mention that in the holographic context, it is more natural to use apparent horizons since their area may be associated with the coarse-grained entropy of the interior [42].

In this Thesis, we will be interested in stationary or asymptotically stationary spacetimes. In this context, one assumes that there is a timelike Killing vector K.

Definition 1.4. [27] A null surface whose normal is the Killing vector field K is called the Killing horizon of K.

Clearly, this is a purely local definition. Its usefulness comes from the Hawking rigidity theorem [60] which states that a real-analytic bifurcated[6] event horizon in a stationary SAP spacetime is a Killing horizon of a certain Killing vector field. The assumption of analyticity can be dropped if one restricts themselves to the neighborhood of the horizon [2].

It is easy to show that all null surfaces are foliated by families of null geodesics. Since K is a null generator of H, it must satisfy

$$\nabla_K K|_H = \kappa^{(K)} K. \tag{1.1}$$

If H is either bifurcated or if the dominant energy condition is satisfied, one can check that $\kappa^{(K)}$ (called surface gravity) is a constant – this is the zeroth law of thermodynamics [8]. This is not only an analogy. In fact, κ is proportional to the Hawking temperature

$$T = \frac{\kappa^{(K)}}{2\pi}, \tag{1.2}$$

assuming that K is appropriately normalized at infinity.

If $\kappa^{(K)} = 0$, it follows that K at H is tangent to affinely parameterized geodesics. The Killing horizons with $\kappa^{(K)} = 0$ are called extremal. They are going to be the main subject of this Thesis.

Clearly, the realistic spacetimes are dynamical which limits the applicability of the Killing horizons. Nevertheless, they are useful as a test-bed for more complicated processes. The following definitions may be seen as intermediate steps between exactly stationary and highly dynamical spacetimes:

Definition 1.5. [6] A null surface Δ is called a non-expanding horizon (NEH) if for every null normal, future-directed ℓ

(i) its expansion $\theta^{(l)}$ vanishes,

(ii) $-T_a \ell^a|_\Delta$ is causal and future directed,

(iii) Δ is topologically $\mathbb{R} \times S$

It is worth mentioning that on a generic null surface, there is no symmetric, metric-compatible connection – a necessary and sufficient condition for its existence is exactly that said surface must be shear and expansion-free. Based on this observation, one can slightly strengthen the def. 1.5 to an isolated horizon:

Definition 1.6. [6] A non-expanding horizon Δ is called an isolated horizon if there is a null normal ℓ such that

$$[D, \mathcal{L}_\ell]|_H = 0, \tag{1.3}$$

where D is a covariant derivative induced on H.

[6] A horizon (of any type) is called a bifurcated horizon if it includes two (or more) transversal components.

Note that in the case of isolated horizons, the obtained structure is more rigid, in particular, ℓ (at the horizon) is defined only up to a rescaling $\ell \mapsto f\ell$, where $\mathcal{L}_\ell f = 0$. One should note that both NEHs and isolated horizons are broader categories than the Killing horizons. They may appear in a spacetime that is for example filled with gravitational waves. A classical example consists of Robinson–Trautman solutions [26].

In a highly-dynamical situation (say during a merger of two black holes) restricting to (even perturbed) NEH is not justified. Then, one should rather work with a dynamical horizon (called also a holographic screen)

Definition 1.7. [7] A codimension one surface Δ is called a dynamical horizon if it can be foliated by a family of surfaces whose ingoing expansion is strictly negative and whose outgoing expansion vanishes.

Note that the main difference between dynamical and apparent horizon lies in the fact that the former does not depend on the choice of a Cauchy slice. It should be mentioned that suitably formulated laws of black hole thermodynamics hold for isolated and dynamical horizons [7].

1.3 Extremal horizons and their near-horizon geometry

Since the extremal horizons are important objects in this Thesis, let us discuss them a little more now. The first examples of extremal horizons are Reissner–Nordström black hole with maximal charge $|Q| = M$ and Kerr black hole with maximal angular momentum $J = M^2$. This should explain the name – they correspond to black holes with extremal admissible physical quantities (at fixed mass). Nevertheless, it is a misnomer – solutions for which parameters are the biggest but the surface gravity is non-vanishing are known [33].

Near any null surface $\mathcal{N}$ (which we take to be topologically a product $\mathbb{R} \times H$) (with a null normal ℓ) we may introduce null gaussian coordinates [96] in the following way: we choose a cross-section H transversal to ℓ and fix any coordinate system x^a on H. Then, we can Lie-drag x^a along the integral lines of ℓ^a. Let v be a unique function on $\mathcal{N}$ which satisfies $v|_H = 0$ and $\mathcal{L}_\ell v = 1$. (v, x^a) is then a good coordinate system on $\mathcal{N}$. At each point we choose also a vector field n (transversal to $\mathcal{N}$) orthogonal to $v = \text{const.}$ slices, normalized in such a way that $\ell^\mu n_\mu = 1$. Then, from any point of $\mathcal{N}$ we may shoot a null geodesics with a tangent vector n. In this way, we extend n into bulk, and to a point lying on this geodesic, we associate coordinates (v, r, x^a), where r is an affine parameter and (v, x^a) is an initial shooting point. Thus, we introduced coordinates in the neighborhood of $\mathcal{N}$. If ℓ is a Killing vector field satisfying $\nabla_\ell \ell|_\mathcal{N} = 0$, it is easy to convince yourself that if the metric is C^2, it takes the following form:

$$g = 2dv(dr + rh_a(r, x^a)dx^a + \frac{1}{2}r^2 C(r, x^a)dv) + \gamma_{ab}(r, x^a)dx^a dx^b. \tag{1.4}$$

Let us now consider a one-parameter family of diffeomorphisms

$$\phi_\epsilon(v, r, x^a) \mapsto (\epsilon^{-1}, \epsilon r, x^a), \tag{1.5}$$

which is well-defined for $\epsilon > 0$. The physical interpretation of these transformations is such that we move observers closer and closer to the horizon (or, equivalently, we boost them faster and faster). Surprisingly, the pull-back $\phi_\epsilon^\star g$ is well-defined even

in the limit when $\epsilon \to 0$. Since it is no longer a diffeomorphism, we obtain a bona fide different spacetime. If the initial metric was Einstein, so is the limiting one. Similar statements hold in the presence of matter fields [7]. The first realization of this limiting procedure (though formulated in a different gauge) was given by Bardeen and Horowitz for the Kerr black hole [9]. One can check that the Maxwell field allows for an analogous limiting procedure. In this way, we obtain physical fields of the form

$$g = 2dv\left(dr + rh_a dx^a + \frac{1}{2}r^2 C dv\right) + \gamma_{ab}dx^a dx^a \tag{1.6a}$$

$$F = Edv \wedge dr + rW_a dv \wedge dx^a + \frac{1}{2}B_{ab}dx^a \wedge dx^b, \tag{1.6b}$$

where now $C, h_a, \gamma_{ab}, E, W_a, B_{ab}$ are functions of x^a only. Metrics of the form (2.19) are called near-horizon geometries. Notice that they have at least two Killing vector fields: not only ∂_v but also a dilation generator $r\partial_r - v\partial_v$. One could now invert the logic. Instead of starting with a known solution and taking an appropriate limit, one could work with (2.19) directly and e.g. classify possible solutions of this form to the appropriate equations of motion which in turn can constraint horizon's geometries in general.

This approach was quite fruitful in the past – for example, it was used to prove that there are no supersymmetric[8] black rings in AdS_5 within a minimal $\mathcal{N} = 1$ gauged supergravity [50, 85]. It was also a first step towards the construction of asymptotically AdS_5 supersymmetric black holes [54]. Our considerations are relatively close to these. Indeed, the bosonic sector of a minimal (gauged) sugra in 4 dimensions is exactly Einstein-Maxwell theory with a negative cosmological constant Λ. In 5 dimensions it is slightly more complicated due to the presence of an additional Chern-Simons term. In this work we will restrict ourselves to black holes which carry only an electric charge[9] and so the Chern-Simons term vanishes identically and we are perfectly justified in omitting it.

Having said that, let us present equations in question explicitly:

$$D_{[c}B_{ab]} = 0, \tag{1.7a}$$

$$D_a E = W_a, \tag{1.7b}$$

$$(D_a - h_a)\, E + \left(D^b - h^b\right) B_{ba} = 0, \tag{1.7c}$$

$$R_{ab} = \frac{1}{2}h_a h_b - D_{(a}h_{b)} + \Lambda\gamma_{ab} + 2B_{ac}B_b^{\ c} + \frac{2}{D-2}\gamma_{ab}E^2 - \frac{1}{D-2}\gamma_{ab}B^2, \tag{1.7d}$$

$$C = \frac{1}{2}h_a h^a - \frac{1}{2}D^a h_a + \Lambda - \frac{2(D-3)}{D-2}E^2 - \frac{1}{D-2}B^2, \tag{1.7e}$$

where D_a and R_{ab} are a covariant derivative and Ricci tensor associated with γ_{ab}, respectively, and D is the number of spacetime dimensions. As we may see, this is a system of equations on a cross-section of the horizon – there is no r dependence.

These Near-Horizon equations were first derived in [96] for the case of four-dimensional vacuum ($F = 0 = \Lambda$). It is not hard to show that when the cross-section is a torus, then $h_a = 0$ and γ_{ab} is flat. All those solutions can be embedded in

[7] It was probably first noticed by Geroch in [45].

[8] Although supersymmetric black holes are not the topic of this thesis, we feel obliged to note that supersymmetry implies extremality.

[9] Note that in four dimensions this is not a real restriction since equations of motion possess a symmetry between electric and magnetic fields.

pp-wave spacetimes. The version with the Maxwell field (still in $4d$ and without a cosmological constant) appeared in [87]. It was also shown there that all axisymmetric solutions correspond to Kerr-Newman. A higher-dimensional vacuum formulation can be for example in [88]. Note that to derive these equations, one needs only properties of an isolated (not necessarily Killing) horizon.

Quite often we will be interested in the static spacetimes additionally satisfying

$$D_a C = h_a C \tag{1.8a}$$

and

$$D_{[a} h_{b]} = 0. \tag{1.8b}$$

One can check that if C is nowhere vanishing, then the static geometries must be a warped product of AdS_2 with a cross-section [86]. Indeed, then we can write $h_a dx^a = d\log(C)$ and rescale $r = \rho C^{-1}$ so that the metric reads

$$g = C^{-1}\left(\rho^2 dv^2 + 2dvd\rho\right) + \gamma_{ab} dx^a dx^b. \tag{1.9}$$

A two-dimensional metric in a bracket is just AdS_2. Instead of assuming $C \neq 0$, we can take the cross-section to be simply connected. A similar statement holds also for axisymmetric spacetimes *on shell* [86]. In D dimensions, if the symmetry group of NHG contains $U(1)^{D-3}$, then (assuming Einstein equations), it must actually contain $G \times U(1)^{D-3}$, where G is either $O(2,1)$ or $2d$ Poincare group [86].

Solutions to (1.7) on a sphere S^2 (when $D = 4$) where classified under either an assumption of staticity [30, 84] or $U(1)$-symmetry [84, 87]. They correspond to the limits of the Reissner-Nordström (AdS) (the limiting case is known as a Robinson-Beltrotti spacetime) and Kerr-Newman (AdS) black holes, respectively. Whether there are any other vacua or electrovacua S^2 is still an open question (for partial negative results, see [29, 75]). More is known about the moduli spaces when the cross-section has a different topology. It was shown in [38] that the only vacuum NHG on a compact two-dimensional surface with a positive genus satisfies

$$R = 2\Lambda \tag{1.10a}$$

and

$$h_a = 0. \tag{1.10b}$$

The most important lesson for us coming from these classification results is that if we look for a static extremal black hole in AdS_4, its horizon geometry cannot depend on any details (like the boundary conditions at infinity).

Much less is known about the extremal black holes in 5 dimensions. Perhaps surprisingly, even in the static case, the full classification is still missing. It was performed only under assumptions of $U(1)^2$ symmetry and a vanishing cosmological constant [83] (and with additional restrictions on the Maxwell field). In particular, when the cross-section is S^3 and the magnetic field vanishes, a two-parameter family of solutions was found. A large part of Chapter 3 is devoted to extending these results to $\Lambda < 0$, albeit with a different symmetry group. For a state-of-the-art review of classifications of near-horizon geometries (in various dimensions and theories), see [82].

So far we have discussed only the geometry of the horizon (understood as the induced metric). However, ultimately we are interested in the full spacetime (with prescribed asymptotics, e.g. asymptotically flat or AdS). Thus, to go beyond the

near-horizon limit, it was proposed in [90] to take $\phi_\epsilon^\star g$ (ϕ_ϵ defined as above) and expand it in a power series in ϵ. Then, Einstein equations would be expanded as well and could be solved order by order. The first-order equations were derived in [90]. They were also obtained in [80] but as constraints for connections admissible on the extremal horizons[10]. These results were extended to the Einstein-Maxwell(-dilation) theory in [44, 89]. Although this elegant program of systematic power series expansion near the horizon, is the initial motivation behind Chapter 2, we will be obliged to abandon it. As we will see, in four dimensions when $\Lambda \neq 0$, a generic extremal black hole is not smooth at the horizon even though it is a limit of finite-temperature perfectly smooth black holes. Thus, it is not justified to treat it as a power series in ϵ. There is no such obstruction when $\Lambda = 0$. However, in higher dimensions, it is going to be true even in this case. This can be seen as a reason behind a well-known fact that Majumdar-Papapetrou solutions are generically singular above 4d [19, 109].

1.4 AdS/CFT correspondence

Since observations indicate that the cosmological constant in our universe is positive [100], an honest physicist needs a good reason to work with negative Λ. A possible (rather vague) justification could be made as follows: since the conformal boundary of (asymptotically) AdS spacetime is timelike, it is not so different than putting gravity into a box. Moreover, since we can (and, in fact, we have to) impose boundary conditions at infinity, it is analogous to controlling what happens at that box's walls.

Instead of working directly with this analogy[11], we will focus on the AdS/CFT correspondence. It was noticed by Maldacena that in the string theory with a coupling constant g_s a stack of N $D3$ branes in an otherwise empty spacetime can be described in various ways [93]. If

$$\lambda \equiv 4\pi g_s N \ll 1, \tag{1.11}$$

the effective action for the low-energy excitations (open strings that begin and ends on $D3$ branes) is $\mathcal{N} = 4$ Yang-Mills theory with the gauge group[12] $SU(N)$ and 't Hooft coupling λ. All the fields are in the adjoint representation, it means they are matrices.

In the opposite limit

$$4\pi g_s N \gg 1, \tag{1.12}$$

the branes gravitate strongly and collapse forming a black brane. In this case, due to the redshift, the low-energy (as observed by a distant observer) excitations are the ones living close to the horizon. Near-horizon region of the solution in IIB supergravity is $AdS_5 \times S^5$. It was proposed that the gravity on that spacetime should be dual to the strongly interacting $\mathcal{N} = 4$ Yang-Mills theory.

AdS_5 radius (that happen to be equal to S^5 radius) can be written as

$$L = \lambda^{\frac{1}{4}} L_s = (4\pi N)^{\frac{1}{4}} L_{Pl}, \tag{1.13}$$

[10] One should note that on a null surface, the metric does not specify the connection uniquely (if at all). Thus, the proper intrinsic geometry of the extremal horizon consists of both the metric and a choice of the metric-compatible covariant derivative.

[11] Though one should not haste too much to abandon it! In fact, it is exactly the timelike nature of the conformal boundary that allows all the constructions in this Section to work.

[12] It is in fact $U(N)$ group but the trace is clearly trivial and does not contribute anything to the correspondence.

where L_s and L_{Pl} are the string and Planck lengths, respectively. Thus, it is much larger than both of them when $\lambda \gg 1, N \gg 1$. That means that the duality is between strongly interacting gauge theory and classical (super)gravity! Although the original argument was for the duality between two very specific theories, it is now believed to be much more general.

1.4.1 GKPW dictionary

Let us now give a more quantitative description of the duality. In the large N limit, a nice set of operators are so-called single trace operators

$$\mathcal{O}_I(x) = \frac{1}{N}\mathrm{Tr}F_I, \tag{1.14}$$

where F_I is a function of physical fields and (a finite number of) their derivatives. To the leading order in N, these operators are classical, which means

$$\langle \mathcal{O}_{I_1}\mathcal{O}_{I_2}...\mathcal{O}_{I_n}\rangle = \langle \mathcal{O}_{I_1}\rangle\langle \mathcal{O}_{I_2}\rangle...\langle \mathcal{O}_{I_n}\rangle. \tag{1.15}$$

All the information about correlators can be obtained from the generating functions

$$Z_{QFT}[\{h\}] = \left\langle \exp\left(i\sum_I \int dx h_I(x)\mathcal{O}_I(x)\right)\right\rangle. \tag{1.16}$$

Observables in GR are much harder to find because of the diffeomorphism invariance. However, in our case, the spacetime has a(n asymptotic) boundary that breaks diff-invariance and can be used to generate observables. Let as assume that we imposed Dirichlet boundary conditions $\phi_i \to h_i$ for all physical fields[13]. Then, we can construct the partition function[14]

$$Z_{grav}[\{h\}] \equiv \int_{\phi_i \to h_i}\left(\prod_i \mathcal{D}\phi_i\right)\exp(iS[\{\phi\}], \tag{1.17}$$

where S is an action of the full gravitational theory.

The AdS/CFT duality claims that there is a one-to-one correspondence between O_I and ϕ_i and (having appropriately identified their sources h_I and h_i) [52, 110]

$$Z_{QFT}[\{h\}] = Z_{grav}[\{h\}]. \tag{1.18}$$

Thus, if we know $Z_{grav}[\{h\}]$ we know everything about the boundary theory as well. The nicest part is the fact that in the regime $L \gg L_{Pl}, L_s$ the gravitational path integral may be calculated in the saddle-point approximation. Thus, an effective description of large N, strongly interacting gauge theory reduces to (semi-)classical gravitational calculations. That is a huge simplification!

The underlying string theory provides a detailed map between single-trace operators, sources, and bulk degrees of freedom. A canonical example is of course the fact that the metric is a source (h) for the energy-momentum tensor ($\mathcal{O}$). In practice, identification is hard, and the symmetry principles may help. For example, from

[13] In general, physical fields may exhibit a power law behavior near infinity. $\phi_i \to h_i$ means that the expansion of ϕ is f_i times an appropriate power law.

[14] In general, to prescribe the partition function we should also impose initial and finial conditions as $t \to 0$. This is equivalent to the choice of the state on the QFT side, see [95] for a relevant discussion.

(large) gauge transformations:

$$A \mapsto A + d\chi, \tag{1.19}$$

we have

$$S \mapsto S + \int \nabla_\mu \chi J^\mu = S - \int \chi \nabla_\mu J^\mu. \tag{1.20}$$

Thus, consistency requires that the operator J for which A is a source must be conserved. In general, bulk gauge fields must source (conserved) currents for *global* symmetries in QFT. Analogously, charged bulk fields are sources for fields with a global charge. In particular, the electric charge of both systems must match.

Let us now give a simple example. On the AdS_{d+1} background:

$$ds^2 = L^2 \left(\frac{\eta_{\mu\nu} dx^\mu dx^\nu + dz^2}{z^2} \right), \tag{1.21}$$

we consider a scalar field of mass m. Near infinity ($z = 0$), it has an expansion

$$\phi = \frac{\phi_{(0)}}{L^{d-1}/2} z^{d+1-\Delta} + ... + \frac{\phi_{(1)}}{L^{d-1}/2} z^\Delta + ..., \tag{1.22}$$

where

$$\Delta(\Delta - d) = (mL)^2. \tag{1.23}$$

We will encounter this behavior very often in this work. $\phi_{(0)}$ is a boundary value of ϕ that we previously denoted by h. The background is scale invariant. If we require that the (radial profile of) ϕ remains invariant, we must have

$$\phi_{(0)}(x) = h(x) \mapsto \lambda^{\Delta - d} h(\lambda x) \tag{1.24a}$$

as

$$(x^\mu, z) \mapsto \lambda (x^\mu, z). \tag{1.24b}$$

It follows that the operator $\mathcal{O}$ that is dual to h must scale as

$$\mathcal{O}(x) \mapsto \lambda^{-\Delta} \mathcal{O}(\lambda x). \tag{1.24c}$$

We thus see that Δ is the scaling dimension of $\mathcal{O}$. The action that properly describes the scalar field is

$$S = -\frac{1}{2} \int_M d^{d+1}x \sqrt{-g} \left((\nabla\phi)^2 + m^2\phi^2 \right) + \frac{\Delta - d}{2L} \int_{\partial M} d^d x \sqrt{-\gamma} \phi^2, \tag{1.25}$$

where γ is the metric induced on the boundary. The last term does not affect equations of motion nor the boundary conditions, it is needed to render the whole expression finite. In general, we choose the boundary at $r = \epsilon$ and then go with $\epsilon \to 0$. Then, a simple calculation shows that (in the saddle-point approximation)

$$\langle \mathcal{O}(x) \rangle = i \frac{\delta}{\delta \phi_{(0)}(x)} S = (2\Delta - d) \phi_{(1)}. \tag{1.26}$$

We thus see that boundary one-point functions are simply prescribed in terms of the asymptotic behavior of the bulk fields.

1.4.2 Holographic renormalization

Another key feature of holography is the fact that it geometrizes the RG (renormalization group) flow of the boundary theory. Behavior close to the asymptotic boundary corresponds to the UV observables (for example, n-point functions) while what happens deep in the bulk encodes the IR. The simplest example is the fact that the entropy is given by the Bekenstein-Hawking formula [10, 59]

$$S = \frac{A}{4}, \tag{1.27}$$

where A is the horizon's area (more generally, the entanglement entropy is given by a Ryu-Takayanagi [102] formula in which the horizon is replaced by the minimal surface and one takes into account also the entropy of the matter fields outside). We will not get into a detailed statement about connections between the RG flow and the radial evolution. A derivation may be found for example in [43, 61, 98]. What matters to us is a simple statement that infrared physics is captured by the near-horizon geometry of the black hole inside[15].

Let us give one more example of that correspondence. It was shown in [57] that if we perturb the boundary Hamiltonian by the translation-invariance-breaking term:

$$H = H_0 - \mathcal{O}(k_L) \tag{1.28}$$

with a characteristic wavelength k_L (given e.g. by a lattice), then the current J^t in the infrared is going to have a scaling dimension Δ_{k_L} (one needs to determine Δ_{k_L} from the equations of motion). It then follows that dc resistivity for low temperatures follows the power law:

$$r \sim T^{2\Delta_{k_L}}. \tag{1.29}$$

A large part of this Thesis is devoted to the study of scaling dimensions in the infrared and on the rôle the spatial symmetry breaking terms have. We thus see that they can be translated into very physical observable quantities such as transport coefficients. More about applications of AdS/CFT to the condensed matter may be found in [58].

1.5 Weak Gravity Conjecture

In 4, we will encounter the Weak Gravity Conjecture (WGC) a few times. It seems appropriate to introduce it already here. One can informally state it as follows: *there must be a particle for which gravity is the weakest force*. One can see this claim as a stronger version of *there are no global symmetries in quantum gravity*. Indeed, if we take any gauge symmetry and consider the limit $g \to 0$ of its coupling constants going to zero, we would obtain *a global symmetry* that is excluded (since its charge would be inevitably lost in a black hole). Thus, there should be a physical principle forbidding such limits [5].

It should be kept in mind that WGC is not actually a single conjecture but rather a bundle of connected ideas. We will only need its mildest version:

Conjecture 1.1. *[5] For any $U(1)$ gauge field, let $(\frac{|Q|}{M})_{ext}$ be a ratio of mass and $U(1)$ charge of the extremal black hole (of that mass). Then, in the spectrum of the theory, there*

[15] Somehow along the line we assumed that there is a black hole inside. In the Einstein-Maxwell theory at a non-zero charge it seems almost necessary because that charge must be stored somewhere.

should be a particle of mass m and $U(1)$ charge q such that

$$\frac{|q|}{m} \geq \left(\frac{|Q|}{M}\right)_{ext} \tag{1.30}$$

Note that in the Einstein-Maxwell theory, the right-hand side is 1. The motivation for this version is very simple. If the bound is not satisfied, then extremal black holes are stable (in a particle physics sense – they cannot decay into lighter particles). Moreover, large black holes sufficiently close to the extremality would actually lower their temperature due to Hawking radiation. Since arbitrarily heavy stable particles (that are not protected by any symmetry) are rather troublesome it was proposed in [5] that there must be always a decay channel.

There are at least a few ways to satisfy WGC[16] The simplest one would be obviously to simply start with a field (say, scalar one) with $|q| > m$. We will encounter consequences of that in Sec. 4.4. Another possibility, somehow subtler, has to do with the higher-curvature corrections. In their presence, $\left(\frac{|Q|}{M}\right)_{ext}$ changes and, in particular, it depends on the mass [76]. If the ratio is larger for small black holes than for big ones, very heavy black holes could decay into smaller ones! That condition puts constraints on a certain field-redefinition invariant combination of the Wilson coefficients (usually denoted d_0). We will see that $d_0 > 0$ also leads to the RG instability of five-dimensional Reissner-Nordström.

Let me end that discussion by pointing out that the version of WGC presented above is too weak to be actually self-consistent if we take into account possible dimensional reductions [62]. Thus, stronger versions (e.g. lattice WGC) are probably required to hold. Nevertheless, it is all we need in this Thesis. A good review of the topic may be found in [55].

1.6 Main results

For the Reader's convenience let us summarize the main results presented in the thesis. Before we shall dive into the detailed description, let me emphasize that virtually all the work constituting the dissertation was performed in the collaboration with my wonderful coauthors. I shall point out where they were published (if applicable) and with whom I collaborated on the topic. The leitmotif of the thesis is (nearly) extremal black holes and their stationary perturbations. I hope the Reader finds them as interesting as I do.

In Chapter 2 we shall describe how small stationary perturbations (induced for example by some distant matter distribution or by non-trivial boundary conditions at infinity) backreact on the background of extremal black holes in AdS_4. Perhaps quite surprisingly we will see that these perturbations transform the horizon into a null singularity. (Hopefully) counter-intuitively in this case the larger the black hole, the worse the singularity. Most of that content is identical with [66], published with Gary Horowitz and Jorge Santos. I feel obliged to emphasize that a large part of the numerical search was (very unfortunately!) not performed by myself. At the same time, I believe them to be crucial to show that the many approximations performed are in fact valid, that no surprising fine-tuning occurs, and to provide examples. This was not my first paper about the neighborhood of extremal horizons. Previously,

[16] Any conditional sentence "... assuming that WGC holds" in this Thesis means actually "... assuming that WGC holds in *a particular way*". To simplify the language, we will not discern between them later on.

I collaborated on the topic with Jerzy Lewandowski and Adam Szereszewski, the results may be found in [79, 80]. The starting point back then was slightly different since we assumed smoothness from the very beginning. As a result, this body of work may be seen as a special case of [66] (with $\gamma = 1$).

Let me emphasize that the singularity discussed here is physical. It describes tidal forces that would be measured by the infalling observer so it is not a gauge artifact. Moreover, there is no reason to reject them [53] (as one would do for example with $M < 0$ Schwarzschild). In particular, we are able to prepare those states using gravitational path integral. Moreover, since all the curvature scalars remain small, we do not expect higher-curvature corrections to change these results in any significant way.

Even at finite temperatures, there are signatures of that singularity. First of all, the tidal forces evaluated at the horizon follow a power law with the temperature:

$$C_{\rho a \rho b} \sim T^{\gamma-2}, \tag{1.31}$$

where $\gamma < 2$ depends on the black hole's parameters. Moreover, the specific heat gains an anomalous term $\sim T^{2\gamma}$. If the scaling dimension γ is smaller than $\frac{1}{2}$, this dominates over a usual (linear) behavior of the specific heat with the temperature. Thus, a small perturbation may drastically change thermodynamics. This should be a very clear prediction for the boundary theory. Incidentally, if the condition $\gamma \leq \frac{1}{2}$ is satisfied, $T \to 0$ limit of the solutions to Einstein-Maxwell equations is not even a weak solution.

Encouraged by the findings in four-dimensional spacetimes we shall move into higher dimensions in Chapter 3. There, we find that the singularity becomes even worse and in fact leads to the RG (renormalization group) instability. That means that a holographic CFT_4 with a non-vanishing $U(1)$ charge when put on a non-symmetric background would behave very differently in the IR than previously believed. On the bulk side, it means that (contrary to what happens in four dimensions) a small change in the boundary conditions can radically deform or even destroy the near-horizon region of the extremal black hole. We are still lacking an understanding of what is the endpoint of this instability (either in the bulk or in the boundary). I hope to try to address this question in the future. These results explain (and perhaps put into a broader perspective?) well-known statements regarding the non-smoothness of the higher-dimensional Majumdar-Papapetrou solutions. This Chapter was again a group effort in collaboration with Gary Horowitz and Jorge Santos, published in [65]. Certain results (in Sec. 3.4 regarding toroidal black holes) are new. In particular, they correspond to the quantum phase transition, and thus *may have* certain condensed matter applications.

Every result mentioned so far was awfully classical. In Chapter 4 we move beyond that and try to include quantum corrections encoded in the effective field theory. This is again a group effort together with Gary Horowitz, Grant Remmen, and Jorge Santos. As we have seen in the previous Chapters, four-dimensional $\Lambda = 0$ extremal black holes are miraculously smooth. This fine-tuning is removed when we include higher-curvature corrections. We found that the singularities are quite robust (albeit they do not have to occur, that depends on either a UV completion or the black hole's size) and do not require a cosmological constant or higher dimensions. The scaling dimensions of the Kerr black hole (but not of Reissner-Nordström) are shifted. For the Standard Model, they become smaller, and thus the horizon is replaced by a null singularity. This happens even *without* any additional sources. If the underlying UV theory was SUSY, the same conclusion would be reached (for *any*

supersymmetric matter content). All the curvature scalars remain finite (and small) and so the higher-curvature expansion seems trustworthy.

In $5d$, quantum corrections lead to the RG instability of Reissner-Nordström black hole provided that the Weak Gravity Conjecture is satisfied. At the same time, I have to emphasize that the curvature (and Maxwell) scalars diverge at the horizon. Thus, it is not clear that we can trust these results. Nevertheless, they are too interesting (at least to me) to ignore them. In $D > 5$, the corrections to the scaling dimensions are negative (also provided that WGC holds). However, in this case, the background was unstable anyway so this does not offer any qualitatively new effects. These EFT results shall appear soon [69].

It is also in Chapter 4 that we show that a scalar field of mass smaller than charge (it means, one satisfying WGC), leads to RG instability also on the background of Kerr-Newman. This effect is slightly more subtle due to the gauge transformations and a non-zero rotation of the background. There is no new solution bifurcating from the onset of the instability for $\Lambda = 0$. The connection between RG instability and WGC is highly suggestive and may shed some light on the nature of extremal black holes in quantum gravity.

Chapter 2

Generic extremal black holes and their singularities

2.1 Motivation

In the last few years, our understanding of (nearly) extremal black holes grew enormously, even at the level of quantum gravity. Indeed, the most important ingredient close to the extremality, the so-called Schwarzian, was identified and non-perturbatively quantized. That allowed for a much more accurate (from the physical point of view) quantum-mechanical description. As an example, let us mention a beautiful calculation of the density of states in four dimensions [72]. This progress did not omit also supersymmetric black holes (see for example [91]) which are special cases of extremal black holes. All of it was possible thanks to the dimensional reduction to JT gravity.

Thus, it may seem surprising that, in these exciting times, the author believes that something physically interesting can be said about the *classical* behavior of the extremal black holes. Even though it was not my initial motivation, I feel obliged to connect the work presented here with the beautiful body of results just mentioned. It is quite often (for example in [72]) to assume that, having done dimensional reduction, Kaluza-Klein modes are not sourced. In this Chapter, we will try to understand: what would be different if we turned the sources on? At this stage, I can only offer a classical answer to that question and I hope to convince my kind Readers that the difference is significant, at least as long as we keep the cosmological constant negative.

Nevertheless, since our description is classical, let us phrase it in the language of general relativity. In this Chapter, we aim to show that generic extremal black holes are in fact singular. Over the years, various examples have been found showing that this may be the case. A mild lack of smoothness (where the metric is C^2 but not C^3) was first noticed in the static multi-black hole solutions to $D = 5$ Einstein-Maxwell theory [109]. This became more serious with the discovery that in $D > 5$, static multi-black hole solutions have curvature singularities on the horizon [19]. These were null singularities in which tidal forces on infalling observers diverge, but all curvature scalars remain finite.

Similar null singularities were also seen in the extremal limit of some black holes in anti-de Sitter (AdS) space. This includes solutions with less symmetry [32, 63, 92], nonsupersymmetric attractor flows [71] and even in some supersymmetric black holes [94]. A natural question to ask is: how common are these singular extremal solutions? Are they exceptional special cases, or indicating a more general phenomenon?

As we will see, in AdS they are very common. In fact, almost all extremal black holes are singular. This is true even in four dimensions (and becomes worse

in higher dimensions). We will focus on four-dimensional solutions of Einstein-Maxwell theory with $\Lambda < 0$. The higher dimensional case will be discussed in Chapter 3. There are many more stationary black holes in AdS than in asymptotically flat spacetime since one has the freedom to choose boundary conditions for the metric and the vector potential at infinity[1]. In particular, static nonspherical charged black holes exist, but we will show they are generically singular. The derived results apply whenever rotational symmetry is broken. For example, if one puts a cage around a static AdS black hole – it becomes singular.

If the horizon was smooth, it is known that in the extremal limit, the only possible static near-horizon geometry is $AdS_2 \times S^2$ [84] so the horizon itself remains spherical. We will see that in four dimensions, even when the horizon becomes singular, a well-defined near-horizon geometry exists and remains $AdS_2 \times S^2$. Intuitively, this is because the radial distance (along a static hypersurface) from the horizon to any point outside is infinite, and thus any nonspherical perturbation[2] should decay before reaching the horizon. But the key point is how quickly they decay. The symmetry of AdS_2 ensures that all perturbations should have power law behavior near an extremal horizon. If the exponent is not an integer, the solution is not C^∞, and if the exponent is too small, the curvature will diverge. We will show that for AdS black holes with topology S^2, an $\ell = 2$ perturbation always falls off slowly enough to produce a singularity on the horizon. So generic extremal black holes with S^2 topology are singular. This singularity is null, and all curvature scalars remain finite. However, the tidal forces on infalling particles diverge.

As one increases the charge, this singularity becomes stronger, and higher ℓ modes also become singular. Similar results hold for static black holes of different topologies (with the exception of small toroidal ones) and for Kerr AdS. In fact, for large hyperbolic black holes, the singularity is so strong that some perturbations diverge at the horizon. Thus, we see that almost all extremal black holes in AdS are singular. The smoothness of the known exact solutions is an artifact of symmetry rather than a basic physical feature. Solutions with extremal AdS black holes in nonspherical backgrounds have been constructed before [70]. Although it was not noticed at the time, the current analysis shows that these "hovering" black holes also have diverging tidal forces on their horizon.

2.2 A simple example

In this Section, we will discuss a simple toy model that aims to explain all relevant phenomena. Let us look for stationary solutions to the massless (neutral) Klein–Gordon equation

$$g^{\mu\nu}\nabla_\mu\nabla_\nu\phi = 0 \tag{2.1}$$

[1] It does not mean that we cannot discuss more general black holes without a cosmological constant. We would just have to assume that there is a matter far away that we keep stationary (for example, by external forces). Our analysis automatically extends to $\Lambda = 0$ case, the answer just happens to be qualitatively different.

[2] One should note that in this work a "perturbation" does not mean any dynamical change, but rather a change in boundary conditions for the elliptic problem of finding static black holes. In particular, this work is different from the Aretakis instability of extremal black holes [3] which results from time-dependent perturbations. Nevertheless, both effects share their geometric origin – symmetries of the near-horizon geometries.

on the background of the RN AdS:

$$ds^2 = -f(r)\,dt^2 + \frac{dr^2}{f(r)} + r^2 d\Omega^2 \tag{2.2}$$

where $d\Omega^2$ is the line element on a unit radius round two-sphere,

$$f(r) = \frac{r^2}{L^2} + 1 - \frac{2M}{r} + \frac{Q^2}{r^2} \tag{2.3}$$

and L is the AdS radius. In the extremal limit, the horizon is at

$$r_+ = \sqrt{\frac{2Q^2}{1+\sqrt{1+12Q^2/L^2}}} \tag{2.4}$$

and

$$f''(r_+) = \frac{6}{L^2} + \frac{2Q^2}{r_+^4}. \tag{2.5}$$

Since the background is spherically symmetric, we may decompose ϕ into spherical harmonics:

$$\phi = \sum_{\ell,m} \phi_{\ell m}(r) Y_{\ell m}. \tag{2.6}$$

Then, Eq. (2.1) reads

$$(f\phi'_{\ell m})' + \frac{2f\phi'_{\ell m}}{r} - \frac{\ell(\ell+1)}{r^2}\phi_{\ell m} = 0 \tag{2.7}$$

This is a simple ODE with $r = r_+$ being a regular singular point. Thus, near $r = r_+$ we can approximate it by the Euler equation:

$$\frac{1}{2}(r-r_+)^2 f''(r_+)\phi''_{\ell m} + (r-r_+)f''(r_+)\phi'_{\ell m} - \frac{\ell(\ell+1)}{r_+^2}\phi_{\ell m} = 0, \tag{2.8}$$

and so near the horizon we have $\phi_{\ell m} \sim (r-r_+)^{\gamma_\pm}$, where

$$\gamma_\pm = \frac{1}{2}\left[\pm\sqrt{1+\frac{4\ell(\ell+1)}{1+6\,r_+^2/L^2}} - 1\right]. \tag{2.9}$$

Since $\gamma_- < 0$, it must be discarded as a diverging solution (mathematically speaking, we choose Dirichlet boundary conditions $\phi(r = r_+) = 0$). Nevertheless, notice that when $\ell = 1$, we have $0 < \gamma_+ < 1$ for all $\frac{r_+}{L} > 0$. Thus, the field is only C^0 at the horizon. Moreover, certain components of the associated energy-momentum tensor:

$$T_{rr} \sim (\phi_{,r})^2 \sim (r-r_+)^{2(\gamma_+ - 1)} \tag{2.10}$$

are divergent. Thus the backreaction on the metric will produce a singularity. Nevertheless, all scalar quantities built from $T_{\mu\nu}$, such as T or $T_{\mu\nu}T^{\mu\nu}$ are finite. Thus, one could be tempted to blame our choice of coordinates for the apparent non-smoothness. However, that would be too naive since r is a good coordinate at the horizon. Moreover, if one replaces t with an ingoing Eddington coordinate v, the

calculation is the same, and now ∂_r is a vector field tangent to the affinely parameterized null geodesics and so it has a clear geometrical meaning. Moreover, T_{rr} enters the Raychaudhuri equation and so its divergence signifies that the family of null rays emanating from the horizon is singular. This is going to be a general lesson for all the examples we consider later in this paper: generic nonspherical perturbations produce a physical curvature singularity along the null horizon, but all curvature scalars are finite. Thus, one needs to be extra careful with the choice of coordinates to properly capture these divergences. A few remarks are in order regarding (2.9):

- Although we assumed that ϕ is massless, similar conclusions would hold also for massive but light fields. Thus, it is a generic result, not just a product of an unfortunate fine-tuning of the model.
- If r_+/L is large enough, $\gamma_+ < 1$ also for higher ℓ's.
- The larger r_+ is, the smaller γ_+ and thus the solutions are more and more divergent. As we will see, this and the previous remark hold also in the nonlinear Einstein-Maxwell theory. This means that (counter-intuitively) large black holes, whose curvature scalars at the horizon are much less than small black holes', nevertheless have stronger singularities if we perturb them a little bit.
- Eq. (2.9) does not depend on any asymptotic conditions. It was derived locally, just near the horizon. The only role of the asymptotic region is to provide a source for non-symmetric modes.
- The case $\Lambda = 0$ can be read off from Eq. (2.9) by taking $L \to \infty$. The result is $\gamma_+ = \ell$, so ϕ remains smooth.
- The case $\Lambda > 0$ can be read off from Eq. (2.9) by analytically continuing $L^2 \to -L^2$. One sees that ϕ is at least C^1 but it is still not smooth. As we will see, for *certain* black holes in dS, the singularity at the horizon may persist, although it will be milder.

Eq. (2.9) can be understood as a special case of a familiar result in gravitational holography. The near-horizon geometry of the extremal RN AdS solution is $AdS_2 \times S^2$ with AdS_2 radius $L_2 = [2/f''(r_+)]^{1/2}$. We may perform (rather trivial) dimensional reduction of the scalar field to the AdS_2 throat. Then, the ℓ^{th} component becomes a free field of mass $m^2 = \ell(\ell+1)/r_+^2$ in this AdS_2 spacetime. In terms of L_2 and m^2, eq. (2.9) becomes

$$\gamma_\pm = \frac{-1 \pm \sqrt{1 + 4m^2 L_2^2}}{2} \tag{2.11}$$

This is a special case of a more general formula that gives the power law behavior of fields with mass m in AdS_D, which is the scaling dimension of the dual operator.[3]

This shows all the important properties of the perturbations we are about to study in this Chapter. They exhibit a power-law behavior near the extremal horizon with a (generically) non-integer scaling dimension and thus are going to be non-smooth. Notice that this is a purely geometrical statement that relies only on the presence of the infinite AdS_2 throat. Only the exact values of the exponents depend on the theory at hand.

[3] Eq. 2.11 differs from the usual scaling dimension by an overall sign, since we have defined it to be the power of $r - r_+$, rather than the more commonly used power of an inverse radius.

2.2.1 BTZ

Although the focus of this Chapter is on four-dimensional extremal black holes, we now briefly comment on the situation with the three-dimensional BTZ black hole (rotating one). This is not at all harder but it will be a nice warm-up before we attack similar problems on the Kerr-Newman background in Sec. Since three-dimensional gravity is purely topological, to perturb BTZ we must add matter fields. We will consider a scalar field of an arbitrary mass μ. The line element (in the near horizon limit) reads:

$$\mathring{g} = 2dvd\rho + \frac{4\rho}{L}dvdx + dx^2 = -\frac{4\rho^2}{L^2}dv^2 + 2dvd\rho + \left(\frac{2\rho}{L}dv + dx\right)^2. \tag{2.12}$$

Near the horizon, solutions to the Klein-Gordon equation may be decomposed into[4]:

$$\phi = \rho^{\alpha} e^{imx}, \tag{2.13}$$

where $\alpha = \frac{1}{2}\left(-1 + iLm \pm \sqrt{1 + L^2\mu^2}\right)$. Only the $+$ choice is continuous at the horizon. Nevertheless, if $0 < L^2\mu^2 < 8$, then the solution is not C^1 and the associated energy-momentum tensor is diverging. Moreover, for $m \neq 0$, the solution is highly oscillating. Notice that the BF bound in three dimensions is

$$\mu^2 \geq m_{BF}^2 = -L^2. \tag{2.14}$$

Thus, there are masses above the BF bound for which $\alpha < 0$. That is a sign of RG instability. A small source for the scalar field would destroy the extremal horizon.

2.3 Linearized Einstein-Maxwell theory

2.3.1 General approach

With all this in mind, let us move towards non-trivial examples such as Einstein-Maxwell theory. The equations of motion read

$$R_{\mu\nu} = 2F_{\mu\sigma}F_{\nu}{}^{\sigma} - \frac{1}{2}g_{\mu\nu}F_{\alpha\beta}F^{\alpha\beta} - \frac{3}{L^2}g_{\mu\nu}, \tag{2.15a}$$

$$\mathrm{d}F = 0, \tag{2.15b}$$

$$\mathrm{d}\star F = 0, \tag{2.15c}$$

where $F = \mathrm{d}A$ is the Maxwell two-form, A is its potential and L is the radius of AdS_4.

We are interested in the solutions to (2.15) which describe a stationary extremal black hole. Near the horizon we may introduce Gaussian null coordinates (v, ρ, x^a) in which the metric and Maxwell field read:

$$g = 2\mathrm{d}v\left(\mathrm{d}\rho + \rho\, h_a\, \mathrm{d}x^a - \frac{1}{2}\rho^2\, C\, \mathrm{d}v\right) + q_{ab}\, \mathrm{d}x^a\, \mathrm{d}x^b \tag{2.16a}$$

$$F = E\, \mathrm{d}v \wedge \mathrm{d}\rho + \rho\, W_a\, \mathrm{d}v \wedge \mathrm{d}x^a + Z_a\, \mathrm{d}\rho \wedge \mathrm{d}x^a + \frac{1}{2}\, B_{ab}\, \mathrm{d}x^a \wedge \mathrm{d}x^b, \tag{2.16b}$$

[4]The physical field is, of course, given by the real and imaginary parts.

where nothing depends on v. In particular, ∂_v is the Killing vector generating the horizon. It is often useful to work with the near-horizon geometry of the spacetimes of the form (2.16). To this end one may consider a one-parameter ($\epsilon > 0$) family of diffeomorphisms

$$\phi_\epsilon(v, \rho, x^a) = (\epsilon^{-1} v, \epsilon\rho, x^a). \tag{2.17}$$

The limits of pull-backs

$$\lim_{\epsilon\to 0}(\phi_\epsilon^\star g, \phi_\epsilon^\star F) = (\mathring{g}, \mathring{F}) \tag{2.18}$$

exist and provide us with a new smooth solution to the Einstein-Maxwell equations. This leads to a significant simplification of (2.16), namely

$$\mathring{g} = 2\,\mathrm{d}v\left(\mathrm{d}\rho + \rho\, h_a\,\mathrm{d}x^a - \frac{1}{2}\rho^2\,\mathrm{C}\mathrm{d}v\right) + q_{ab}\,\mathrm{d}x^a\,\mathrm{d}x^b \tag{2.19a}$$

$$\mathring{F} = E\,\mathrm{d}v\wedge\mathrm{d}\rho + \rho\, W_a\,\mathrm{d}v\wedge\mathrm{d}x^a + \frac{1}{2}B_{ab}\,\mathrm{d}x^a\ \wedge\mathrm{d}x^b, \tag{2.19b}$$

where now all the ρ-dependence is explicit. Notice that $\mathring{g}$ posses a new Killing vector: $\rho\partial_\rho - v\partial_v$. This should not come as a surprise since the action of ϕ_ϵ is generated by $\rho\partial_\rho - v\partial_v$. Also, (2.15) simplifies significantly for $(\mathring{g}, \mathring{F})$. This allowed for the classification (under the assumption of smoothness and either staticity or axial symmetry) of geometries of the extremal horizons in four dimensions. The only possible geometries are either those of Reissner-Nordström (AdS) or Kerr-Newman (AdS) (in the static or the axially symmetric case, respectively). Below we consider how stationary solutions to (2.15) behave near those horizons.

Since we are interested only in near-horizon behavior, we may write our (generic yet stationary) fields as

$$g = \mathring{g} + \delta g, \tag{2.20a}$$

$$F = \mathring{F} + \delta F \tag{2.20b}$$

where $(\delta g, \delta F)$ are supposed to vanish on the horizon (and by continuity, are small nearby). Thus, it seems reasonable to expect that $(\delta g, \delta F)$ satisfies *linearized* Einstein-Maxwell equations on the background of $(\mathring{g}, \mathring{F})$. Due to the symmetries, we may decompose our perturbations into eigenspaces of $\rho\partial_\rho - v\partial_v$ [5] They are thus of the form

$$\delta g = \rho^\gamma\left(\delta F\,\rho^2\,\mathrm{d}v^2 + 2\,\rho\,\delta h_a\,\mathrm{d}v\,\mathrm{d}x^a + \delta q_{ab}\,\mathrm{d}x^a\,\mathrm{d}x^b\right) \tag{2.21a}$$

$$\delta\mathcal{F} = \rho^\gamma\left(\delta E\,\mathrm{d}v\wedge\mathrm{d}\rho + \rho\,\delta W_a\,\mathrm{d}v\wedge\mathrm{d}x^a + \rho^{-1}\delta Z_a\,\mathrm{d}\rho\wedge\mathrm{d}x^a + \frac{1}{2}\,\delta B_{ab}\,\mathrm{d}x^a\wedge\mathrm{d}x^b\right). \tag{2.21b}$$

This ansatz implies

$$\delta C_{\rho a\rho b} \sim \gamma(\gamma-1)\rho^{\gamma-2} \tag{2.22a}$$

$$\delta R_{\rho\rho} \sim \gamma(\gamma-1)\rho^{\gamma-2}, \tag{2.22b}$$

where $C_{\alpha\beta\mu\nu}$ is the Weyl tensor. The derivation is quite simple and does not require any calculation. Let $D = \rho\partial_\rho - v\partial_v$. It is a Killing vector field of the background, so it holds that[6]

$$\mathcal{L}_D\delta R_{\mu\nu}[\delta g] = \delta R_{\mu\nu}[\mathcal{L}_D\delta g] = \delta R_{\mu\nu}[\gamma\delta g] = \gamma\delta R_{\mu\nu}[\delta g]. \tag{2.23}$$

[5] Although $partial_v$ and $\rho\partial_\rho - v\partial_v$ do not commute, they do so on the stationary fields.

[6] One should note that $R_{\mu\nu}$ below is a Ricci tensor written in the abstract-index notation, whereas $R_{\rho\rho}$ is a particular component of this object.

Thus it follows that $\delta R_{\mu\nu}[\delta g]$ must have an expansion similar to Eq. (2.21), with the same exponent γ. We are interested in $R_{\rho\rho}$, which stands in front of $d\rho d\rho$. Since $\mathcal{L}_D d\rho d\rho = 2 d\rho d\rho$, $R_{\rho\rho}$ must be proportional to $\rho^{\gamma-2}$. $\gamma = 0$ and $\gamma = 1$ correspond to smooth perturbations and so there will be factors of $\gamma(\gamma-1)$ in front to ensure it does not diverge for those values. The same reasoning holds for the Weyl tensor. The only remaining question is whether the coefficient in front is non-zero. A simple calculation (e.g. for the RN AdS black hole discussed below) shows that generically it does not vanish.

Thus, we see that if $1 \neq \gamma < 2$, then our linearized solutions are singular. I will show that there are indeed solutions with $0 < \gamma < 1$ which strongly suggests that generically the spacetime is singular at the horizon.[7] Notice that since the diverging components always involve a ρ index and the inverse of the metric in (2.19) has $\mathring{g}^{\rho\rho} = C\rho^2$, all curvature invariants will remain finite at the horizon. Nevertheless, $C_{\rho a \rho b}$ and $R_{\rho\rho}$ are physically measurable quantities. They encode tidal forces acting on a body. Thus, the singularity present for $\gamma < 1$ is not a mere coordinate singularity but a physical issue.

2.3.2 Finite temperature

Of course, black holes with $T = 0$ are not present in nature. Before we will proceed with our investigations of γs, let us look for finite temperature traces of this singularity. For simplicity, we will restrict to RN AdS but the main reasoning remains the same also on different backgrounds.

Let us fix a charge Q and a temperature $T \approx 0$. In Schwarzschild coordinates, the horizon is now located at $r_h \approx r_0 + 2\pi T L_2^2$, where

$$L_2 = \frac{L r_0}{\sqrt{L^2 + 6 r_0^2}} \tag{2.24}$$

is the AdS_2 radius and r_0 is the radius of the horizon of the extremal black hole with the same charge. In the region $\rho \equiv r - r_0 \ll r_0$, the metric can be approximated as

$$g \approx \frac{\rho^2 - (r_h - r_0)^2}{L_2^2} \mathrm{d}t^2 + \frac{L_2^2}{\rho^2 - (r_h - r_0)^2} \mathrm{d}\rho^2 + (r_0 + \rho)^2 \mathrm{d}\Omega^2. \tag{2.25}$$

The first two terms are just AdS_2 in Rindler coordinates. Thus, a little bit from the horizon, any perturbation in this region should behave in the same way as in the $T = 0$ case, i.e., the Weyl tensor should grow like

$$C_{\rho a \rho b} \sim \rho^{\gamma-2}, \tag{2.26}$$

where γ is the same as for the black hole with the same charge at $T = 0$. When $\rho = O(r_h - r_0) = O(T)$, the Weyl tensor will be

$$C_{\rho a \rho b}(\rho = O(T)) \sim T^{\gamma-2}. \tag{2.27}$$

It is not clear what happens very close to the horizon. Nevertheless, if the resulting spacetime is smooth, it cannot change very much. Thus, we expect that on the

[7] Weak solutions of the Einstein-Maxwell equations can be defined if the curvature is integrable. This requires the Christoffel symbols to be square integrable. If $\gamma > \frac{1}{2}$ this is the case, so one can extend the fields inside the horizon as a weak solution, but the extension is not unique. As we will see, for sufficiently large black holes, that condition is not satisfied and no extension is possible.

horizon

$$C_{\rho a \rho b}|_H \sim T^{\gamma-2} \tag{2.28}$$

As we will see later on, this is truly the case. Thus, even at finite T, tidal forces (though finite) can be arbitrarily large.

It turns out that those $T = 0$ singularities may have an important effect on standard black hole thermodynamics. Most notably, if $\gamma < 1/2$, the increase in black hole entropy with T acquires an anomalous scaling at low T, which in turn yields an anomalous scaling for the specific heat at low temperatures. Intuitively, this can be seen as follows. The perturbation to the metric on the horizon decays like ρ^γ. As we will see, linearized analysis shows that the volume element does not change in the first order. Thus, the leading correction to the area comes from the second-order contribution which scales like $\rho^{2\gamma}$. One may now use the above scaling argument to relate ρ to the near extremal horizon temperature T to obtain

$$S \approx S_0 + S_2\, T^{2\gamma} \tag{2.29}$$

where S_0 and S_2 are suitable constants. This implies that the specific heat at constant charge scales like

$$C_Q = T\frac{\mathrm{d}S}{\mathrm{d}T} \;\propto\; T^{2\gamma} \tag{2.30}$$

It still could happen that the horizon's area at the second order is not corrected (if appropriate coefficients cancel out). In the Appendix, it will be shown explicitly that this is not the case. Moreover, we will see that $S_2 > 0$ if $\gamma < \frac{1}{2}$ so that C_Q is positive and the system is thermodynamically stable. We will also see that for $\gamma = 1/2$, there is an anomalous $T \log T$ scaling of the specific heat.

We have discussed so far how the perturbations behave near the (nearly extremal) horizon but we omitted their source. The easiest way to obtain such solutions is to consider slightly deformed boundary conditions. Indeed, a standard (spherically symmetric) black hole spacetimes satisfy

$$A_t|_{\partial M} = \mu_0, \tag{2.31}$$

where μ_0 is a constant. By the AdS/CFT dictionary, it corresponds to the chemical potential for the dual theory. We perturb this boundary condition by writing

$$A_t|_{\partial M} = \mu(\theta, \phi), \tag{2.32}$$

where μ is still time-independent. We look for static black hole solutions (of fixed temperature T) satisfying this condition and we monitor their Weyl tensor at the horizon.[8] Note that in this scheme, the total charge Q is determined by the solution and not prescribed apriori. Of course, we also need to specify the metric at infinity. For simplicity, we will keep it spherical.

2.3.3 Reissner–Nordström AdS

We will start our investigations by considering static NHG. Since in four dimensions, there is a duality between electric and magnetic charges, we may put the latter to

[8] We will see the anomalous scaling of the specific heat in the next section, in a theory where it is easier to reach the low temperatures required.

zero. It was shown in [84] that the only such solutions are of the form:

$$\mathring{g} = 2\,\mathrm{d}v\left(\mathrm{d}\rho - \frac{1}{2}\rho^2\,C\,\mathrm{d}v\right) + q_{ab}\,\mathrm{d}x^a\,\mathrm{d}x^b \tag{2.33a}$$

$$\mathring{F} = E\,\mathrm{d}v\wedge\mathrm{d}\rho, \tag{2.33b}$$

where now C, E are constants and q is a two-dimensional metric of constant curvature. The first term is just AdS_2 with a length scale set by C. The field equations require:

$$R = -\frac{6}{L^2} + 2E^2 \tag{2.34a}$$

$$C = \frac{3}{L^2} + E^2, \tag{2.34b}$$

where R is the Ricci scalar of q. In short, this says that the near-horizon solution has a product structure $AdS_2 \times H$, where H has a constant curvature (of any sign).

Although it is possible to solve Einstein-Maxwell equations for the ansatz (2.21) directly, it is not the most convenient way to find exponents γ. Indeed, we perturb a highly symmetrical background so one should take an advantage of that. We may thus decompose δg and δF into the eigentensors of the Laplacian on H and then use the Kodama-Ishibashi formalism[9]. Since our usage of these methods is rather simple, for the sake of completeness, we will provide a short introduction here. We will restrict ourselves to the scalar-derived perturbations. The inclusion of the vector perturbations is rather immediate and one reproduces the same exponents.

If q_{ab} has a positive (negative) curvature, we may normalize it[10] $q_{ab} = r_+^2\mathring{q}_{ab}$ in such a way that $\mathring{R} \in \{-2, +2\}$. (And obviously $\mathring{R} = 0$ for a torus.) Let $\mathbb{S}$ be a non-constant eigenfunction of the Laplacian $\mathring{\Delta}$:

$$\left(\mathring{\Delta} + k^2\right)\mathbb{S} = 0 \tag{2.35}$$

and

$$\mathbb{S}_a = -\frac{1}{k}\mathring{D}_a\mathbb{S}, \tag{2.36a}$$

$$\mathbb{S}_{ab} = \frac{1}{k^2}\mathring{D}_a\mathring{D}_b\mathbb{S} + \frac{1}{2}q_{ab}\mathbb{S}. \tag{2.36b}$$

Then, we may decompose our perturbation as:

$$\delta F = f\,\mathbb{S}\,, \quad \delta h_a = h\,\mathbb{S}_a\,, \quad \delta q_{ab} = h_L\,\mathring{\gamma}_{ab}\mathbb{S} + h_T\,\mathbb{S}_{ab} \tag{2.37a}$$

$$\delta E = q\,\mathbb{S}\,, \quad \delta W_a = w\,\mathbb{S}_a\,, \quad \delta Z_a = z\,\mathbb{S}_a\,, \quad \delta B_{ab} = 0, \tag{2.37b}$$

where all new variables are simply constants. In this way, the problem of solving linearized Einstein-Maxwell reduces to solving a system of linear (algebraic) equations:

$$\left[\frac{k^2}{2} - \frac{1}{2}C\,r_+^2\gamma\,(1+\gamma) - r_+^2E^2 + \frac{3r_+^2}{L^2}\right]h_T - \frac{4\,E\,r_+^2\,k}{\gamma}z + k^2h_L = 0, \tag{2.38a}$$

$$\frac{k^2 - 2\mathring{R}}{2k}\,E\,\gamma\,h_T + \left[C\,r_+^2\,(1+\gamma)\,\gamma - k^2 - 4E^2r_+^2\right]z + k\,E\left(\frac{3}{2} - \gamma\right)h_L = 0, \tag{2.38b}$$

[9] One important difference between the proper Kodama-Ishibashi formalism [78] and the treatment presented here is our assumption of stationarity. Certain formulas derived in [78] are written after a Fourier transform in the time variable and thus their time-independent limit requires extra care.

[10] From now on, all objects with a little circle are associated with $\mathring{q}$.

$$\gamma(\gamma-1)h_L = 0, \tag{2.38c}$$

$$(\gamma+1)w + qk = 0, \tag{2.38d}$$

$$q = \frac{k}{\gamma\, r_+^2} z - \frac{E}{r_+^2} h_L, \tag{2.38e}$$

$$\frac{1}{2}\gamma(1+\gamma)\, h + \frac{k^2 - \mathring{R}}{4kr_+^2}\gamma\, h_T - 2\, E\, z = 0, \tag{2.38f}$$

$$\frac{1}{2}(1+\gamma)(2+\gamma) f + \frac{1}{2r_+^2}(1+\gamma)\, k\, h - \frac{1}{r_+^2}\, C\, \gamma h_L + 2\, E\, q = 0. \tag{2.38g}$$

For $\gamma(\gamma-1) \neq 0$ we obtain $h_L = 0$. As a result, the first two equations are decoupled from the rest and can be solved. Then, all the other equations have unique solutions in terms of h_T and z. Thus, the whole system (2.38) has a non-zero solution if and only if its two first equations constitute an underdetermined system.
The case $\gamma = 0$ reproduces a linearized NHG solution. It does not have any non-trivial solutions in four dimensions so we will skip it. The case $\gamma = 1$ (first derived in [89] and solved in [79]) is somewhat special. As shown in [89], there is an additional gauge freedom then. It may be used to put $\mathring{\gamma}^{ab}\delta q_{ab} = const.$ and that implies $h_L = 0$ for $k \neq 0$. Besides that point, all other calculations are equivalent to the ones presented in this Section.

We will now go through the solutions in different cases, corresponding to the different geometries of H.

Spherical black holes

We start by considering the case $H = S^2$. There is, obviously, only one (up to scale) constant-curvature geometry on S^2. Then, $k^2 = \ell(\ell+1)$, and r_+ is related to the electric charge Q by (2.4). Solutions to (2.38) exist only when

$$\gamma_{\pm\pm} = \frac{1}{2}\left[-1 \pm \sqrt{\frac{4\ell(\ell+1) + 5\sigma \pm 4\sqrt{\sigma^2 + 2\ell(\ell+1)(1+\sigma)}}{\sigma}}\right], \tag{2.39a}$$

where

$$\sigma \equiv 1 + \frac{6\, r_+^2}{L^2}. \tag{2.39b}$$

There are a total of four solutions for each ℓ and r_+. We are free to choose a boundary condition at the horizon to remove two of them. Since $\gamma_{--}, \gamma_{-+} < 0$ the solution blows up at the horizon for this choice. Thus, the physical perturbations are $++$ and $+-$. The values of γ for a few ℓs are plotted in Fig. 2.1. As one may see, for $\ell = 2, 3$ and for $+-$ modes, the Weyl tensor

$$C_{\rho a \rho b} = \rho^{\gamma-2} h_T \mathrm{S}_{ab} \tag{2.40}$$

is divergent for any value of r_+. Moreover, the larger $\frac{r_+}{L}$, the stronger the divergence. In particular, for sufficiently large black holes, the perturbation is not even a weak solution. The associated region is represented in gray. Since a generic nonspherical perturbation includes the $\ell = 2$ mode, we see that a generic perturbation would replace the horizon with a null singularity. One may notice from Eq. (2.39a) that $\gamma_{+-} = 0$ for $\ell = 1$ (and any r_+). Since it does not decay, one might be tempted to interpret it as a deformation that changes the horizon geometry itself (and not just

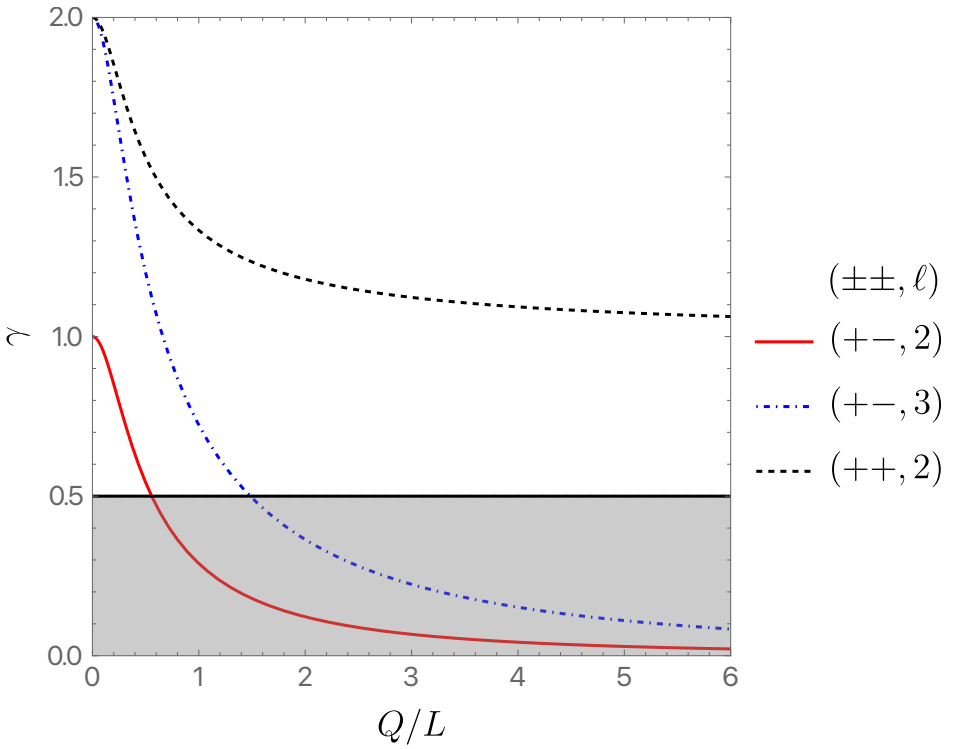

FIGURE 2.1: Scaling exponents for different ℓ as a function of Q/L. The shaded region indicates values of γ for which no weak solution exists. The solid red line is a $+-$ mode with $\ell = 2$, the blue dash-dotted line is a $+-$ mode with $\ell = 3$ and the black dashed line is a $++$ mode with $\ell = 2$. All $\gamma < 2$ (except $\gamma = 1$) lead to a singularity on the horizon via Eq. (2.22a).

a neighborhood of it). This is however not justified since the system of equations (2.38) was derived using a decomposition into $\mathbb{S}$,$\mathbb{S}_a$ and $\mathbb{S}_{ab}$. When $\ell = 1$, $\mathbb{S}_{ab} = 0$ and so all equations proportional to it are automatically satisfied. Instead, we are left with a simpler constraint ($k^2 = 2$):

$$\left[-2 + Cr_+^2(1+\gamma)\gamma - 4E^2 r_+^2\right] z = 0, \tag{2.41}$$

which has non-trivial solutions only when

$$\gamma_\pm = \frac{1}{2}\left(-1 \pm \sqrt{\frac{16+9\sigma}{\sigma}}\right). \tag{2.42}$$

We have only two solutions, so our boundary conditions can get rid of γ_- (which would lead to the mode diverging at the horizon). Since $\gamma_+ > 1$, this solution is at least C^1 (but not necessarily C^2). The fact that $\ell = 1$ perturbation behaves slightly differently should not be a surprise. It is always an exceptional mode in the Kodama-Ishibashi formalism. It is connected to the fact that gravity is a quadrupole force and so $\ell = 1$ mode describes in a sense only Maxwell field (in particular, $\delta q_{ab} = 0$).

For completeness, let us now discuss here what happens when $\Lambda \geq 0$. If $\Lambda = 0$, we have simply $\sigma = 1$ and $\gamma_{+\pm} = \ell \pm 1 \in \mathbb{N}$. As a result, perturbations are perfectly smooth. The case of $\Lambda > 0$ may be obtained by replacing $L^2 \to -L^2$. Then, $\gamma_{+\pm}$ are generically not going to be integers so the perturbations have only a finite degree of smoothness. In this case, the singularity is stronger for small black

holes. In particular, if $\frac{r_+^2}{L^2}$ is small enough, it is only C^1 and it still suffers from the diverging tidal forces at the horizon. A static extremal black hole in our universe would certainly have small $\frac{r_+^2}{L^2}$, and nonspherical perturbations from other galaxies, so if they existed, they would have singular horizons.

Toroidal black holes

Analogous analysis can be performed in the toroidal case. This was done previously in [92] for flat, non-compact cross-sections. As we will see, compactness changes the results qualitatively for small enough black holes. For definiteness, we compactify the space directions in such a way that the cross-section of the horizon has volume $L_x L_y r_+^2$, where x and y are periodic coordinates with $x \sim x + L_x$ and $y \sim y + L_y$. From (2.34a), it follows that

$$E = \frac{\sqrt{3}}{L} \tag{2.43}$$

and

$$C = \frac{6}{L^2}. \tag{2.44}$$

Consequently, the charge confined within a black hole is:

$$Q = \frac{\sqrt{3} L_x L_y r_+^2}{4\pi L} \tag{2.45}$$

Note that in contrast to a sphere, we have a larger family of geometries on a two-dimensional torus – it is encoded in periods of x and y coordinates and the angle between ∂_x and ∂_y.

We may now repeat our scheme and calculate the associated exponent. Perturbations are again scalar derived, however, this time we need to decompose them into eigenfunctions of the Laplacian on $\mathbb{T}^2$, namely $\mathrm{Re}\, e^{i(k_x x + k_y y)}$ and $\mathrm{Im}\, e^{i(k_x x + k_y y)}$. The exponent turns out to be[11]

$$\gamma = \frac{1}{6}\left(\sqrt{45 + 6\tilde{k}^2 - 36\sqrt{1 + \frac{\tilde{k}^2}{3}}} - 3\right), \tag{2.46}$$

where $\tilde{k} \equiv kL/r_+$ with $k = \sqrt{k_x^2 + k_y^2}$. As usual, the (linearized) Weyl tensor diverges when $\gamma < 2$. Not surprisingly, for k large enough, γ given by the expression above is larger than 2 and thus modes with high momenta are not singular, just as in the spherical case. However, if the black hole is toroidal, we can make it arbitrarily small and then γ is arbitrarily large. Thus, the toroidal black holes which are small enough are not going to become singular under an arbitrary (small) perturbation. It happens when

$$\tilde{k}^2 > 36 + 12\sqrt{3} \tag{2.47}$$

for all non-zero eigenvalues of the minus Laplacian $\mathring{\Delta}$. In particular, for a torus that is obtained from a square with $L_x = L_y = 2\pi$, the minimal k is 1 and this translates into

$$\frac{r_+}{L} < \frac{1}{\sqrt{36 + 12\sqrt{3}}} \tag{2.48}$$

[11] As before, there are four values of γ. Two of them are excluded automatically since they are negative. Below we focus only on the smaller positive value since we are interested in possible singularities.

This explains the 'almost all' in the title of this paper – there is a finite volume in the moduli space of extremal black holes which are singularity-free. On the opposite end of this spectrum are planar black holes for which there are infinitely many singular modes (of small momentum), as pointed out in [92].

Hyperbolic black holes

Let us now consider a case when H has a constant negative curvature. All such surfaces are given by a quotient of a hyperbolic space $\mathbb{H}^2$ by a discrete group. As follows from Eq. (2.34a), such solutions exist even without a Maxwell field. To begin, we will restrict ourselves to this case. As we noticed earlier, the larger the charge on a black hole, the more singular it becomes so we can expect that the inclusion of charge will make the perturbations even more divergent. This will be confirmed below. With $E = 0$, it follows from (2.34a) that $R = -\frac{6}{L^2}$ and so $r_+ = \frac{L}{\sqrt{3}}$. The analysis follows exactly in the same way as in the spherical case (except that only gravitational modes are included).

We find that the perturbed solutions (for gravity modes) exist only when

$$\gamma_{grav} = \frac{1}{2}\left(-1+\sqrt{9+4k^2}\right). \tag{2.49}$$

As before, the perturbation is singular if $\gamma_{grav} < 2$, or equivalently $k^2 < 4$. The first non-zero eigenvalue of the Laplacian on a compact Riemann surface is bounded by [39, 111]

$$k^2 \leq \frac{2}{g-1}\lfloor\frac{g+3}{2}\rfloor \leq 4, \tag{2.50}$$

where g is a genus of H and $\lfloor z\rfloor$ denotes the largest integer in z. Note that the last inequality is saturated only when $g = 2$. We thus see that for $g > 2$ and for any geometry of the horizon, at least one mode in the perturbation is singular. For $g = 2$, a recent bootstrap calculation has shown that $k^2 \leq 3.839$ [15, 81], so generic gravitational perturbations of all extremal hyperbolic black holes are singular. It is immediate to see that the same holds true also when the cross-section of the horizon is non-compact. Indeed, then the first non-zero eigenvalue is $\frac{1}{4}$ which is clearly less than 4.

If we next consider a test Maxwell field on this neutral extremal black hole, the appropriate exponent reads

$$\gamma_{EM} = \frac{1}{2}\left(-1+\sqrt{1+4k^2}\right) < \gamma_{grav}. \tag{2.51}$$

Notice that this perturbation may cause a singularity through its backreaction. Thus, the metric would be singular only if $\gamma_{EM} < 1$ which translates to $k^2 < 2$. Thus, there are geometries on H (for example, the Bolza surface which nearly saturates the above $g = 2$ bound) for which the Maxwell field would not produce a singularity. Nevertheless, when the black hole is charged, the situation is very different. Gravitational and Maxwell perturbations are then coupled to each other, and the two physical exponents become:

$$\gamma_{+\pm} = \frac{1}{2}\left[-1+\sqrt{5+\frac{4k^2 \pm 4\sqrt{\sigma^2+2(\sigma-1)(k^2+2)}}{\sigma}}\right], \tag{2.52}$$

where $\sigma = 6\frac{r_+^2}{L^2} - 1$. The minimal radius of the hyperbolic extremal horizon is obtained with no charge, $r_+ = \frac{L}{\sqrt{3}}$, so $\sigma \geq 1$. Notice that when $\sigma > \frac{1}{4}\left(4 + 2k^2 + k^4\right)$, γ_{+-} becomes *negative*. Thus the perturbation blows up on the horizon and our perturbative scheme breaks down. It is likely that some curvature invariants will now diverge. This also signals an RG instability - a small change in the boundary conditions at asymptotic infinity (UV) would lead to a drastic change in the near-horizon (IR) region. At the moment we are not sure what the endpoint of this instability is. Indeed, all smooth static near-horizon geometries are classified in four dimensions [84] so the endpoint cannot be described by a single component extremal black hole with a smooth horizon. Most likely, the horizon just develops a strong singularity in which the metric is not even continuous.

2.3.4 Kerr AdS

So far, we have considered only static solutions and their perturbation. This is of course far from any reasonable notion of 'all extremal black holes'. To gain more completeness, let us now consider perturbations of the extremal Kerr AdS with a mass $\frac{M}{(1-a^2/L^2)^2}$, an angular momentum $\frac{Ma}{(1-a^2/L^2)^2}$, and an angular velocity Ω. It will be convenient to express these parameters in terms of the horizon radius r_+ $\left(< \frac{L}{\sqrt{3}}\right)$:

$$M = \frac{r_+\left(1+\frac{r_+^2}{L^2}\right)^2}{1-\frac{r_+^2}{L^2}}, \quad a = r_+\sqrt{\frac{3r_+^2+L^2}{L^2-r_+^2}}, \quad \Omega = \frac{\sqrt{L^4+2r_+^2L^2-3r_+^4}}{2r_+L^2} \tag{2.53}$$

Though very useful, r_+ has no geometric meaning *per se*. Indeed, it is simply the location of the horizon measured in a particular coordinate system. We thus introduce the areal radius, defined as the square root of the area of the spatial section of the event horizon, divided by 4π

$$R_+ \equiv \frac{\sqrt{r_+^2+a^2}}{\sqrt{1-\frac{a^2}{L^2}}}. \tag{2.54}$$

It is convenient to use the Teukolsky formalism [35]. This is especially useful since one works directly with the Weyl tensor. We want to consider only stationary perturbations. However, stationarity is ambiguous in this context since one could consider perturbations annihilated either by ∂_t (which are stationary at infinity) or by the helical Killing vector $\partial_t + \Omega\partial_\phi$ (which are stationary at the horizon). Since we are interested in the behavior near the horizon, we choose the latter. Notice that this is the choice that corresponds to the black resonators at finite temperature [36]. Following [35] we use the Kinnersly tetrad and Boyer-Lindquist coordinates for a non-rotating frame at infinity for the Kerr AdS. Rather than restrict to pure gravitational perturbations, it is no more difficult to consider a spin s perturbation (with $s = \pm 2$ corresponding to pure gravity). We want to separate variables for the spin s field:

$$\Psi^{(s)} = e^{-i\omega t}e^{im\phi}\Phi^{(s)}_{lm\omega}(r)S_{lm\omega}(\theta). \tag{2.55}$$

Then, the radial (homogeneous) equation reads:

$$\Delta_r^{-s}\partial_r\left[\Delta_r^{s+1}\partial_r\Phi^{(s)}(r)\right] + H(r)\Phi^{(s)}(r) = 0 \tag{2.56}$$

and the angular equation is

$$0 = \Bigg[(a\omega\cos\theta)^2\frac{\Xi}{\Delta_\theta} - 2sa\omega\cos\theta\frac{\Xi}{\Delta_\theta} + s + \hat{\Lambda}_{\omega lm} - \left(m + s\cos\theta\frac{\Xi}{\Delta_\theta}\right)^2\frac{\Delta_\theta}{\sin^2\theta} - 2\delta_s\frac{a^2}{L^2}\sin^2\theta\Bigg]S^{(s)}_{\omega lm}(\theta) + \frac{1}{\sin\theta}\partial_\theta\left(\sin\theta\Delta_\theta\partial_\theta S_{lm\omega}\right), \tag{2.57}$$

where

$$\Delta_r = (r^2+a^2)\left(1+\frac{r^2}{L^2}\right) - 2Mr\,, \quad \Xi = 1-\frac{a^2}{L^2}\,, \quad \Delta_\theta = 1-\frac{a^2}{L^2}\cos^2\theta, \tag{2.58a}$$

$$H(r) = \frac{K_T^2 - is\Delta_r' K_T}{\Delta_r} + 2isK_T' + \frac{s+|s|}{2}\Delta_r'' - \hat{\lambda}_{\omega lm} - |s|(|s|+1)(2|s|-1)(2|s|-7)\frac{r^2}{3L^2} - |s|(|s|-2)(4s^2-12|s|+11)\frac{a^2}{3L^2}, \tag{2.58b}$$

$$K_T = \omega(r^2+a^2) - ma\left(1+\frac{r^2}{L^2}\right), \tag{2.58c}$$

$$\hat{\lambda}_{\omega lm} = \hat{\Lambda}_{\omega lm} - 2am\omega + a^2\omega^2 + s + |s|, \tag{2.58d}$$

$\hat{\Lambda}_{\omega lm}$ is a separation constant and $\delta_s = 1$ for $s \neq 0$ and $\delta_s = 0$ for $s = 0$.

Since we want the perturbation to be invariant under $\partial_t + \Omega\partial_\phi$, we only consider fields satisfying $\omega = \Omega m$. Given $m \in \mathbb{Z}$, one first solves (2.57) (treating it as an eigenproblem for $\hat{\Lambda}_{\omega lm}$) and then inserts the obtained values of that constant into the radial equation (2.56). This equation for the extremal Kerr AdS has a regular singular point at $r = r_+$. Thus, one finds that $\Psi_0 \sim (r-r_+)^\gamma$ and $\Psi_4 \sim (r-r_+)^{\gamma'}$.[12] As usual, there are two possible values of γ and γ' - one is always negative, so must be discarded. In general, $s = 2$ modes (which describe the perturbation of Ψ_0) have smaller exponent. Their values for the $\ell = 2, m = 0$ mode are depicted in Fig. 2.2. It is clear that this particular mode is always divergent. Since Ψ_0 measures the tidal forces in the direction transversal to the horizon, this is the same type of singularity as the one encountered for static black holes. In general, increasing ℓ increases γ, so $\ell = 3, m = 0$ mode is non-singular for small black holes. If $m \neq 0$, γ may become complex (even with $\Lambda = 0$) – this is a sign of the superradiant instability.

For completeness, let us discuss what happens when one changes the cosmological constant. For simplicity, we restrict to $m = 0$ perturbations. In the Ricci flat $\Lambda = 0$ case, all the exponents are (with reasonable accuracy) integers. For $\Lambda > 0$, we found all γ to be positive (at least while real). Thus, Kerr (dS) seems to be free of this type of singularity at the horizon. However, even a small charge appears to change this conclusion. In the Kerr-Newman dS background, the electromagnetic and gravitational perturbations are intertwined. On the neutral background, the former has a smaller scaling dimension γ. Since introducing a small charge will not change its value too much, it follows that this will cause diverging curvature for Kerr-Newman dS black holes. At the same time, when the cosmological constant vanishes, both scaling dimensions remain integer and thus no singularity develops.

[12] Note that here γ, γ' denote the exponents for the curvature perturbation, not the metric perturbation.

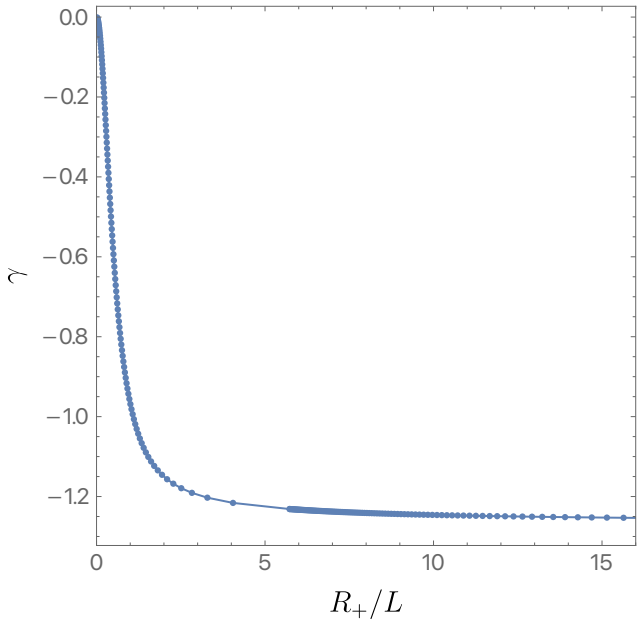

FIGURE 2.2: Curvature exponent γ as a function of the area radius, R_+/L, for the $\ell = 2$, $m = 0$ mode of extremal Kerr AdS. The fact that it is negative shows that the curvature diverges on the horizon.

2.4 Einstein-Maxwell theory beyond the linear approximation

2.4.1 Numerical scheme

To construct solutions at nonzero T, we will work directly in Bondi-Sachs coordinates. The reason for this is two-fold: 1) in Bondi-Sachs coordinates there are no non-analyticities near the conformal boundary, and we thus expect numerical methods to exhibit stronger convergence properties; 2) we need to work in a coordinate system where ingoing null geodesics are easy to determine so that one can easily calculate tidal force singularities. Our work will roughly follow [14, 23], but with some important differences.

We thus take the following metric and gauge field Ansätze

$$\begin{aligned} \mathrm{d}s^2 = \frac{L^2}{y^2}\Bigg\{ &-(1-y)(1+y\,A_1)\frac{\mathrm{d}v^2}{L^2} - \frac{2\,\mathrm{d}v\,\mathrm{d}y}{L} \\ &+ A_2\left[A_3\left(\mathrm{d}x + \frac{A_4(1-y)\sin x\,\mathrm{d}v}{L}\right)^2 + \frac{\sin^2 x}{A_3}\mathrm{d}\phi^2\right]\Bigg\}, \end{aligned} \tag{2.59a}$$

$$A = (1-y)A_5\mathrm{d}v + L\,\sin x\,A_6\,\mathrm{d}x\,, \tag{2.59b}$$

where all A_i are functions of (x, y) and ϕ is a periodic coordinate with $\phi \sim \phi + 2\pi$. Note that $x \in [0, \pi]$ is an angular coordinate and $y = [0, 1]$ is a radial coordinate, with $x = 0, \pi$ being the poles of the two-sphere and $y = 0, 1$ being the conformal boundary and black hole event horizon, respectively. We note that $\partial/\partial y$ is *globally* null and is thus a physical coordinate with respect to which one can easily compute tidal force singularities by looking at certain components of the Weyl tensor in (v, y, x, ϕ) coordinates.

It remains to explain how Eqs. (2.59) together with the Einstein-Maxwell equations give rise to a well-defined system of Elliptic equations which can be solved using standard numerical methods, such as the ones in [37].

Instead of using the trace-reversed version of the Einstein equation, we are going to use the Einstein equation itself. The reason for this is that we will take advantage of the constraint equations to proceed. We thus consider the following equations of motion

$$E_{\mu\nu} \equiv R_{\mu\nu} - \frac{R}{2} g_{\mu\nu} - \frac{3}{L^2} g_{\mu\nu} - 2\left(F_{\mu\alpha} F_{\nu}{}^{\alpha} - \frac{g_{\mu\nu}}{4} F_{\alpha\beta} F^{\alpha\beta} \right) = 0 \,, \tag{2.60a}$$

$$P_{\mu} \equiv \nabla^{\nu} F_{\nu\mu} = 0 \,. \tag{2.60b}$$

Note that we have more independent components of the Einstein equations than variables to solve for. We thus need to choose a subset of the equations and show that, given appropriate boundary conditions, the remaining equations are solved. We thus label the equations we actually solve for as dynamical, and the ones that are enforced via the Bianchi identities as constraints (in analogy with the constraint and dynamical equations of the initial value problem in general relativity).

For dynamical equations we take $E^{\mu\nu}$ and P^{μ} with $\mu = \{v, x, \phi\}$. This gives us exactly six equations to solve for within our symmetry class. For the constraint equations, we take $E^{y\mu}$ and P^{y}. Now, we would like to show that if we impose $E^{y\mu}$ and P^{y} at either $y = 0$ or $y = 1$, then by virtue of the dynamical equations and the Bianchi identities, the constraint equations $E^{y\mu}$ and P^{y} should be satisfied everywhere[13]. This is a relatively simple exercise that we leave to the reader. We do, however, have to check that the dynamical equations form a well-posed Elliptic problem. This, in particular, means that near each boundary we must have a number of free constants of integration that matches the order of the differential equation. That is to say, near the conformal boundary and black hole event horizon, we expect to find six functions of integration.

In four spacetime dimensions, when using Bondi-Sachs coordinates and focusing on the Einstein-Maxwell equations, one can show that the asymptotic expansion of the A_i functions near the boundary is a power-law in y. As such, we take

$$A_i(x, y) = \sum_{I=0}^{+\infty} y^I A_i^{(I)}(x) \,. \tag{2.61}$$

As boundary conditions we impose

$$A_2(x,0) = A_3(x,0) = 1 \,, \quad A_4(x,0) = A_6(x,0) = 0 \,, \quad \text{and} \quad A_5(x,0) = \mu(x) \,, \tag{2.62}$$

with $\mu(x)$ being our boundary chemical potential. Note that we have not yet detailed what boundary condition we take for A_1. One can input the above expansion in the dynamical equations and work out which coefficients are left free. It turns out that all remaining coefficients are uniquely fixed in terms of $\mu(x)$ and

$$\left\{ A_1^{(0)}(x), A_1^{(1)}(x), A_1^{(2)}(x), A_3^{(3)}(x), A_4^{(3)}(x), A_5^{(1)}(x), A_6^{(1)}(x) \right\} \tag{2.63}$$

and their derivatives with respect to x. These are seven free functions (once we fix $\mu(x)$), and thus one too many with respect to what we are expecting. To remove this

[13] It might appear confusing that we only need to impose the constraint at a single boundary, but this is the result of the Bianchi identities being first order in $E_{\mu\nu}$.

redundancy we impose the constraint equation E^{yv} asymptotically. This constraint then imposes

$$\left.\frac{\partial A_1}{\partial y}\right|_{y=0} = \frac{1}{4}\left[5 + 2A_1(x,0) + A_1(x,0)^2\right] , \tag{2.64}$$

which fixes $A_1^{(1)}(x)$ in terms of $A_1^{(0)}(x)$. We thus have the expected number of integration functions near the conformal boundary and have imposed one of the constraint equations.

We now turn our attention to the black hole event horizon located at $y = 1$. The powers of $(1-y)$ in the Ansatz for the gauge field and metric (see Eqs. (2.59)) were chosen in such a way that P^y and E^{yx} are automatically satisfied at the black hole event horizon. The savvy reader will note that we have not yet imposed E^{yy}, but we shall shortly. We again expand all equations in power series in $(1-y)$ near the black hole event horizon

$$A_i(x,y) = \sum_{I=0}^{+\infty} (1-y)^I \tilde{A}_i^{(I)}(x) . \tag{2.65}$$

We also impose E^{yy} at the horizon, which demands that $\tilde{A}_1^{(0)}$ be a constant. In fact, if we set

$$\tilde{A}_1^{(0)} = T_0 - 1 \tag{2.66}$$

we find that the black hole temperature is given by

$$4\pi L T = T_0 . \tag{2.67}$$

All coefficients appearing in the expansion near the horizon Eq. (2.65) are uniquely fixed in terms of T_0 and

$$\left\{\tilde{A}_1^{(1)}(x), \tilde{A}_2^{(0)}(x), \tilde{A}_3^{(0)}(x), \tilde{A}_4^{(0)}(x), \tilde{A}_5^{(0)}(x), \tilde{A}_6^{(0)}(x)\right\} , \tag{2.68}$$

which is precisely the number of expected integration constants near $y = 1$.

All we need to discuss are the axes of symmetry, located at $x = 0, \pi$. We will focus on $x = 0$, but $x = \pi$ has identical boundary conditions. Since we want ϕ to have period 2π, we must demand $A_3(0,y) = A_3(\pi,y) = 1$. Regularity at the axis further imposes

$$\left.\frac{\partial A_i}{\partial x}\right|_{x=0} = 0 . \tag{2.69}$$

One can check that the above boundary conditions are consistent with the constraint equations, and provide the right number of integration functions near the axis of symmetry. We have thus sketched in some detail that our dynamical equations, together with our choice of boundary conditions, enforce the constraint equations and give rise to a well-posed Elliptic problem.

Before presenting the results, we shall detail a little about the numerical method we used. Since the functions A_i develop enormous gradients close to the black hole event horizon as $T \to 0$, we discretize the integration domain into two patches $[0, y_c] \cup [y_c, 1]$. Chebyshev-Gauss-Lobatto grids are placed in each patch using transfinite interpolation (see [37]). At the patch boundaries, we require the metric and its first derivative to be continuous (continuity of the remaining derivatives is then enforced via the equations of motion). We then implement a standard Newton-Raphson routine, solving each linear iteration via a LU decomposition. Since large gradients develop near the horizon, we typically take $y_c = 0.95$. On the patch near the event horizon, we had to resort to enormous resolutions (with more than 100

points in the y direction) to resolve the gradients and achieve convergence. With these high resolutions, we were able to reach as low as $4\pi LT = 10^{-3}$.

2.4.2 Results

For the boundary profile, we take

$$\mu(x) = \bar{\mu} + \mu_1 \cos x \,. \tag{2.70}$$

This corresponds to a dipole-type perturbation, where the inhomogeneous component of the chemical potential is given entirely in terms of an $\ell = 1$ harmonic on the round two-sphere.

The most interesting quantity to plot is the $C_{\rho\phi\rho\phi}$ component of the Weyl tensor evaluated on the event horizon, *i.e.* at $y = 1$, for which the scaling given in Eq. (2.28) should apply. In Bondi-Sachs coordinates, this component is simply given by

$$C_{\rho\phi\rho\phi} = -\frac{\sin^2 x}{2y^2 A_3^2}\left[\frac{A_2}{A_3}\left(\frac{\partial A_3}{\partial y}\right)^2 - \frac{\partial A_2}{\partial y}\frac{\partial A_3}{\partial y} - A_2\frac{\partial^2 A_3}{\partial y^2}\right] . \tag{2.71}$$

In Fig. 2.3 we plot the maximum value of $C_{\rho\phi\rho\phi}$ on the black hole event horizon, *i.e.* $\max_{\mathcal{H}^+} C_{\rho\phi\rho\phi}$, as a function of $4\pi TL$ in a log-log scale, for fixed values of $\bar{\mu} = 2$ and $\mu_1 = 0.1$. We have tried other values of $\bar{\mu}$ and μ_1 and the results remain qualitatively similar. If the scaling given in Eq. (2.28) holds, we should see a straight line in a log-log plot appearing at low T. This appears evident from Fig. 2.3. Furthermore, the slope of this linear behavior should be given precisely by $\gamma - 2$, with γ being computed by the limiting Q at zero temperature. We can extract such Q from the numerical results via a linear fit

$$\frac{G_4 Q}{L} = q_0 + q_1 T \tag{2.72}$$

in the range $4\pi TL \in [10^{-3}, 10^{-2}]$. We find $q_0 \approx 2.00181$ which, as expected is very close to $\bar{\mu}$, since μ_1 is small. This is the value of Q that controls the smallest value of γ. This occurs for the $\ell = 2$ mode with the minus sign in Eq. (2.39a). For this value of Q, we find $\gamma \approx 0.122025$. On the other hand, the solid black line in Fig. 2.3 is well fit by a function of the form

$$a_0 T^{\tilde{\gamma}-2} \tag{2.73}$$

and via a fit in the region $4\pi T \in [10^{-3}, 10^{-2}]$ we find $\tilde{\gamma} \approx 0.122401$ and $a_0 \approx 0.00166763$. The agreement between γ computed with the limiting value of Q and according to Eq. (2.39a) and the value extracted from the fit ($\tilde{\gamma}$) is striking: the difference is below 0.5%. Furthermore, we expect the $\ell = 2$ mode to be nonlinearly sourced by the $\ell = 1$ boundary mode. As such, the expectation is that this mode at the horizon must have a magnitude that scales as a power of μ_1. This is precisely what we find for a_0.

We have also looked at curvature invariants, such as the maximum value of the *square* of the Weyl tensor at the black hole horizon. For an extremal RN AdS black hole of *any* size, we find that the square of the Weyl tensor on the horizon $\mathcal{H}^+$ is simply

$$L^4 C^2\Big|_{\mathcal{H}^+} \equiv L^4\, C^{\mu\nu\rho\lambda} C_{\mu\nu\rho\lambda}\Big|_{\mathcal{H}^+} = 48 \,. \tag{2.74}$$

If our linear results are to hold, we should see all curvature invariants approaching their AdS_2 value at small temperatures. In Fig. 2.4 we plot the maximum value of

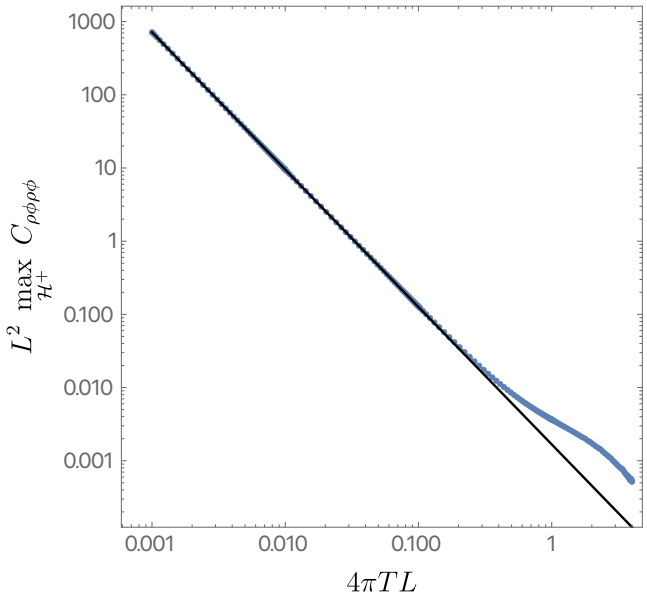

FIGURE 2.3: A plot showing the maximum of $C_{\rho\phi\rho\phi}$ on the horizon as a function of $4\pi TL$, computed for $\bar{\mu} = 2$ and $\mu_1 = 0.1$. The solid black line shows the best fit to the functional form given in Eq. (2.73) in the range $4\pi T \in [10^{-3}, 10^{-2}]$ yielding $\tilde{\gamma} \approx 0.122401$ and $a_0 \approx 0.00166763$. The blue disks correspond to the numerical data points extracted from our simulations.

the square of the Weyl tensor on the black hole event horizon as a function of the temperature in a log-linear plot. The blue disks are the exact numerical results and the dashed black horizontal line is the AdS_2 prediction. Clearly, the square of the Weyl tensor on the horizon not only remains finite as we cool down the system but it also approaches its unperturbed value, as predicted by perturbation theory.

2.5 Nonlinear scalar field model

It is difficult to numerically construct the $T = 0$ limit of the solution in the previous section, or get T low enough to see the anomalous scaling of the specific heat predicted in Sec. 2.3. To remedy this, in this section we consider a simpler model in which both can be achieved. We confirm that the exact $T = 0$ solution has diverging tidal forces as predicted by the linear analysis and that the specific heat has anomalous scaling.

Our model consists of adding $2\ell + 1$ neutral, massless, minimally coupled scalar fields to the Einstein-Maxwell theory. By cleverly choosing their angular dependence, one can keep the stress tensor spherically symmetric, so the metric remains spherical. From the behavior of a test field in Sec. 2.2, we still expect the scalars will develop power-law behavior with non-integer exponents near the horizon which will backreact on the metric.

The scalar fields can be viewed as components of a vector $\vec{\Phi}$:

$$(\vec{\Phi})_m = \phi_m \,, \tag{2.75}$$

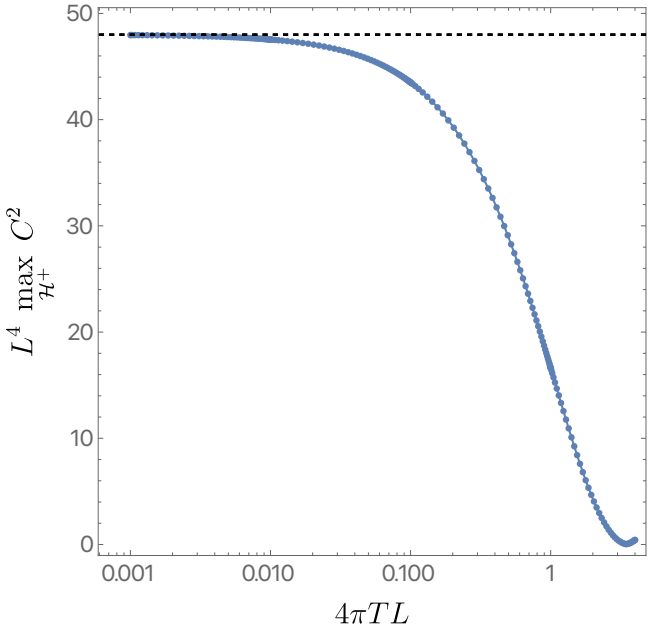

FIGURE 2.4: A plot showing the square of the Weyl tensor on the black hole event horizon as a function of $4\pi TL$, computed for the same black holes as Fig. 2.3. The solid black line shows the AdS_2 prediction of Eq. (2.74). The blue disks correspond to the numerical data points extracted from our simulations.

with $|m| \leq \ell$. The action is then simply

$$S = \frac{1}{16\pi G}\int_{\mathcal{M}} \mathrm{d}^4x\,\sqrt{-g}\left[R + \frac{6}{L^2} - F_{\mu\nu}F^{\mu\nu} - (\nabla_\mu\vec{\Phi})\cdot(\nabla^\mu\vec{\Phi})\right]. \tag{2.76}$$

where $\cdot$ denotes the usual Cartesian dot product between vectors in $\mathbb{R}^{2\ell+1}$ and G is Newton's constant. One could generalize this by adding the same mass to all scalars without changing the conclusion.

The equations of motion derived from (2.76) read

$$\begin{aligned} R_{\mu\nu} - \frac{R}{2}g_{\mu\nu} - \frac{3}{L^2}g_{\mu\nu} = 2\left(F_\mu{}^\alpha F_{\nu\alpha} - \frac{g_{\mu\nu}}{4}F_{\alpha\beta}F^{\alpha\beta}\right) \\ + (\nabla_\mu\vec{\Phi})\cdot(\nabla_\nu\vec{\Phi}) - \frac{g_{\mu\nu}}{2}(\nabla_\alpha\vec{\Phi})\cdot(\nabla^\alpha\vec{\Phi})\,, \end{aligned} \tag{2.77a}$$

$$\nabla^\nu F_{\mu\nu} = 0\,, \tag{2.77b}$$

and

$$\nabla_\mu\nabla^\mu\vec{\Phi} = 0\,. \tag{2.77c}$$

We will focus on static black holes with a spherically symmetric stress-energy tensor. We then introduce ingoing Eddington-Finkelstein coordinates (v, r, θ, ϕ) in which the metric and gauge field take the form

$$\mathrm{d}s^2 = -f(r)\,\mathrm{d}v^2 + 2\,\mathrm{d}v\,\mathrm{d}r + r^2\,p(r)\left(\mathrm{d}\theta^2 + \sin^2\theta\mathrm{d}\phi^2\right), \tag{2.78a}$$

and

$$A = A_v(r)\,\mathrm{d}v \tag{2.78b}$$

with f and p functions of r to be determined by our numerical scheme.

As promised, we would like to retain non-homogeneity in the scalar field, and at the same time ensure that the resulting stress energy-momentum tensor is spherically symmetric. We can achieve this by choosing

$$\phi_m(\hat{r},\theta,\phi) = \phi(r) \times \sqrt{\frac{(\ell-m)!}{(\ell+m)!}} \times P_m^\ell(\cos\theta) \times \begin{cases} \sqrt{2}\,\sin(m\,\phi)\,, & \text{for} \quad m<0 \\ 1\,, & \text{for} \quad m=0 \\ \sqrt{2}\,\cos(m\,\phi)\,, & \text{for} \quad m>0 \end{cases}, \tag{2.79}$$

where $P_m^\ell(x)$ are the standard associated Legendre polynomials. The normalizations are chosen so that

$$\sum_{m=-\ell}^{\ell} \phi_m(r,\theta,\phi)^2 = \phi(r)^2\,. \tag{2.80}$$

We first solve Eq. (2.77b). This is a simple exercise since the scalars are uncharged under the Maxwell field and the solution is spherically symmetric. We thus find

$$A_v'(r) = \frac{Q}{r^2\,p(r)}\,, \tag{2.81}$$

where Q is an integration constant and $'$ denotes differentiation with respect to r. It is a simple exercise to show that in fact Q is the charge of the black hole solutions we seek to construct so long as we demand $\lim_{r\to+\infty} p(r) = 1$. We can use this relation in the remaining Einstein and scalar field equations to eliminate all dependence on A_v. The Einstein and scalar field equations reduce to

$$\frac{(r^2\,p)'}{p}\frac{f'}{f} + \frac{1}{2}\frac{(r^2p)'^2}{r^2p^2} - \frac{6r^2}{fL^2} + \frac{2Q^2}{r^2\,f\,p^2} - \frac{2}{f\,p} + \frac{\ell(\ell+1)\phi^2}{f\,p} - r^2\phi'^2 = 0\,, \tag{2.82a}$$

$$\frac{1}{r^2p}(r^2\,p\,f\,\phi')' - \frac{\ell(\ell+1)}{r^2p}\phi = 0\,, \tag{2.82b}$$

$$\frac{1}{r^2p}(r^2p')' + \phi'^2 - \frac{p'^2}{2p^2} = 0\,. \tag{2.82c}$$

The line element Eq. (2.78a) has residual gauge freedom. Namely, we are free to shift r by a constant. We fix this freedom by demanding $p(r_+) = 1$, where $r = r_+$ is the black hole event horizon (extremal or otherwise) defined by $f(r_+) = 0$.

2.5.1 Zero temperature results

For zero-temperature black holes, we want $f(r)$ to have a double zero at the black hole horizon $r = r_+$. We shall also assume that near the horizon $\phi \propto (r-r_+)^\gamma$ for some power $\gamma > 0$ to be determined shortly. From Eq. (2.82a) it easy to see that the requirement that f has a double zero at $r = r_+$ implies

$$Q = r_+\sqrt{1+\frac{3\,r_+^2}{L^2}}\,. \tag{2.83}$$

We thus choose this value throughout and parameterize our extremal black holes by $r_+/L > 0$.

We now write

$$f = f_0(r-r_+)^2\,(1+\delta f)\,, \tag{2.84}$$

where δf is a function we wish to determine next as a function of γ. The first non-trivial order in Eq. (2.82a) determines f_0 as a function of r_+, and we find

$$f_0 = \frac{L^2 + 6r_+^2}{L^2 r_+^2} = \frac{1}{L_2^2}\,. \tag{2.85}$$

where L_2 is the AdS_2 radius. The next to leading order terms in Eq. (2.82a) determine δf. The leading contribution to δf is of the form

$$(r - r_+)^2 \delta f' \;\propto\; (r - r_+)^{2\hat{\gamma}+1} \Rightarrow \delta f \;\propto\; (r - r_+)^{2\hat{\gamma}}\,, \tag{2.86}$$

where $\hat{\gamma} = \min(\gamma, 1/2)$.

Similarly, p admits an expansion

$$p = 1 + p_1 (r - r_+)^{2\hat{\gamma}}\,, \tag{2.87}$$

where p_1 is a known constant. For $\gamma = 1/2$, there are logarithmic terms appearing in the expansions of both f and p.

It remains to determine γ. These we read off from the scalar equation, which to leading order off the extremal horizon yield

$$\gamma = \frac{1}{2}\left[\sqrt{1 + \frac{4\ell(\ell+1)}{1 + 6\,y_+^2}} - 1\right]\,, \tag{2.88}$$

where y_+ is again the dimensionless radius $y_+ \equiv r_+/L$. Note that this agrees with the linear result (2.9).

To proceed numerically, we introduce a compact coordinate

$$r = \frac{r_+}{1 - y} \tag{2.89}$$

so that the extremal horizon is located at $y = 0$, whereas the conformal boundary is located at $y = 1$. To implement our boundary conditions, we also define

$$f(r) \equiv \frac{(r - r_+)^2 \left(L^2 + r^2 + 3r_+^2 + 2rr_+\right)}{L^2 r^2} q(r)\,. \tag{2.90}$$

and regard q, ϕ and p as functions of y. The boundary conditions are now simply $q(0) = 1$, $\phi(0) = 0$, $p(0) = 1$ at the extremal horizon. At the conformal boundary we demand $q(1) = 1$, $\phi(1) = V$ and $p(1) = 1$. The conditions on q and p just ensure that the spacetime is asymptotically AdS. V is the amount that we turn on the scalars asymptotically. If there were a holographic dual to this theory, V would be the source of the operator dual to ϕ.

After obtaining the exact solution, we extract the exponents by computing logarithmic derivatives as a function of radius

$$\gamma_y(y) \equiv \frac{y}{\phi}\frac{\mathrm{d}\phi}{\mathrm{d}y} \quad \text{and} \quad \tilde{\gamma}_y(y) \equiv \frac{y}{p-1}\frac{\mathrm{d}p}{\mathrm{d}y} \tag{2.91}$$

If our linear analysis is accurate, we expect $\gamma_y(0) = \gamma$ and $\tilde{\gamma}_y(0) = 2\gamma$ if $\gamma < 1/2$. If $\gamma > 1/2$, we expect $\tilde{\gamma}_y(0) = 1$. In this case, even though the leading correction to the metric looks smooth, at the next order there are fractional powers that make the horizon singular. The results are shown in Fig. (2.5) as a function of y for $\ell = 1$ and $V = 1$. On the top row we have $\gamma = 1/4$ ($y_+ = 3/\sqrt{10}$), whereas on the

bottom row we have $\gamma = 3/4$ ($y_+ = \sqrt{11/126}$). On the left column, we plot $\gamma_y(y)$, whereas on the right column, we plot $\tilde{\gamma}_y(y)$. The numerical data is represented in blue, and the linear analytic prediction is given as a red disk at $y = 0$. The agreement between the numerical results and the analytic analysis is reassuring and shows that, despite starting the scalars with magnitude one asymptotically and having a horizon singularity, the linear near horizon calculation is reproduced at the non-linear level. Note that our boundary conditions at no point assumed power law decay. Indeed, our boundary conditions assumed only that $\phi(r_+) = 0$ and that $p(r_+) = q(r_+) = 1$. In this sense, our nonlinear confirmation of the linear results is non-trivial.

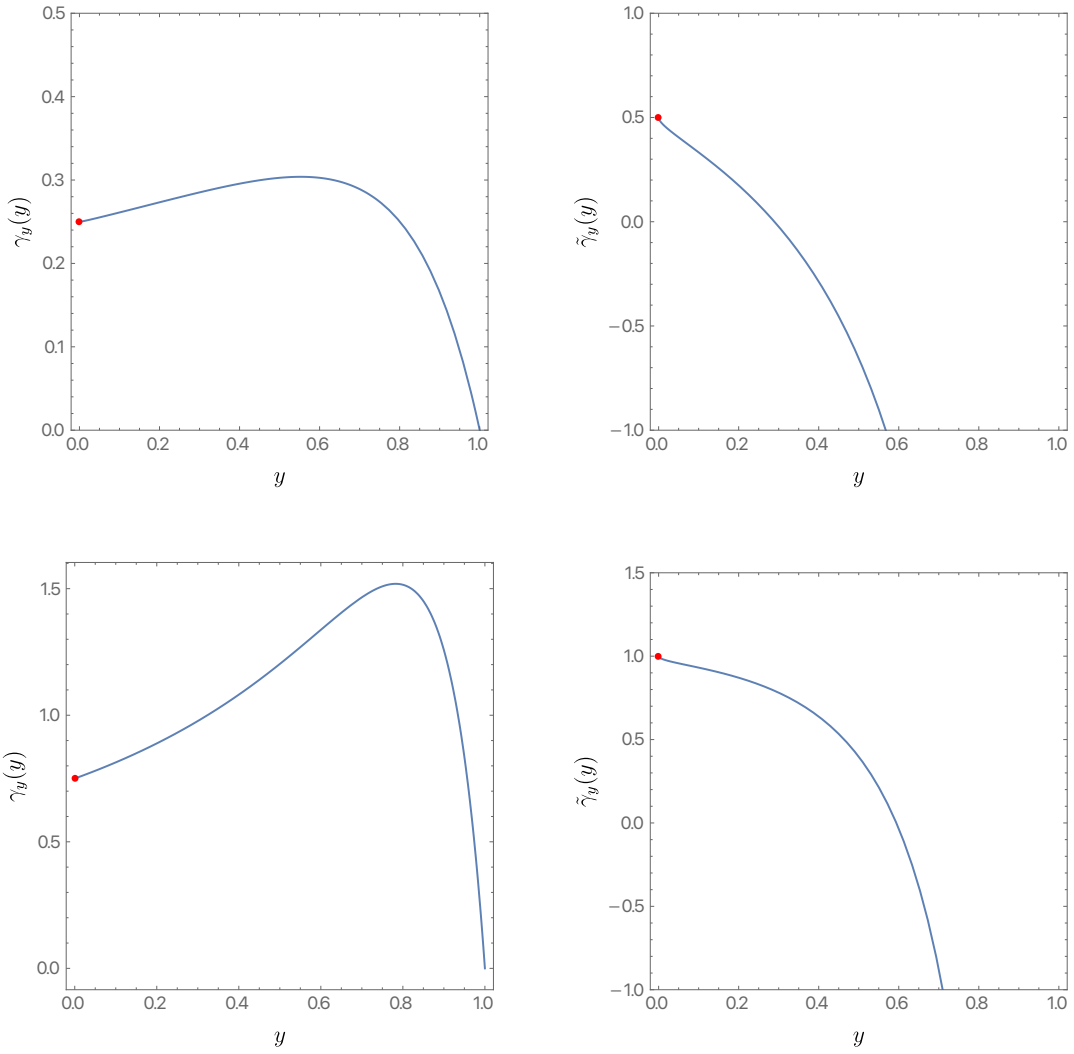

FIGURE 2.5: **Left column**: Plots of $\gamma_y(y)$ as a function of y. **Right column**: Plots of $\tilde{\gamma}_y(y)$ as a function of y. The top row has $\gamma = 1/4$ and the bottom row has $\gamma = 3/4$. In all cases, $\ell = 1$ and $V = 1$. The red dots denote the scaling exponents derived from the linear analysis.

2.5.2 Non-zero temperature results

Having discussed the zero temperature limit, we now turn our attention to the non-extremal case. In particular, in this section, we aim to show that whenever the linear analysis predicts $\gamma < 1/2$, the specific heat at constant charge Q, *i.e.* C_Q, will show

a leading *anomalous scaling* in the small temperature expansion. In particular, according to the general arguments established in section 2.3.2 we expect the leading behavior at small T of the specific heat to be $C_Q \propto T^{2\gamma}$.

We will again use the ingoing Eddington-Finkelstein coordinates of (2.78a). Since we want a non-degenerate horizon we demand that f has a simple zero at $r = r_+$. Under this assumption, Eq. (2.82a) and Eq. (2.82b) develop a regular singular point at $r = r_+$. To implement the boundary conditions we define

$$f(r) = \left(1 - \frac{r_+}{r}\right)\left(\frac{r^2}{L^2} + 1 + \frac{r_+ r}{L^2} + \frac{r_+^2}{L^2} - \frac{Q^2}{r\, r_+}\right) q(r)\,. \tag{2.92}$$

Again, we introduce a compact coordinate as in Eq. (2.89), and regard q, ϕ, and p as functions of y, with $y = 0$ being the location of the event horizon and $y = 1$ the conformal boundary.

At the conformal boundary we demand $q(1) = p(1) = 1$ and $\phi(1) = V$, just like we did for the extremal case. We are thus left with specifying the boundary conditions at the event horizon. Since $r = r_+$ is a regular singular point of Eq. (2.82a) and Eq. (2.82b), the boundary conditions for q and ϕ follow from demanding regularity at $r = r_+$ and in particular yield

$$q(0)\left(\left.\frac{\mathrm{d}p}{\mathrm{d}y}\right|_{y=0} + 2\right) = \left[2 - \frac{y_+^2\,\ell(\ell+1)\phi(0)^2}{y_+^2 + 3y_+^4 - \tilde{Q}^2}\right] \tag{2.93a}$$

and

$$\left.\frac{\mathrm{d}\phi}{\mathrm{d}y}\right|_{y=0} = \frac{y_+^2\,\ell(1+\ell)\phi(0)}{\left(y_+^2 + 3y_+^4 - \tilde{Q}^2\right) q(0)}\,, \tag{2.93b}$$

where we defined $y_+ \equiv r_+/L$ and $\tilde{Q} = Q/L$. For $p(y)$, we again demand $p(0) = 1$.

Having determined the boundary conditions, we can now readily compute all quantities of interest. We are particularly interested in the behavior of the specific heat at constant charge C_Q. This is obtained via the usual thermodynamic relation

$$C_Q = T\left(\frac{\partial S}{\partial T}\right)_Q\,. \tag{2.94}$$

In order to determine C_Q as a function of T, we need to find the entropy S and temperature T of our novel black holes. These are given by

$$S = \frac{\pi\, y_+^2\, p(0)}{G} L^2 \quad \text{and} \quad \tilde{T} \equiv L\,T = \frac{y_+^2(1+3y_+^2) - \tilde{Q}^2}{4\pi y_+^3} q(0)\,. \tag{2.95}$$

The strategy is clear: we hold fixed a particular value of $\tilde{Q}$, and decrease y_+ thus decreasing the temperature. The expected low-temperature scaling depends on γ which is uniquely determined by $\tilde{Q}$. So we can predict γ from the onset. It remains then to check whether C_Q does exhibit the scaling predicted in section 2.3.2. For an RN AdS black hole, it is relatively easy to check that

$$\frac{G\, C_Q^{\mathrm{RN}}}{L^2} = \frac{2\pi y_+^2}{3\tilde{Q}^2 - y_+^2 + 3y_+^4}\left[y_+^2\left(1 + 3y_+^2\right) - \tilde{Q}^2\right] \tag{2.96}$$

and thus near $\tilde{T} \approx 0$ we find

$$\frac{G\, C_Q^{\rm RN}}{L^2} \approx \frac{\pi^2}{3}\sqrt{\frac{2}{3}}(1+12\tilde{Q}^2)^{1/4}\left(1-\frac{1}{\sqrt{1+12\tilde{Q}^2}}\right)^{3/2}\tilde{T}+\mathcal{O}(\tilde{T}^2) \tag{2.97}$$

In Fig. 2.6 we plot the logarithmic derivative of C_Q, at constant charge Q, with respect to T. This particular data was collected for $\ell = 1$, $\gamma = 1/4$, and thus $\tilde{Q} = 3\sqrt{37}/10$. Furthermore, we have chosen $V = 1/2$. The purple disks are the numerical data, the solid black curve is given in Eq. (2.96) for the same charge $\tilde{Q}$ and the red horizontal line shows $1/2$ and is there to guide the eye. We can see that the logarithmic derivative approaches $2\gamma = 1/2$ at low temperatures, as expected from our scaling in section 2.3.2. For smaller values of V we need to resort to (even) smaller temperatures to see the scaling emerging at small T. We have probed other values of $\tilde{Q}$ and find that whenever $\gamma < 1/2$, we see an anomalous scaling. For $\gamma > 1/2$, we return to the standard AdS_2 linear scaling given in (2.97).

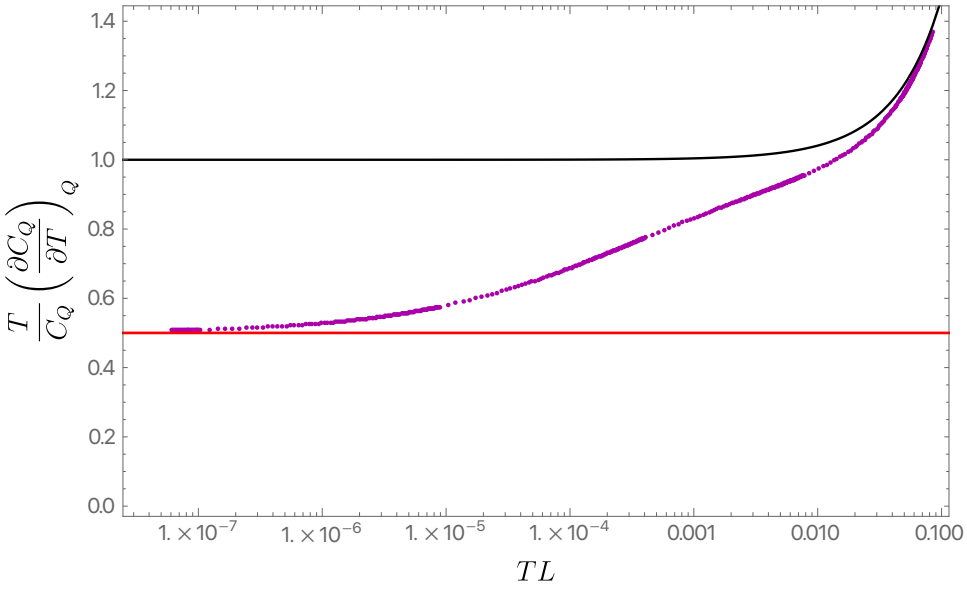

FIGURE 2.6: Logarithmic derivative of C_Q, at constant charge Q, with respect to T. For the data shown we have used $\ell = 1$ and $Q/L = 3\sqrt{37}/10$. The anomalous scaling predicted in section 2.3.2 is marked as a horizontal red line showing $2\gamma = 1/2$, the purple disks are the exact numerical data collected at finite temperature and the solid black line shows the standard AdS_2 result of Eq. (2.96).

2.6 Discussion

We have seen that as soon as one breaks the usual spatial symmetry, almost all stationary black holes in AdS_4 develop curvature singularities on their horizon in the extremal limit. (The main exceptions are small toroidal black holes.) This singularity results in infinite tidal forces for infalling observers. Contrary to the usual situation where the horizon curvature increases when the black hole becomes smaller, this singularity becomes stronger when the black hole becomes larger. Since the singularity arises in the limit of a family of smooth black holes, the solution is clearly physical [53], and not like the singularity of $M < 0$ Schwarzschild.

The diverging tidal forces close to the horizon should be proportional to the deviation from spherical symmetry at infinity. Thus, one could be tempted to infer that (close to the spherical symmetry) the physical effects are negligibly small, despite the null singularity. However, to properly account for e.g. the *total* deformation an infalling observer experiences, one should look at the integrated tidal forces rather than their pointwise values. If the scaling dimension of the metric perturbation satisfies $\gamma > 1$, the forces are integrable, so the deformation would be finite and indeed small for the boundary conditions close to the spherical symmetry. However, for $\gamma < 1$, the forces are not integrable. Thus, the total deformation remains infinite for arbitrary small deviations from the spherical symmetry. In particular, this is the case for RN AdS of any charge and for sufficiently large Kerr AdS black holes.

Many supersymmetric solutions have been found in AdS with smooth horizons.[14] However, if one deforms the boundary conditions slightly, supersymmetry will be broken and we expect that the horizon will become singular. (We have checked this explicitly in one case.) So supersymmetric solutions are very special, like Reissner-Nordström, and do not see these singularities.

The Einstein-Maxwell theory that we studied can be embedded in supergravity in different ways. In some embeddings, there are charged scalars with mass m and charge q. Depending on (m, q), there may be a range of r_+ in which the extremal black hole is unstable to turning on the scalar field [34]. In this case, the singularity is likely to become much worse, as we will see in the $\Lambda = 0$ case in Sec. 4.4. However, even with charged scalars, there is usually a space of parameters for which there is no instability to turning on the scalar field, and in those cases, our tidal force singularity will remain. (An extensive discussion of the near-horizon scaling dimensions of supergravity fields is given in [22].)

It is natural to ask how stringy or quantum effects will modify this singularity. Although we cannot fully answer this at the moment, let us make the following comments. Infalling strings will certainly become excited by the large tidal forces and should backreact on the geometry. Quantum effects are often discussed in the context of Euclidean theory. To this end, let us focus for a moment on static solutions since they have a real Euclidean analytic continuation.[15] In the extremal limit, the horizon moves off to infinity and becomes another asymptotic boundary to the Euclidean solution. All curvature invariants of the Euclidean solution are the same as the Lorentzian solution. Since the latter remains finite, and the Euclidean curvature is completely determined by its scalar invariants, the Euclidean solution is completely nonsingular! The only remnant of the tidal force singularity seen in the Lorentzian solution is that the solution decays with noninteger powers of the radius in the asymptotic region associated with the horizon. But that also occurs near the boundary at infinity for most massive fields in AdS and does not cause any problems. Thus there is no reason to discard these solutions. In particular, they are proper saddles for the Euclidean path integral with appropriate boundary conditions. It follows, that such black holes may be also prepared (as quantum states) using the Euclidean path integral.

As we have discussed, when these tidal force singularities are strong enough, there is a clear signal of them in a holographic dual theory. Various quantities such as the specific heat will exhibit anomalous scaling with temperature as $T \to 0$. For topologically spherical, charged black holes, this applies whenever the black hole is

[14] See [94] for an example of a supersymmetric solution with a singular horizon.

[15] The Maxwell field will also remain real if we consider the magnetic rather than electrically charged solutions. Since the four-dimensional Maxwell stress tensor is symmetric with respect to exchanging magnetic and electric fields, the metric remains the same.

larger than roughly the AdS radius. We have also discussed two examples of extreme black holes in pure gravity: Kerr AdS and hyperbolic black holes. These black holes exhibit more mild singularities which holographically appear in anomalous higher-order corrections to the leading (linear in T) behavior of the specific heat. DC resistivity also exhibits power law behavior dictated by the scaling dimensions we found [57].

Finally, there is an interesting holographic argument that a singularity should perhaps be expected on the horizon of an extremal black hole and not be resolved by quantum effects.[16] The entanglement wedge of the entire boundary of an extremal black hole only covers the region of spacetime outside the horizon (that becomes a Cauchy horizon in the extremal limit). Since there is no other boundary, it appears that the region inside the horizon cannot be described in terms of the dual theory. If the theories are really equivalent, then perhaps spacetime should end at a singular horizon. Note that this argument does not depend on having a timelike singularity inside the black hole. The event horizon is a Cauchy horizon for any complete spacelike surface outside the black hole.

There is still a lot for me (and, hopefully, for an interested Reader) to understand, for example, what happens in supergravity theories. Probably the most important question is connected with the recent developments regarding nearly extremal black holes' entropy [72] (see also [16] for the supersymmetric part of this story). These highly sophisticated calculations start with the dimensional reduction to the JT gravity (with many matter fields). Although the authors do not ignore Kaluza-Klein modes in their path-integral calculations, they assume that those modes are not sourced. As we have seen, at least classically, when they are sourced they may drastically change the thermodynamics of the system. A naive calculation shows that (as $T \to 0$) they are more important than the classical Schwarzian but less significant than the quantized one. It is not clear what will happen with the Kaluza-Klein modes when we will treat them quantum-mechanically as well. Moreover, the scaling dimensions of those modes depend on the black hole's charge. This begs the question of how to describe them in the holographic (one-dimensional) dual.

Let me end this chapter by emphasizing that the arguments presented here are mainly geometric in nature. The fact that all (weak) fields exhibit a power-law behavior close to the extremal horizon is independent of any equations of motion and comes simply from the fact that *any* near-horizon geometry is scale invariant. Only the values of the exponent are to be determined from the dynamics. Thus, we may expect similar behavior in other dimensions, in theories with more derivatives or more matter fields. In retrospect, it seems almost necessary that generic extremal black holes are non-smooth and it is rather a mystery why all four-dimensional examples without a cosmological constant are perfectly regular.

[16] I am grateful to Leonel Queimada for suggesting this during our ride from Davis to Santa Barbara.

Chapter 3

A deformed IR

3.1 Introduction

It has been said already a few times in this Thesis that the dual of a thermal state of a field theory at temperature T and chemical potential μ is described by an asymptotically anti-de Sitter (AdS) charged black hole [56]. Assuming that the spherical symmetry, the black hole is obviously given by the Reissner-Nordström (RN) AdS solution. Since another tenet of holography is that the radial direction corresponds to an energy scale in the field theory [97], the IR behavior of the theory is described by the near-horizon limit of the extremal solution, which for RN AdS is $AdS_2 \times S^n$.

In four bulk dimensions, $AdS_2 \times S^2$ remains the near-horizon geometry of the extremal black hole even if one deforms the chemical potential or the boundary metric to a static, non-spherical configuration [66]. (For smooth horizons, it has been shown that the only static near-horizon solutions in Einstein-Maxwell theory are $AdS_2 \times H$ where H is a space of constant curvature, i.e., a sphere, torus, or a compact Riemann surface [82]. Even though this theorem does not apply to generic non-spherical solutions since the horizon is singular, the conclusion still holds as follows from the previous Chapter.) Intuitively, this is because the extremal horizon is infinitely far away from any effect outside the horizon (along a static surface). From the dual field theory perspective, $AdS_2 \times S^2$ describes a stable IR fixed point. Note that we are not referring to dynamical stability, but rather stability in the RG sense, which is a property of the space of static solutions. It is widely believed that in higher dimensions, $AdS_2 \times S^n$ similarly describes a stable IR fixed point.

We will show that this common belief is incorrect. For all $n > 2$, generic static non-spherical perturbations of $AdS_2 \times S^n$ blow up on the horizon, even though the horizon is still infinitely far away. We will construct a new near-horizon geometry in $D = n + 2 = 5$ that is invariant under only $SO(3)$ (and not $SO(4)$) symmetry and show that it is stable to $SO(3)$-preserving perturbations. In addition, we construct an open set of non-extremal, $SO(3)$-invariant black holes and show that as $T \to 0$, they approach our new near-horizon geometry. This shows that, within this symmetry class, our new solution is a stable IR fixed point for four-dimensional holographic theories. Of course, $SO(4)$-symmetry is a special point in our class, and if one imposes it, one still flows to $AdS_2 \times S^3$, but this is now seen as an unstable fixed point. This is illustrated in Fig. 3.1.

There is actually a one-parameter family of these new IR geometries which are conveniently labeled by the total charge Q. While we do not have analytic expressions for the new solutions, we can construct them numerically and (for small Q) check them with an analytic perturbative expansion. When Q is small, the solutions are close to $AdS_2 \times S^3$. However, as Q increases, the curvature near the poles of the S^3 decreases so the sphere becomes flattened. For even larger Q, this curvature becomes negative. In the limit $Q \to \infty$ the curvature near the poles approaches a

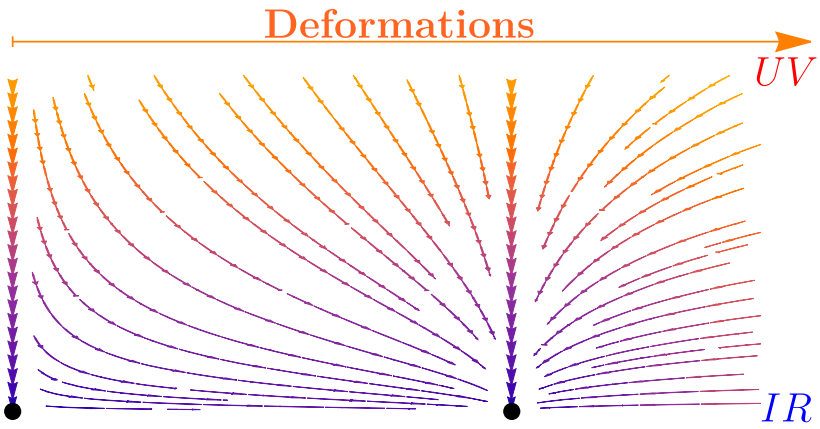

FIGURE 3.1: Illustration of stable and unstable fixed points in the RG sense.

finite negative value, so the sphere looks like two large hyperbolic disks joined by a positive curvature ring around the equator. There is still an AdS_2 factor, but now it is warped as one moves around the deformed sphere.

The solutions we find turn out to be unstable to perturbations that break the $SO(3)$ symmetry, so they do not describe true stable IR fixed points. It is an important open problem to find the gravitational description of these true stable fixed points. One might think that a reasonable approach to this problem is to first classify all possible near-horizon geometries in higher dimensions and then study their stability. However, this approach is doomed to failure since we expect there to be an infinite number of (RG unstable) near-horizon geometries [66].

We will also show that the toroidal black holes exhibit a phase transition. Small ones are RG stable and larger ones become unstable. For a generic solution at the threshold of instability, there is no new geometry bifurcating. We constructed perturbatively two new families of solutions that start from very special ones. One may show that they are the only bifurcating ones (from those points in the moduli space). Unfortunately, they are still RG unstable.

3.2 Reissner-Nordström AdS is IR unstable in $D = 5$

To study IR fixed points of four-dimensional holographic theories, we work with the $D = 5$ Einstein-Maxwell theory

$$S = \frac{1}{16\pi G_5}\int_{\mathcal{M}} \mathrm{d}^5x\sqrt{-g}\left(R - F_{ab}F^{ab} + \frac{12}{L^2}\right) + S_{\partial\mathcal{M}}\,, \tag{3.1}$$

where $F = \mathrm{d}A$, A is the Maxwell 1-form potential, L is the AdS_5 length scale and G_5 is the five-dimensional Newton's constant. The equations of motion derived from this action read

$$R_{ab} - \frac{R}{2}g_{ab} - \frac{6}{L^2}g_{ab} = 2\left(F_a{}^cF_{bc} - \frac{g_{ab}}{4}F_{cd}F^{cd}\right) \tag{3.2a}$$

and

$$\nabla^a F_{ab} = 0\,. \tag{3.2b}$$

There is a unique two-parameter spherical solution to these equations (with a non-constant areal radius) which is given by

$$\mathrm{d}s^2_{\mathrm{RN}} = -f(r)\mathrm{d}t^2 + \frac{\mathrm{d}r^2}{f(r)} + r^2\mathrm{d}\Omega_3^2\,, \tag{3.3a}$$

$$A_{\mathrm{RN}} = \frac{q}{r_+^2}\left(1 - \frac{r_+^2}{r^2}\right)\mathrm{d}t\,, \tag{3.3b}$$

where $\mathrm{d}\Omega_3^2$ is the metric on a unit radius round three-sphere and

$$f(r) = \frac{r^2}{L^2} + 1 - \frac{r_+^2}{r^2}\left(\frac{r_+^2}{L^2} + 1 + \frac{4q^2}{3r_+^4}\right) + \frac{4q^2}{3r^4}\,. \tag{3.4}$$

This is the familiar Reissner-Nordström AdS solution (RN AdS).

We will take $|q| \leq q_{\mathrm{ext}}$, with

$$q_{\mathrm{ext}} = \frac{\sqrt{3}}{2}\sqrt{1 + 2\frac{r_+^2}{L^2}}\,r_+^2\,, \tag{3.5}$$

so that $r = r_+$ is the largest root of $f(r) = 0$. The black hole event horizon is then the null hypersurface $r = r_+$, where $f(r)$ vanishes. For $|q| < q_{\mathrm{ext}}$, $f(r)$ vanishes linearly and the black hole has non-vanishing Hawking temperature

$$T_H = \frac{|f'(r_+)|}{4\pi} = \frac{2\,q_{\mathrm{ext}}^2}{3\,\pi\,r_+^4}\left(1 - \frac{q^2}{q_{\mathrm{ext}}^2}\right)\,, \tag{3.6}$$

whereas for $q = q_{\mathrm{ext}}$, $f(r)$ vanishes quadratically at $r = r_+$ and the hole is said to be extremal and has vanishing temperature. The parameter q determines the total charge of the black hole by

$$Q = \frac{\pi\,q}{G}\,, \tag{3.7}$$

while its energy E, chemical potential μ and entropy S are given by

$$E = \frac{3\pi r_+^2}{8G}\left(\frac{r_+^2}{L^2} + 1 + \frac{4q^2}{3r_+^4}\right)\,, \quad \mu = \frac{q}{r_+^2}\,, \quad \text{and} \quad S = \frac{\pi^2}{2G}r_+^3\,, \tag{3.8}$$

respectively. It is a simple exercise to show that all of these thermodynamic quantities satisfy the first law of black hole mechanics

$$\mathrm{d}E = T_H\,\mathrm{d}S + \mu\,\mathrm{d}Q\,. \tag{3.9}$$

Hereafter we will focus on the extremal case. In particular, we are interested in the near-horizon geometry of the RN AdS black hole. To obtain this, we take a limit where we zoom near the extremal horizon located at $r = r_+$. Define new coordinates ρ, T by

$$r = r_+(1 + \lambda\rho) \quad \text{and} \quad t = \frac{L_{\mathrm{AdS}_2}^2}{r_+}\frac{T}{\lambda}\,, \tag{3.10}$$

where λ is a constant and we defined

$$L_{\mathrm{AdS}_2}^2 \equiv \frac{r_+^2 L^2}{4(L^2 + 3r_+^2)}\,. \tag{3.11}$$

We then take the limit $\lambda \to 0$. The resulting line element is the Robinson-Bertotti solution (or a five-dimensional version thereof), which takes the familiar $AdS_2 \times S^3$ form

$$\mathrm{d}s^2_{\mathrm{RB}} = L^2_{\mathrm{AdS}_2}\left(-\rho^2\,\mathrm{d}T^2 + \frac{\mathrm{d}\rho^2}{\rho^2}\right) + r_+^2\,\mathrm{d}\Omega_3^2\,, \tag{3.12a}$$

and

$$A_{\mathrm{RB}} = \frac{2q_{\mathrm{ext}}}{r_+^3}\,\rho\,L^2_{\mathrm{AdS}_2}\,\mathrm{d}T\,, \tag{3.12b}$$

with $\rho = 0$ being the black hole horizon, which in this limit yields the AdS_2 Poincaré horizon. The Robinson-Bertotti solution is itself a solution of the Einstein-Maxwell equations, since it is just a particular limit of the RN AdS black hole.

This near-horizon geometry, according to the standard rules of AdS/CFT [31], controls the IR of the dual theory. For this reason zero temperature solutions such as the one above, are often called IR geometries. To understand whether a given IR geometry is stable, in the RG sense, we perturb the IR geometry by time-independent perturbations (h, a), where h and a are metric and gauge field perturbations, respectively.

One might think that perturbing (3.12) is a complicated task, but it turns out that symmetry can help us. We first note that AdS_2 has constant curvature. This means we can use harmonic functions on AdS_2 as building blocks for constructing our generic perturbations (h, a). For time independent perturbations, harmonic functions on AdS_2 take a particularly simple form:

$$\Box_{\mathrm{AdS}_2}\mathbb{S}_\gamma(\rho) - \frac{\gamma(\gamma+1)}{L^2_{\mathrm{AdS}_2}}\mathbb{S}_\gamma(\rho) = 0 \quad \Rightarrow \quad \mathbb{S}_\gamma(\rho) = C\,\rho^\gamma\,. \tag{3.13}$$

where C is a normalization constant.

To construct perturbations (h, a) we use $\mathbb{S}_\gamma(\rho)$ as building blocks. Let I be an AdS_2 index and $\hat{I}$ an index on S^3. It then follows that metric perturbations with indices on the S^3 only behave as scalars under coordinate transformations on AdS_2, so we take

$$h_{\hat{I}\hat{J}} = \mathbb{S}_\gamma(\rho)\,\hat{h}_{\hat{I}\hat{J}} \tag{3.14}$$

where $\hat{h}_{\hat{I}\hat{J}}$ is a symmetric 2-tensor on S^3. The metric components $h_{I\hat{J}}$, on the other hand, behave as vectors, so we set

$$h_{I\hat{J}} = D_I\mathbb{S}_\gamma(\rho)\,\hat{h}_{\hat{J}} \tag{3.15}$$

where D_I is the covariant derivative on AdS_2 and $\hat{h}_{\hat{J}}$ a vector on S^3.

Finally, we come to metric perturbations with indices on AdS_2. These behave as symmetric 2-tensors with respect to coordinate transformations on AdS_2. Any symmetric 2-tensor can be built from a trace and a traceless symmetric 2-tensor. The latter two need to be built from $\mathbb{S}_\gamma(\rho)$. We thus set

$$h_{IJ} = \mathbb{S}_\gamma\,\hat{h}_L\,g_{IJ} + \hat{h}_T\mathbb{S}_{IJ} \tag{3.16}$$

with

$$\mathbb{S}_{IJ} \equiv D_ID_J\mathbb{S}_\gamma(\rho) - \frac{1}{2}\frac{\gamma(\gamma+1)}{L^2_{\mathrm{AdS}_2}}g_{IJ}\mathbb{S}_\gamma(\rho) \tag{3.17}$$

where g_{IJ} is the metric on AdS_2 and $\hat{h}_L$ and $\hat{h}_T$ are functions on S^3.

We now discuss the thorny issue of gauge invariance. A generic gauge transformation ξ can be written using the same procedure as above. In particular we find

$$\xi_a \mathrm{d}x^a = \hat{\xi}_S \, D_I \mathbb{S}_\gamma(\rho) \, \mathrm{d}x^I + \hat{\xi}_{\hat{I}} \, \mathbb{S}_\gamma(\rho) \, \mathrm{d}x^{\hat{I}} \,, \tag{3.18}$$

where $\hat{\xi}_S$ is a scalar on S^3 and $\hat{\xi}_{\hat{I}}$ is a vector on S^3. The metric perturbations will transform under an infinitesimal transformation generated by ξ according to

$$\delta h = \mathcal{L}_{\xi} g_{\mathrm{RB}} \,, \tag{3.19}$$

which induces

$$\delta \hat{h}_L = \frac{\gamma(\gamma+1)}{L^2_{\mathrm{AdS}_2}} \hat{\xi}_S \tag{3.20a}$$

$$\delta \hat{h}_T = 2 \, \hat{\xi}_S \tag{3.20b}$$

$$\delta \hat{h}_{\hat{I}} = 2(\hat{D}_{\hat{I}} \hat{\xi}_S + \hat{\xi}_{\hat{I}}) \tag{3.20c}$$

$$\delta h_{\hat{I}\hat{J}} = (\mathcal{L}_{\hat{\xi}} \hat{g})_{\hat{I}\hat{J}} \tag{3.20d}$$

where $\hat{g}_{\hat{I}\hat{J}}$ is the metric on a unit radius round S^3 and $\hat{D}_{\hat{I}}$ its metric preserving covariant derivative. We will work in a gauge where we choose $\hat{\xi}_S$ and $\hat{\xi}_{\hat{I}}$ so that $\hat{h}_T = \hat{h}_{\hat{I}} = 0$.

For the gauge field perturbation, we have

$$a = \hat{a}_S \, \mathbb{S}_\gamma(\rho) \, \mathrm{d}T \,, \tag{3.21}$$

where $\hat{a}_S$ is a function on S^3. Our perturbed gauge and metric field configurations are thus, in our gauge, parameterized by $\hat{h}_L$, $\hat{h}_{\hat{I}\hat{J}}$ and $\hat{a}_S$, which depend on the S^3 angles only.

Next we repeat the procedure and decompose the remaining perturbations in terms of spherical harmonics on the S^3. These, in turn, are parameterized by a quantum number $\ell \in \mathbb{N}$. Since we want to study non-spherical perturbations, we are interested in $\ell > 0$.

We are left with a linear system of homogeneous, algebraic equations for the coefficients, whose nontrivial solutions can be studied by computing the corresponding characteristic polynomial. This reduces to a fourth-order polynomial equation in the scaling exponent γ, with coefficients depending on ℓ and r_+. All the roots of the polynomial, which provide the non-trivial solutions to the homogeneous equations, are real. We can eliminate two of the four solutions with boundary conditions at the horizon. Since the two *smallest* roots are negative, the corresponding perturbation would blow up as $\rho \to 0$. We therefore discard them as our choice of boundary conditions. The remaining two roots give the physical scaling of the non-spherical perturbations near the $\rho = 0$ horizon. If one of them is again negative, it cannot be removed by boundary conditions, and indicates that the perturbation is singular on the horizon.

It is convenient to view the roots as functions of the dimensionless horizon radius $y_+ = r_+/L$. The largest two roots are:

$$\gamma_\pm(\ell, y_+) = \frac{1}{2} \left[\sqrt{5 - \lambda_\ell - 12\beta_+\lambda_\ell \pm 8\sqrt{\frac{1}{4} + 12\left(\beta_+^2 - \frac{1}{144}\right)\lambda_\ell}} - 1 \right] \,, \tag{3.22a}$$

where

$$\beta_+ \equiv \frac{L^2_{\mathrm{AdS}_2}}{L^2} - \frac{1}{6} \quad \text{and} \quad \lambda_\ell = \ell(\ell+2)\,. \tag{3.22b}$$

Note that λ_ℓ is the eigenvalue of spherical harmonics on S^3 and L_{AdS_2}/L^2 is only a function of y_+ (see Eq. (3.11)).

It remains then to check whether $\gamma_\pm(\ell, y_+)$ are positive. It turns out that the scaling dimension $\gamma_+(\ell, y_+)$ is positive for all values of ℓ and y_+ but $\gamma_-(\ell, y_+)$ is not. In particular, **for $\ell = 2$, γ_- is negative for all $y_+ > 0$!** Since a generic linear perturbation will always contain the $\ell = 2$ mode with some coefficient, we conclude that generic non-spherical perturbations blow up on the $AdS_2 \times S^3$ horizon. Nonlinearly, even if one starts with a deformation on the boundary that does not include an $\ell = 2$ mode, it will be generated as one evolves in to smaller radius. This means that from the standpoint of the RG flow of a dual field theory, $AdS_2 \times S^3$ is an unstable IR fixed point.

We now comment on the $\ell = 0, 1$ modes. In this case one has to repeat the above analysis separately, since some of the structures that are used to decompose our perturbations with respect to coordinate transformations on S^3 turn out to vanish. A deformation with $\ell = 0$ corresponds to an infinitesimal deformation of the background charge. For $\ell = 1$, the calculation is more subtle. Once the dust settles, one finds a single pair of modes, with one being negative and another positive. Again, we discard the smallest exponent based on boundary conditions as $\rho \to 0$. We thus restrict to the positive exponent, which is precisely given by $\gamma_+(1, y_+)$ with $\gamma_+(\ell, y_+)$ given in Eq. (3.22a).

For modes with $\ell \geq 3$, $\gamma_-(\ell, y_+)$ becomes negative whenever the horizon is large enough. The condition is:

$$y_+ \geq y_+^c(\ell) = \frac{1}{2\sqrt{2}}\sqrt{(\ell-2)(\ell+4)}\,, \tag{3.23}$$

In Fig. 3.2 we plot $\gamma_-(\ell, y_+)$ for several values of ℓ. Note that these higher ℓ modes become more divergent on the horizon of a large black hole.

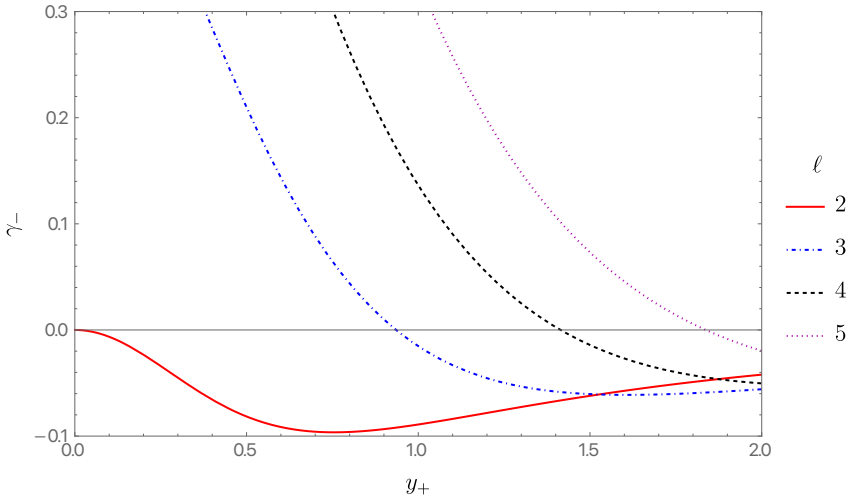

FIGURE 3.2: The scaling exponents γ_- for perturbations of $AdS_2 \times S^3$, as a function of $y_+ = r_+/L$, computed for several values of ℓ shown on the legend on the right.

The instability of the near-horizon geometry that we found above in $D = 5$ becomes even worse in higher dimensions, where the solution is $AdS_2 \times S^n$. The computation detailed above can be readily generalized to $n > 3$. The corresponding scaling dimensions are now given by

$$\gamma_\pm(\ell, y_+) = \frac{1}{2}\Bigg\{ 5 - \frac{2\,\lambda_\ell}{n-1} - \frac{4\,n\,(n+1)\,\lambda_\ell}{(n-1)^2}\beta_+ \pm \frac{4\,(n+1)}{n-1}\sqrt{4\,n\,\lambda_\ell\left[\beta_+^2 - \frac{1}{4\,n^2}\left(\frac{n-1}{n+1}\right)^2\right] + \left(\frac{n-1}{n+1}\right)^2}\Bigg\}^{1/2} - \frac{1}{2}\,, \tag{3.24a}$$

with

$$\beta_+ = \frac{y_+^2}{(n-1)^2 + n(n+1)y_+^2} - \frac{1}{2n} \quad \text{and} \quad \lambda_\ell = \ell(\ell+n-1)\,. \tag{3.24b}$$

There are now more modes that are always unstable. In analogy with the $D = 5$ ($n = 3$) case, we see that for $\ell = n - 1$, we have

$$\gamma_-(n-1, 0) = 0\,. \tag{3.25a}$$

However,

$$\gamma_-(2, 0) = \frac{1}{2}\left(\frac{|n-5|}{n-1} - 1\right)\,, \tag{3.25b}$$

which is negative for all $n > 3$. In fact, for $\ell \leq n - 1$, $\gamma_-(\ell, y_+) < 0$ for all $y_+ > 0$. Which modes dominates near the horizon depends on the size of the black hole. This is illustrated in Fig. 3.3 where we plot $\gamma_-(\ell, y_+)$ for $n = 5$ and $\ell = 2, 3, 4, 5$. Since Reissner-Nordström with $\Lambda = 0$ corresponds to $y_+ = r_+/L = 0$, this shows that the near-horizon region of RN in $D > 5$ is also unstable to non-spherical perturbations.

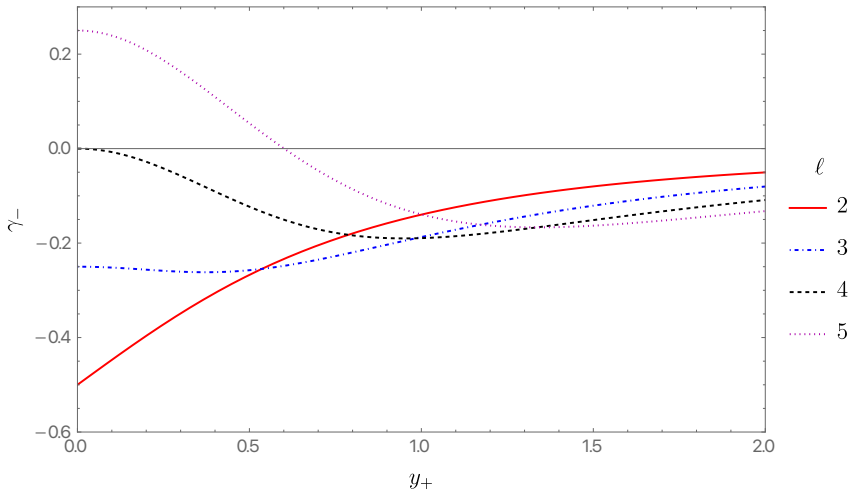

FIGURE 3.3: The scaling exponents γ_- for perturbations of $AdS_2 \times S^5$, as a function of $y_+ = r_+/L$, computed for several values of ℓ shown on the legend on the right.

An electrically charged BTZ black hole (whose near-horizon geometry is described by $AdS_2 \times S^1$) is different from the above discussion. This stems from the fact $D_A D_B f$ on S^1 (for any function f) is a pure trace. Moreover, gravity has no local degrees of freedom. In this way, three-dimensional Einstein–Maxwell theory has a lot in common with the $\ell = 1$ sector of its higher-dimensional counterparts. The background reads:

$$g = \frac{L^2}{2}\left(-\rho^2 \mathrm{d}t^2 + \frac{\mathrm{d}\rho^2}{\rho^2}\right) + r_+^2 \mathrm{d}\phi^2 \tag{3.26a}$$

and

$$A = \frac{L}{2}\rho \mathrm{d}t. \tag{3.26b}$$

Notice that r_+ is an arbitrary parameter. We may again decompose perturbations in terms of $\mathrm{S}_\gamma(\rho)$ and Fourier modes $e^{im\phi}$ on S^1. Then, we find two possible values of γ:

$$\gamma_\pm = -\frac{1}{2} \pm \frac{3}{2}\sqrt{1 + \frac{2m^2L^2}{9r_+^2}}. \tag{3.27}$$

The boundary conditions at the horizon choose $\gamma_+ \geq 1$. Thus, we see that the BTZ black hole is RG stable. Nevertheless, it may suffer from (rather mild) tidal-force singularities as long as $1 < \gamma < 2$.

3.3 A new $SO(3)$-invariant IR geometry

In this section, we construct a new near-horizon geometry that is only invariant under an $SO(3)$ subgroup of the $SO(4)$ rotational symmetry. We will show that it is stable to small $SO(3)$-invariant perturbations. Since the charge is conserved in Einstein-Maxwell theory, we need a near-horizon geometry for each Q. For $AdS_2 \times S^3$ this just corresponds to a trivial overall rescaling. However, our new solutions will depend non-trivially on Q, so we actually construct a one-parameter family of new IR geometries.

These new geometries can be written as a warped product of AdS_2 with a deformed three-sphere, where the AdS_2 length scale depends on the angles of the S^3. The S^3 is deformed in such a way that preserves a round S^2. In order to describe these solutions we first introduce an angle $\theta \in [0, \pi]$ and write the metric on the unit round S^3 as

$$\mathrm{d}\Omega_3^2 = \mathrm{d}\theta^2 + \sin^2\theta \mathrm{d}\Omega_2^2 \tag{3.28}$$

where $\mathrm{d}\Omega_2^2$ is the metric on a unit radius round S^2.

We then write our full IR metric and gauge field configuration as

$$\mathrm{d}s^2 = L^2\left\{B(\theta)\left(-A_0^2\rho^2\frac{\mathrm{d}t^2}{L^2} + \frac{\mathrm{d}\rho^2}{\rho^2}\right) + \Upsilon_+^2\left[H(\theta)^2\mathrm{d}\theta^2 + \frac{\sin^2\theta}{H(\theta)}\mathrm{d}\Omega_2^2\right]\right\} \tag{3.29a}$$

and

$$A = -\rho_{\mathrm{IR}}\, A_0\, \rho\, \mathrm{d}t\,, \tag{3.29b}$$

Note that the factor in parenthesis is just AdS_2 with the Poincare horizon at $\rho = 0$. Our *Ansatz* depends on two constants, Υ_+ and ρ_{IR}, that determine the size of the horizon and charge density respectively. We have introduced a third constant A_0 that just rescales t. It will play no role in constructing the near-horizon geometries but will be useful when we later relate these geometries to full asymptotically AdS solutions. The function $B(\theta)$ describes the warping of the AdS_2, and the function

$H(\theta)$ describes the distortion of the S^3. The entropy, S, and total electric charge, Q, of our field configuration are given by

$$S = \frac{\pi^2 Y_+^3}{2G_5} \quad \text{and} \quad Q = \frac{\rho_{\rm IR}}{G_5} Y_+^3 \int_0^\pi \frac{\sin^2\theta}{B(\theta)} \mathrm{d}\theta \,, \tag{3.30}$$

Note that since the charge is conserved, Q can be computed at the boundary or the horizon.

The Maxwell equation is automatically satisfied using Eq. (3.29b), whereas the Einstein equation yields a pair of nonlinear ordinary differential equations

$$\left(\frac{\sin^2\theta}{H^2} B'\right)' + 2\, Y_+^2 \, \sin^2\theta \left(1 - \frac{4}{3}\frac{\rho_{\rm IR}^2}{B} - 4B\right) = 0 \tag{3.31a}$$

where $'$ denotes differentiation with respect to θ and

$$\frac{1}{B^2 \sin^2\theta}\left[\left(\frac{B^2 \sin^2\theta}{H}\right)'\right]^2 - 4B^2 H - \frac{3\sin^2\theta}{H^2} B'^2 - 4\, Y_+^2 \, \sin^2\theta \left(\rho_{\rm IR}^2 - B + 6B^2\right) = 0 \,. \tag{3.31b}$$

Note that, as advertised, A_0 does not appear in these equations of motion. Regularity at the poles requires the boundary conditions $B'(0) = B'(\pi) = 0$ and $H(0) = H(\pi) = 1$.

From Eq. (3.31a) it is clear that $\rho_{\rm IR}$ is not a free parameter. Indeed, one can integrate both sides of Eq. (3.31a) and use the above boundary conditions to find the following relation

$$\int_0^\pi \sin^2\theta \left[1 - \frac{4}{3}\frac{\rho_{\rm IR}^2}{B(\theta)} - 4B(\theta)\right] \mathrm{d}\theta = 0 \,, \tag{3.32}$$

Thus, although our *Ansatz* depends on two free parameters $(Y_+, \rho_{\rm IR})$ the relation above fixes one of them, so that we only have a single parameter free.

3.3.1 Perturbative analytic treatment

We have not managed to find closed form solutions of Eqs. (3.31). We have, however, found an analytic perturbative scheme which we can extend to whatever order in perturbation theory we wish. The idea is the following. We have seen in section 3.2 that $\ell = 2$ perturbations have $\gamma_-(2,0) = 0$. This suggests that there might exist a new family of near-horizon geometries with AdS_2 symmetry that branches off from the zero size limit of $AdS_2 \times S^2$. Since the zero size limit is singular, this is an unconventional perturbation expansion. Nevertheless we will see that it is well defined.

We thus expand

$$B(\theta) = \sum_{i=1}^{+\infty} b^{(i)}(\theta)\varepsilon^i\,, \tag{3.33a}$$

$$H(\theta) = 1 + \sum_{i=1}^{+\infty} h^{(i)}(\theta)\varepsilon^i\,, \tag{3.33b}$$

$$\rho_{\rm IR}^2 = \sum_{i=1}^{+\infty} \Xi^{(i)}\varepsilon^i\,, \tag{3.33c}$$

$$Y_+^2 = \sum_{i=1}^{+\infty} \Sigma_+^{(i)}\varepsilon^i\,, \tag{3.33d}$$

where ε is a book-keeping parameter, whose normalization we choose to be

$$\int_0^\pi B\sin^2\theta\, Y_{\ell=2}(\theta)\mathrm{d}\theta = \varepsilon^2\,. \tag{3.34}$$

where $Y_\ell(\theta)$ is a spherical harmonic on the three-sphere preserving $SO(3)$, which we choose to be given by

$$Y_\ell(\theta) = \sqrt{\frac{2}{\pi}}\frac{\sin[(\ell+1)\theta]}{\sin\theta} \quad \text{so that} \quad \int_0^\pi Y_\ell(\theta)Y_{\tilde\ell}(\theta)\mathrm{d}\theta = \delta_{\ell,\tilde\ell} \quad \text{and} \quad Y_\ell(0) > 0\,. \tag{3.35}$$

Note that H starts with 1 to satisfy our boundary conditions, and $\epsilon > 0$ is required since Y_+^2 begins at order ϵ.

Despite the fact that $\varepsilon = 0$ corresponds to a *singular* solution, at each order in ε our boundary conditions are sufficient to solve for each of the functions above. In particular, for any finite value of ε our perturbative expansion yields a completely smooth solution. We carried this expansion all the way to $\mathcal{O}(\varepsilon^7)$. The first few coefficients are

$$\begin{aligned}
b^{(1)}(\theta) &= \frac{\sqrt{7}}{2(2\pi)^{1/4}}\,, \quad b^{(2)}(\theta) = \frac{56\cos(2\theta) - 61}{14\sqrt{2\pi}}\,,\\
b^{(3)}(\theta) &= \frac{588\cos(2\theta) + 588\cos(4\theta) + 6354}{147\sqrt{7}(2\pi)^{3/4}}\,,\\
h^{(1)}(\theta) &= -\frac{4\,2^{3/4}\sin^2\theta}{\sqrt{7}\pi^{1/4}}\,, \quad h^{(2)}(\theta) = -\frac{496}{49}\sqrt{\frac{2}{\pi}}\sin^2\theta\,,\\
h^{(3)}(\theta) &= -\frac{162^{1/4}\sin^2\theta}{1029\sqrt{7}\pi^{3/4}}\left[2891\cos(2\theta) + 11442\right]\,,\\
\Xi^{(1)} &= \frac{3\sqrt{7}}{8(2\pi)^{1/4}}\,, \quad \Xi^{(2)} = -\frac{561}{56\sqrt{2\pi}}\,, \quad \Xi^{(3)} = \frac{15525}{98\sqrt{7}(2\pi)^{3/4}}\,,\\
\Sigma_+^{(1)} &= \frac{2^{3/4}\sqrt{7}}{\pi^{1/4}}\,, \quad \Sigma_+^{(2)} = \frac{205}{7}\sqrt{\frac{2}{\pi}}\,, \quad \Sigma_+^{(3)} = \frac{373602^{1/4}}{49\sqrt{7}\pi^{3/4}}\,.
\end{aligned} \tag{3.36}$$

Note that since the solution starts with an $\ell = 2$ perturbation, there is a reflection symmetry about $\theta = \pi/2$ which is preserved to all orders.

With the above it is a simple exercise to compute the total charge and entropy as a function of ε. These turn out to be given by

$$\frac{G_5\,Q}{L^2} = \frac{\sqrt{21}\pi^{3/4}}{2^{1/4}}\varepsilon\left[1+\frac{303}{7\sqrt{7}(2\pi)^{1/4}}\varepsilon+\frac{36369}{343}\sqrt{\frac{2}{\pi}}\varepsilon^2+\frac{15631151}{2401\sqrt{7}(2\pi)^{3/4}}\varepsilon^3 + \frac{682434694}{50421\pi}\varepsilon^4+\frac{630372065550}{823543\sqrt{7}(2\pi)^{5/4}}\varepsilon^5+\mathcal{O}(\varepsilon^6)\right] \tag{3.37a}$$

and

$$\frac{G_5\,S}{L^3} = 2^{1/8}7^{3/4}\pi^{13/8}\varepsilon^{3/2}\left[1+\frac{615}{14\sqrt{7}(2\pi)^{1/4}}\varepsilon+\frac{574395}{2744\sqrt{2\pi}}\varepsilon^2+\frac{34688917}{5488\sqrt{7}(2\pi)^{3/4}}\varepsilon^3 + \frac{392491070291}{30118144\pi}\varepsilon^4+\frac{309058579837106}{421654016\sqrt{7}(2\pi)^{5/4}}\varepsilon^5+\mathcal{O}(\varepsilon^6)\right], \tag{3.37b}$$

respectively. The parameter ε, though very useful for practical implementations, has little physical meaning. We shall see that the entropy of this novel solution is not very different from that of an extremal RN AdS black hole with the same total charge Q. For this reason, we define

$$\Delta S = S(Q) - S_{\rm RN}(Q) \tag{3.38}$$

which gives the difference in entropy between one of the solutions we are seeking to construct and an extreme RN AdS black hole with the same total charge Q. It is then a simple exercise to compute ΔS as a function of ε (or alternatively, Q through Eq. (3.37a)). The final result, consistent with our $\mathcal{O}(\varepsilon^7)$ expansion for B and H, turns out to be

$$\begin{aligned}\frac{G_5\,\Delta S}{L^3} &= -2^{3/8}7^{1/4}8\pi^{7/8}\varepsilon^{9/2}-\frac{34682^{1/8}\pi^{5/8}}{7^{5/4}}\varepsilon^{11/2}-\frac{987123\pi^{3/8}}{2^{1/8}7^{3/4}49}\varepsilon^{13/2}+\mathcal{O}(\varepsilon^{15/2})\\ &= -\frac{16\sqrt{2}}{441\pi^{5/2}3^{1/4}}\left(\frac{G_5\,Q}{L^2}\right)^{9/2}\left\{1-\frac{310\sqrt{3}}{49\pi}\left(\frac{G_5\,Q}{L^2}\right)+\frac{415279}{4802\pi^2}\left(\frac{G_5\,Q}{L^2}\right)^2 + \mathcal{O}\left[\left(\frac{G_5\,Q}{L^2}\right)^3\right]\right\}\end{aligned} \tag{3.39}$$

This analytic expression works remarkably well when $Q/L^2 \ll 1$.

3.3.2 Exact numerical results

We now solve Eqs. (3.31) fully non-linearly using numerical methods. It is easy to see that, at least locally, Eqs. (3.31) gives a one-parameter family of solutions. It might appear that Eqs. (3.31) depends on two parameters, $\rho_{\rm IR}^2$ and Y_+^2, but because of the global constraint in Eq. (3.32), one of these parameters gets locked in terms of the other.

We discretize the θ direction with a Chebyshev-Gauss-Lobatto collocation grid, and solve the resulting equations using a Newton-Raphson method. These methods have been reviewed in the literature in [37]. The size of the horizon is determined

by Y_+, and the charge Q is a monotonically increasing function of Y_+. We are able to construct solutions for all Q up to about $G_5Q/L^2 \sim 3 \times 10^4$ without encountering any numerical issues. We believe they extend to arbitrarily large Q.

In Fig. 3.4 we show ΔS for charges up to $G_5Q/L^2 \sim 100$. Note that $\Delta S < 0$ for all Q, showing that the new IR geometries have smaller entropy than RN AdS with the same charge.

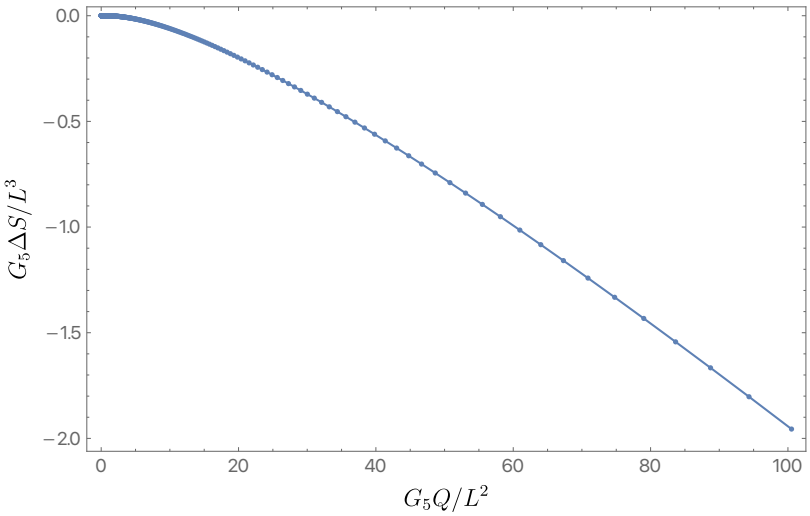

FIGURE 3.4: The difference in entropy between the new near-horizon geometries and RN AdS, as a function of charge.

We now explore the geometry of a spatial cross section of the horizon. It is topologically S^3, but is no longer round. The reflection symmetry about $\theta = \pi/2$ that we saw in the perturbative solution remains in the exact solutions for all Q. To begin, let us try to embed it into $\mathbb{R}^4$. To do this we set

$$\begin{aligned} y_1 &= L\, Z(\theta)\,, \\ y_2 &= L\, R(\theta) \cos\theta_1\,, \\ y_3 &= L\, R(\theta) \sin\theta_1 \cos\phi\,, \\ y_4 &= L\, R(\theta) \sin\theta_1 \sin\phi\,, \end{aligned}$$

with $\theta_1 \in [0, \pi]$ and $\phi \sim \phi + 2\pi$ the usual latitude and longitude angles on a two-sphere, respectively. We then compare the induced metric on

$$\mathrm{d}s^2 = \sum_{i=1}^{4} \mathrm{d}y_i^2 \tag{3.40}$$

with that of a spatial cross section of our horizon obtained from Eq. (3.29a). We thus obtain

$$R(\theta) = \frac{Y_+ \sin\theta}{\sqrt{H(\theta)}} \quad \text{and} \quad Z'(\theta)^2 = Y_+^2 H(\theta)^2 - R'(\theta)^2\,. \tag{3.41}$$

The latter equation can be solved using numerical methods. For small Y_+ (i.e. small Q) the horizon is only slightly distorted from a round S^3, consistent with the previous perturbative results. For sufficiently large values of Y_+ (i.e. large Q) there is no solution to (3.41), showing that the near-horizon geometry stops being embeddable into $\mathbb{R}^4$. This is similar to Kerr and Kerr-Newman black holes near extremality [103]. The isometric embedding of the horizon for $G_5Q/L^2 \approx 1.61$ is shown in Fig. 3.5.

One can see that the horizon becomes flattened like a pancake. The black dashed line shows what a perfect sphere would look like, for comparison. The blue disks correspond to the numerical embedding obtained by solving Eq. (3.41).

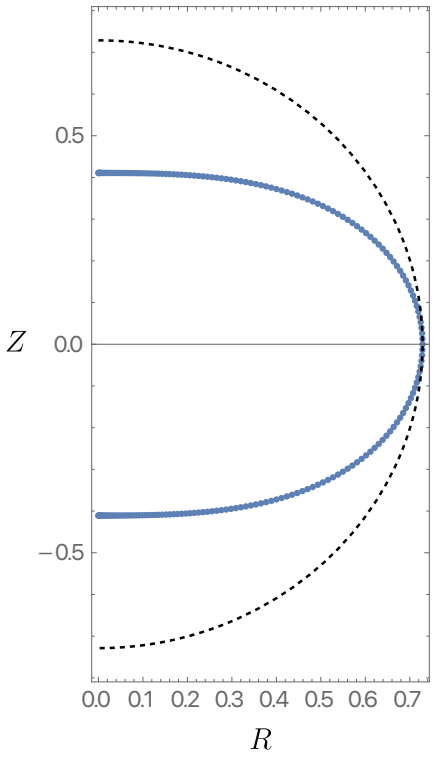

FIGURE 3.5: Isometric embedding of the near-horizon geometry into $\mathbb{R}^4$. The black dashed line shows what a perfect sphere would look like and the blue disks represent our novel pancaked IR geometry. This particular embedding was generated for $G_5Q/L^2 \approx 1.61$.

In order to picture the large Q solution, we first plot $\mathcal{R}$ and F^2 on the horizon, as a function of θ for $G_5Q/L^2 \approx 100$. This is shown in Fig. 3.6. We can see that near the equator, *i.e.* $\theta = \pi/2$, the Ricci scalar $\mathcal{R}$ is positive as expected, but $\mathcal{R}$ becomes *negative* near the poles. In addition, we see that the electric field is stronger at the equator and weaker near the poles.

To map out how a round sphere with a uniform electric field (for small Q) evolves to something like Fig. 3.6 (for large Q), we plot $\mathcal{R}(0)$, $\mathcal{R}(\pi/2)$, $F^2\big|_{\theta=0}$ and $F^2\big|_{\theta=\frac{\pi}{2}}$ as one increases Q. This is shown in Fig. 3.7. One clearly sees that the curvature at the poles decreases rapidly as Q increases from the large positive curvature of a small sphere to a constant negative value. The curvature at the equator also decreases but settles down to a constant positive value. The limiting behavior at large Q is

$$\lim_{Q\to+\infty} L^2\mathcal{R}(0) \equiv \mathcal{R}_0 \approx -9.3913\,, \qquad \lim_{Q\to+\infty} L^2\mathcal{R}(\pi/2) \equiv \mathcal{R}_e \approx 9.3058\,, \tag{3.42a}$$

and

$$\lim_{Q\to+\infty} F^2\big|_{\theta=0} \approx -2.5947\,, \qquad \lim_{Q\to+\infty} F^2\big|_{\theta=\frac{\pi}{2}} \approx -18.9797\,. \tag{3.42b}$$

Since the horizon volume is growing with Q, but the curvature is not decreasing, the horizon must look like a large three-dimensional hyperbolic space near each pole, joined together by a positive curvature ring around the equator.

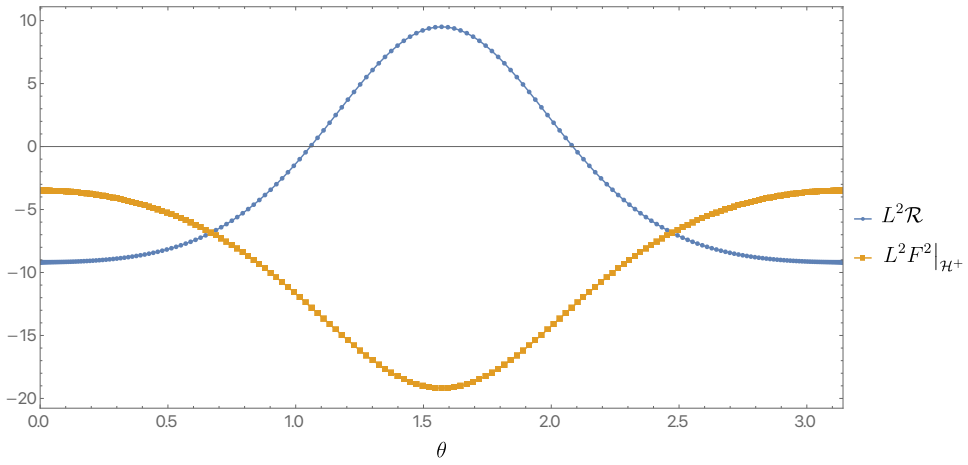

FIGURE 3.6: $\mathcal{R}$ and F^2 on the horizon, as a function of θ for $Q \approx 100.523$.

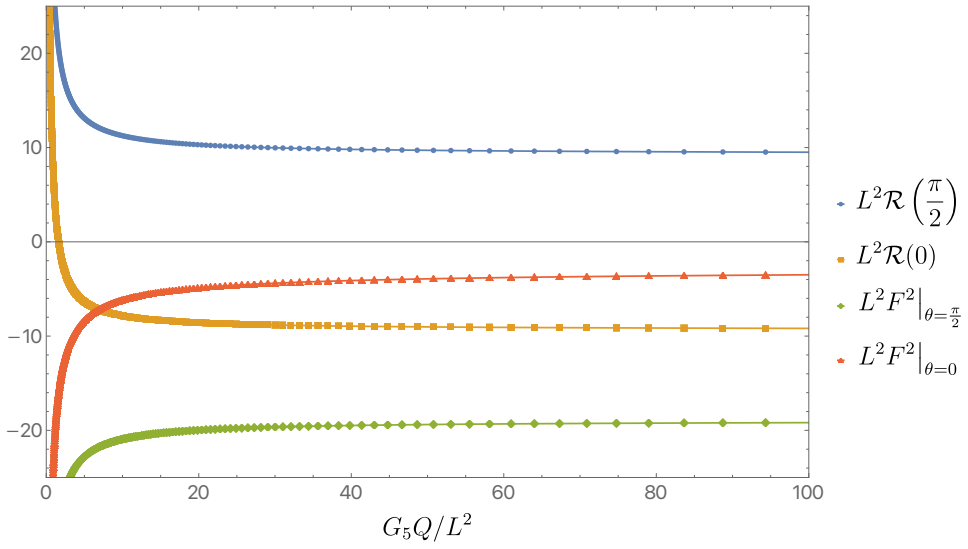

FIGURE 3.7: $\mathcal{R}(\pi/2)$ (blue disks), $\mathcal{R}(0)$ (orange squares), $F^2|_{\theta=\frac{\pi}{2}}$ (green diamonds) and $F^2|_{\theta=0}$ (red triangles) as a function of Q.

To understand the limiting geometry more explicitly, we will change gauge. Consider

$$\mathrm{d}s^2 = L^2\left\{B(\chi)\left(-A_0^2\rho^2\frac{\mathrm{d}t^2}{L^2}+\frac{\mathrm{d}\rho^2}{\rho^2}\right)+\tilde{Y}_+^2\left[\tilde{H}(\chi)\mathrm{d}\chi^2+\sin^2\chi\,\mathrm{d}\Omega_2^2\right]\right\} \tag{3.43}$$

instead of Eq. (3.29a). This amounts to a simple change of coordinates. We are interested in the large $\tilde{Y}_+$ limit of the resulting equations of motion. The advantage of this coordinate system is that we have to solve just a single second order equation of motion for B. Indeed, after some algebra, we find that $\tilde{H}$ can be expressed in terms of B and its first derivative:

$$\begin{aligned}&4\left(B^2+\tilde{Y}_+^2\left[\rho_{\mathrm{IR}}^2-B\left(1-6B\right)\right]\sin^2\chi\right)\tilde{H}(\chi)=\\&=\left(\sin\chi\,\frac{\partial B}{\partial\chi}+4\cos\chi\,B\right)^2-12\,B^2\,\cos^2\chi\,.\end{aligned} \tag{3.44a}$$

while $B(\chi)$ satisfies the following second order differential equation

$$\frac{\partial}{\partial\chi}\left(\frac{\sin^2\chi}{\sqrt{\tilde{H}}}\frac{\partial B}{\partial\chi}\right)-\frac{2\tilde{Y}_+^2\sqrt{\tilde{H}}}{3B}\sin^2\chi\left(4\rho_{\rm IR}^2-3B+12B^2\right)=0\,. \tag{3.44b}$$

Note that near the poles, located at $\chi=0\,,\pi$, Eq. (3.44a) automatically yields $\tilde{H}=1$, as it should from regularity. The solution we seek to construct is even around $\chi=\pi/2$, so we have

$$\left.\frac{\partial B}{\partial\chi}\right|_{\chi=\frac{\pi}{2}}=0\,. \tag{3.45}$$

From Eq. (3.44a) we find that in order for $H(\pi/2)$ *not* to vanish we must demand

$$\rho_{\rm IR}^2=B\left(\frac{\pi}{2}\right)\left[1-B\left(\frac{\pi}{2}\right)\left(6+\frac{1}{\tilde{Y}_+^2}\right)\right]\,. \tag{3.46}$$

The above equation, so long as $B(\pi/2)$ is non-vanishing, provides a simple relation between $\rho_{\rm IR}^2$ and $B(\pi/2)$. In particular, in the large $\tilde{Y}_+$ limit we find

$$\rho_{\rm IR}^2=B\left(\frac{\pi}{2}\right)\left[1-6\,B\left(\frac{\pi}{2}\right)\right]\,. \tag{3.47}$$

We would like to find a similar relation, in the large $\tilde{Y}_+$ limit, between $\rho_{\rm IR}^2$ and $B(0)$. However, it is clear from Eq. (3.44a) that the expansion near $\chi=0$ needs to be treated with care, since the factor of $\tilde{Y}_+^2$ appearing in the denominator comes multiplied by $\sin^2\chi$. In order to deal with this, we first change into a new variable

$$\xi\equiv\tilde{Y}_+^2\sin\chi \tag{3.48}$$

and take the large $\tilde{Y}_+$ limit *a posteriori*, while keeping ξ fixed. This ensures that while we take $\tilde{Y}_+$ to be large, we are zooming in to $\chi=0$. This procedures then yields

$$\rho_{\rm IR}^2=\frac{3}{4}\left[1-4B(0)\right]B(0)\,, \tag{3.49}$$

to leading order at large $\tilde{Y}_+$. We have thus found a relation between $B(0)$ and $B(\pi/2)$ for large horizons, by combining Eq. (3.47) and Eq. (3.49).

We can use this result to obtain analytic expressions relating $\mathcal{R}$ and F^2 at the equator and at the poles. Let us start with $\mathcal{R}$. This is a function of $\tilde{H}(\chi)$ and its first derivative only. However, from Eq. (3.44a) we can alternatively express $\mathcal{R}$ as a function of B and its first and second derivatives. By using the equation of motion for B (see Eq. 3.44b) we can eliminate all second derivatives, thus finding an expression for $\mathcal{R}$ as a function of B and its first derivative only. Finally we note that the first derivative of B vanishes at $\theta=0,\pi/2$, so we are left with an expression for $\mathcal{R}(0)$ and $\mathcal{R}(\pi/2)$ as a function of $B(0)$ and $B(\pi/2)$, respectively.

We can now substitute in the above relation between $B(0)$ and $B(\pi/2)$ to obtain an analytic relation between $\mathcal{R}_0\equiv\mathcal{R}(0)$ and $\mathcal{R}_e\equiv\mathcal{R}(\pi/2)$, valid for large Q. The result is:

$$\mathcal{R}_0=\frac{9}{128(\mathcal{R}_e+16)}\left[(3\mathcal{R}_e+32)\,(\mathcal{R}_e-32)-(\mathcal{R}_e+32)\sqrt{9\mathcal{R}_e^2+64\mathcal{R}_e+1024}\right]\,. \tag{3.50}$$

We have tested this relation with the values in Eq. (3.42a) and find that it matches the numerical results to within 0.1%.

Since F^2 only depends on B and ρ_{IR} (which is determined in terms of B via (3.47) or (3.49)) we clearly have a relation between F^2 at $\chi = 0$ and at $\chi = \pi/2$. But we can also express both of them in terms of $\mathcal{R}_e$:

$$\lim_{\tilde{Y}_+ \to +\infty} L^2 F^2\big|_{\chi=\frac{\pi}{2}} = -\frac{3}{4}\left(\mathcal{R}_e + 16\right) , \tag{3.51a}$$

and

$$\lim_{\tilde{Y}_+ \to +\infty} L^2 F^2\big|_{\chi=0} = -\frac{3072\left(\mathcal{R}_e + 16\right)}{\left(3\mathcal{R}_e + 96 + \sqrt{9\mathcal{R}_e^2 + 64\mathcal{R}_e + 1024}\right)^2} . \tag{3.51b}$$

Using the value quoted in Eq. (3.42a) for $\mathcal{R}_e$, we find that these expressions reproduce the values quoted in Eq. (3.42b) to within 0.25%. So we see that the large Q limits of the curvature and Maxwell field at the equator and the pole are all determined by $\mathcal{R}_e$.

3.3.3 RG stability of the new IR geometries with respect to $SO(3)$ preserving deformations

In this section, we study the RG stability of our new near-horizon geometries. The analysis developed here has a drawback: it is a linear analysis and it could well be that nonlinearities change the overall picture. In the next section, we study fully nonlinear deformations and show that this is not the case.

Before proceeding let us briefly discuss what the expectations are. When we studied the RG stability of $AdS_2 \times S^3$, we decomposed all perturbations in terms of spherical harmonics on S^3, which in turn were labeled by a quantum number ℓ. For each value of ℓ we can find a total of *four* scaling exponents γ. Two of these are eliminated via boundary conditions at the horizon since they turn out to always be negative. The remaining two roots are then studied as a function of y_+, or equivalently Q. We would like to keep this procedure as much as possible.

However, once we break $SO(4)$ we need to find a way to articulate what we mean by a perturbation having a certain ℓ. We do this by counting nodes along the θ direction. This allows us to make sense of ℓ beyond spherical symmetry. Note that a given standard ℓ-harmonic on the three-sphere *does* have ℓ nodes along the polar direction. For each value of $\ell \neq 0, 1$ we are then supposed to find four values for the scaling exponents. We discard the two most negative exponents, which connect to the unphysical scaling exponents when $SO(4)$ symmetry is restored (*i.e.* $Q = 0$). Unlike for the perturbations of $AdS_2 \times S^3$, we now need to resort to solving an honest quadratic Stürm-Liouville problem, which we will detail next.

First, we present our perturbative Ansatz, which is a function of the scaling exponents γ. We then take $g = \bar{g} + h$, $A = \bar{A} + a$, with bared quantities being our novel IR geometries, and set

$$\delta \mathrm{d}s^2 \equiv h_{ab}\mathrm{d}x^a \mathrm{d}x^b = \rho^\gamma L^2 \Bigg\{ B(\theta)\frac{q_1(\theta)}{\gamma}\left(-A_0^2\rho^2\frac{\mathrm{d}t^2}{L^2} + \frac{\mathrm{d}\rho^2}{\rho^2}\right) + Y_+^2\left[q_2(\theta)\, H(\theta)^2 \mathrm{d}\theta^2 + q_3(\theta)\,\frac{\sin^2\theta}{H(\theta)}\mathrm{d}\Omega_2^2\right]\Bigg\} \tag{3.52a}$$

and

$$\delta A \equiv a_a \mathrm{d}x^a = -\rho_{\rm IR}\, A_0\, \rho^{1+\gamma}\, q_4(\theta)\, \mathrm{d}t\,. \tag{3.52b}$$

Note that the perturbations preserve an $SO(3)$ symmetry. This form of the metric is already gauged fixed, in the sense that h_{tt} and $h_{\rho\rho}$ are not independent components, and metric components of the form $h_{\rho\theta}$ are absent. These conditions fix both infinitesimal reparametrizations of θ and ρ, as it should. It then remains to find q_1, q_2, q_3, q_4 and γ from the Einstein-Maxwell equations.

The procedure is somehow tedious, so we will only present the final results. Setting $\lambda = \gamma(\gamma+1)$, we find

$$q_2 = -2\, q_3\,, \tag{3.53a}$$

$$\begin{aligned} q_3 = \frac{1}{\mathcal{H}_\lambda}\Bigg\{ & 2Y_+^2\left[4\rho_{\rm IR}^2 + (\lambda-2)B\right]\sin\theta H^3 \frac{q_1}{\gamma} - 8\rho_{\rm IR}^2 Y_+^2(\gamma+1)\sin\theta H^3 q_4 \\ & + 3B^2\left(2\cos\theta H - \sin\theta H'\right)\frac{q_1'}{\gamma} - \left[4B\sin\theta H' - 8H\left(B\cos\theta + \sin\theta B'\right)\right]\frac{\rho_{\rm IR}^2 q_4'}{\gamma}\Bigg\}\,, \end{aligned} \tag{3.53b}$$

$$\begin{aligned} & \frac{\mathcal{H}_\lambda^2}{B^2\sin^3\theta H}\left(\frac{B^2\sin^3\theta H\, q_1'}{\mathcal{H}_\lambda}\right)' + \left(\alpha_0\,\mathcal{H}_\lambda + \alpha_1 + \alpha_2\,\lambda\right) q_4' \\ & \quad + \left(\beta_0\,\mathcal{H}_\lambda + \beta_1 + \beta_2\,\lambda + \beta_3\lambda^2\right) q_1 + \left(\kappa_0\,\mathcal{H}_\lambda + \kappa_1 + \kappa_2\lambda\right)\,\lambda\, q_4 = 0\,. \end{aligned} \tag{3.53c}$$

$$\left(\frac{\sin^2\theta\, q_4'}{H^2}\right)' - \frac{Y_+^2\sin^2\theta}{B}\left(q_1 - \lambda q_4\right) = 0\,. \tag{3.53d}$$

where α_0, α_1, α_2, β_0, β_1, β_2, β_3, κ_0, κ_1 and κ_2 are functions of B, B', H, H' and θ given in Appendix B and are independent of λ, and

$$\mathcal{H}_\lambda \equiv \sin\theta\Big\{4Y_+^2\left[\rho_{\rm IR}^2 - (\lambda+1-6B)B\right]H^3 - 3HB'^2 + 6BB'H'\Big\} - 12B\cos\theta HB'\,. \tag{3.53e}$$

Once q_1 and q_4 are known from Eq. (3.53c) and Eq. (3.53d), q_2 and q_3 are fixed in terms of Eq. (3.53a) and Eq. (3.53b). We are thus left with solving Eq. (3.53c) and Eq. (3.53d), which should determine q_1, q_4 and λ. As boundary conditions we demand

$$q_1'(0) = q_1'(\pi) = q_4'(0) = q_4'(\pi) = 0\,, \tag{3.54}$$

which render Eq. (3.53c) and Eq. (3.53d) a quadratic Stürm-Liouville eigenvalue problem in λ. Note that once a solution for q_1 and q_4 has been found, we still need to a posteriori check that q_3 given in Eq. (3.53b) is everywhere smooth. The present work only discusses modes for which all of the functions q_i are smooth for $\theta \in [0,\pi]$.

We solved Eq. (3.53c) and Eq. (3.53d) in two different manners, which agree well with each other in the regime where both methods are applicable. First, by using our perturbative scheme, we determine λ as a function of ε (see section 3.3.1), which

gives an expansion valid at small Q. We set

$$q_1(\theta) = \sum_{i=0}^{+\infty} q_1^{(i)}(\theta)\varepsilon^i \tag{3.55a}$$

$$q_4(\theta) = \sum_{i=0}^{+\infty} q_4^{(i)}(\theta)\varepsilon^i \tag{3.55b}$$

$$\gamma = \sum_{i=0}^{+\infty} \gamma^{(i)}\varepsilon^i \tag{3.55c}$$

and solve order by order in ε. The most problematic mode is the mode that goes negative for all $Q > 0$ for $AdS_2 \times S^3$. This mode has $\ell = 2$, which is the mode we would like to disentangle.

To start our perturbative treatment we take

$$\gamma^{(0)} = 0\,, \quad q_1^{(0)} = \sqrt{\frac{2}{\pi}}[2 + \cos(2\theta)] \qquad \text{and} \quad q_4^{(0)} = 0\,. \tag{3.56}$$

Note that $q_1^{(0)}(\theta)$ is an $\ell = 2$ harmonic on a round three-sphere, as expected. One can now proceed to solve these equations order by order in ε. For instance, one finds

$$\begin{aligned}
\gamma^{(1)} &= \frac{2\,2^{3/4}\sqrt{7}}{3\pi^{1/4}}\,, \quad \gamma^{(2)} = -\frac{3686}{189}\sqrt{\frac{2}{\pi}}\,, \quad \gamma^{(3)} = \frac{5022016\,2^{1/4}}{11907\sqrt{7}\pi^{3/4}}\,,\\
q_1^{(1)}(\theta) &= -\frac{2\,2^{1/4}}{\sqrt{7}\pi^{3/4}}[2\cos(4\theta) + 2\cos(2\theta) - 1]\,,\\
q_1^{(2)}(\theta) &= -\frac{8}{147\pi}[25\cos(2\theta) + 25\cos(4\theta) - 21\cos(6\theta) + 166]\,,\\
q_4^{(1)}(\theta) &= -\frac{2\,2^{1/4}\sqrt{7}}{3\pi^{3/4}}[2\cos(2\theta) + 1]\,,\\
q_4^{(2)}(\theta) &= -\frac{2}{189\pi}[430\cos(2\theta) + 1727]\,.
\end{aligned} \tag{3.57}$$

Note that the fact that $\gamma^{(1)} > 0$ indicates that at least for sufficiently small Q, the mode that used to go negative for $AdS_2 \times S^3$, becomes positive! We shall see that this remains the case for all values of Q we have managed to probe.

For any other perturbation with $\ell \geq 3$ our perturbative scheme starts with non-trivial $\{\gamma^{(0)}, q_1^{(0)}, q_4^{(0)}(\theta)\}$, since $\gamma^{(0)}$ is non-zero at $Q = 0$ for any other value of $\ell \geq 3$ (see Fig. 3.2). For instance, for the $\ell = 3$ mode we find

$$\gamma = \frac{1}{2} - \frac{5\sqrt{7}}{4(2\pi)^{1/4}}\varepsilon + \frac{2987}{672\sqrt{2\pi}}\varepsilon^2 - \frac{317057}{6272\sqrt{7}(2\pi)^{3/4}}\varepsilon^3 + \mathcal{O}(\varepsilon^4)\,. \tag{3.58}$$

We now proceed using our exact numerical solutions for the background and by solving Eq. (3.53c) and Eq. (3.53d) numerically. We again use the numerical methods detailed in [37] to do this calculation. The results are displayed in Fig. 3.8 where we track the two lowest-lying modes. These are associated with $\ell = 2$ and $\ell = 3$ perturbations, respectively. Recall that for each $\ell \geq 2$ perturbation of $AdS_2 \times S^3$, there are two physical scaling exponents γ, which we labeled $\gamma_\pm(\ell, y_+)$. The perturbations we study naturally connect to $\gamma_-(\ell, 0)$ for $\ell = 2, 3$. Recall that for each value of ℓ, horizon boundary conditions allow us to discard two negative values of γ (which connect to the values of γ that we discard when we plot Fig. 3.2). Since the

lowest scaling exponent in Fig. 3.8 remains positive, this conclusively shows that the novel IR geometry is RG stable at the linear level to $SO(3)$-symmetric deformations. Furthermore, when Q is small enough, our perturbative results in Eq. (3.57) (dashed red line) and Eq. (3.58) (dotted black line) match well our exact numerical results given by the blue disks and orange squares for $\ell = 2, 3$, respectively.

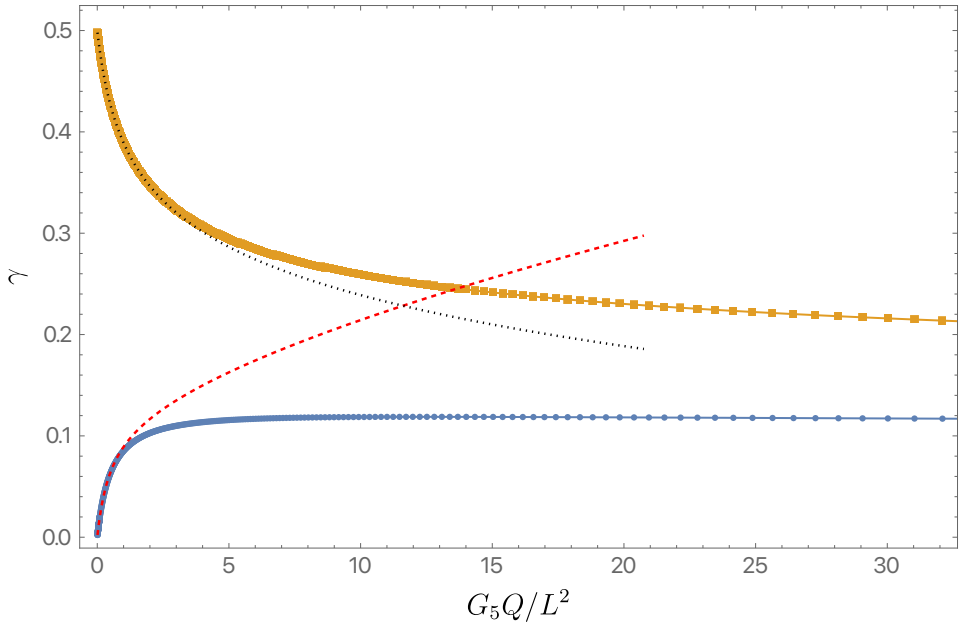

FIGURE 3.8: The two lowest lying modes of the quadratic Stürm-Liouville equations Eq. (3.53c) and Eq. (3.53d) governing perturbations of the new near-horizon geometries. The red dashed line shows the perturbative result displayed in Eq. (3.57), whereas the black dotted line shows γ given in Eq. (3.58). The blue disks have $\ell = 2$ and the orange squares have $\ell = 3$. In the language used in section 3.2, the modes shown both connect to $\gamma_-(\ell, 0)$.

We tracked the lowest lying mode all the way to $G_5 Q/L^2 \sim 3 \times 10^4$ and it remains positive, saturating at around $\gamma \approx 0.1013$.

3.3.4 RG instability of the new IR geometries with respect to $SO(3)$ breaking deformations

Having investigated the stability properties of the new IR geometries with respect to $SO(3)$-preserving deformations, we now ask whether the new geometries are stable with respect to deformations that break $SO(3)$. Unfortunately, this is *not* the case, as we show below.

We start by presenting an Ansätze for the metric and gauge field perturbations. These are necessarily more involved than the $SO(3)$ symmetric case. Since we want to break the symmetries of the round S^2, we expand all perturbations in terms of standard spherical harmonics $Y_{k\,m}(\chi, \phi)$ on S^2, where $\chi \in [0, \pi]$ and $\phi \sim \phi + 2\pi$ are the standard latitude and longitude angles on the round S^2, respectively. Spherical harmonics on the S^2 obey

$$\Box_{\Omega_2} Y_{k\,m} + k(k+1) Y_{k\,m} = 0\,, \tag{3.59}$$

with $k = 0, 1, 2, \ldots$ and $|m| \leq k$ being the standard quantum numbers of the spherical harmonics and $\Box_{\Omega_2}$ the standard Laplacian on the round two-sphere. The sector

with $k = 0$ was studied in the previous section, and the sector with $k = 1$ has to be treated separately. For this reason, we take $k \geq 2$ from here onward.

There are *two* types of gravito-electromagnetic perturbations that we can consider here. Perturbations built from scalar harmonics are often called scalar-derived gravito-electromagnetic perturbations, while perturbations built from vector harmonics are often coined vector-derived gravito-electromagnetic perturbations. The former sector is one of interest to us since one can easily show that vector-derived gravito-electromagnetic perturbations are RG stable.

Let $\check{D}$ be the metric preserving connection on the round two-sphere, so that $\check{D}_\alpha \check{D}^\alpha = \Box_{\Omega_2}$, with lower case Greek indices running on S^2, *i.e.* $\alpha = \{\chi, \phi\}$. We then introduce

$$S^{k\,m}_{\alpha\beta} \equiv \check{D}_\alpha \check{D}_\beta Y_{k\,m} + \frac{k(k+1)}{2}\, g_{\alpha\beta}\, Y_{k\,m}\,, \tag{3.60}$$

where $g_{\alpha\beta}$ being the metric on the round two-sphere. By construction, $S_{\alpha\beta}$ is traceless. We then write the following Ansätze for the metric and gauge field perturbations

$$\begin{aligned}\delta \mathrm{d}s^2 \equiv h_{ab}\mathrm{d}x^a \mathrm{d}x^b = L^2 \rho^\gamma \Bigg\{ & B(\theta)\, \frac{\hat{q}_1(\theta)}{\gamma}\, Y_{k\,m} \left(-A_0^2 \rho^2 \frac{\mathrm{d}t^2}{L^2} + \frac{\mathrm{d}\rho^2}{\rho^2} \right) \\ & + Y_+^2 \Big[H(\theta)^2\, \hat{q}_2(\theta)\, Y_{k\,m}\, \mathrm{d}\theta^2 + \frac{\sin^2\theta}{H(\theta)} \hat{q}_3(\theta)\, Y_{k\,m}\, \mathrm{d}\Omega_2^2 \\ & + 2\, \frac{\hat{q}_5(\theta)}{\gamma\, k}\, \mathrm{d}\theta\, (\check{D}_\alpha Y_{k\,m}) \mathrm{d}x^\alpha + \hat{q}_6(\theta)\, S^{k\,m}_{\alpha\beta} \mathrm{d}x^\alpha\, \mathrm{d}x^\beta \Big] \Bigg\}\,, \end{aligned} \tag{3.61a}$$

and

$$\delta A \equiv a_a \mathrm{d}x^a = -\rho_{\mathrm{IR}}\, A_0\, \rho^{1+\gamma}\, \hat{q}_4(\theta)\, Y_{k\,m}\, \mathrm{d}t\,. \tag{3.61b}$$

There are total of six functions of θ to solve for, namely $\{\hat{q}_1, \ldots, \hat{q}_6\}$. After some considerable algebra, one can express $\hat{q}_2$, $\hat{q}_3$ and $\hat{q}_6$ as a function of the remaining unknown functions and their first derivatives with respect to θ. We are thus left with three second-order ordinary differential equations in θ for $\{\hat{q}_1, \hat{q}_4, \hat{q}_5\}$. Regularity at the poles demands

$$\hat{q}_1(\theta) \approx \sin^k\theta\, \hat{C}_1\,, \quad \hat{q}_4(\theta) \approx \sin^k\theta\, \hat{C}_2 \quad \text{and} \quad \hat{q}_5(\theta) \approx \sin^{k-1}\theta\, \hat{C}_3\,, \tag{3.62}$$

where $\hat{C}_1$, $\hat{C}_2$ and $\hat{C}_3$ are constants. In order to impose these, we change to a new set of variables

$$\hat{q}_1(\theta) = \sin^k\theta\, \hat{Q}_1(\theta)\,, \quad \hat{q}_4(\theta) = \sin^k\theta\, \hat{Q}_2(\theta) \quad \text{and} \quad \hat{q}_5(\theta) = \sin^{k-1}\theta\, \hat{Q}_3(\theta) \tag{3.63}$$

with regularity at the poles now simply demanding

$$\hat{Q}_1'(0) = \hat{Q}_2'(0) = \hat{Q}_3'(0) = \hat{Q}_1'(\pi) = \hat{Q}_2'(\pi) = \hat{Q}_3'(\pi) = 0\,. \tag{3.64}$$

It is possible to cast, with the above boundary conditions, the second order differential equations for $\hat{Q}_1$, $\hat{Q}_2$ and $\hat{Q}_3$ as a Sturm-Liouville problem, where the combination $\gamma(\gamma+1)$ appears as the eigenvalue. This is the system we solve numerically using the numerical methods detailed in [37].

We start by using the perturbative scheme of section 3.3.1, which allows us to predict γ for small enough charge Q. Indeed, for $k = 2$ we find that

$$\gamma = -\frac{4\,2^{3/4}\sqrt{7}}{3\pi^{1/4}}\varepsilon + \frac{496}{27}\sqrt{\frac{2}{\pi}}\varepsilon^2 + \frac{6259984\,2^{1/4}}{11907\sqrt{7}\pi^{3/4}}\varepsilon^3 + \frac{52933540168}{26254935\pi}\varepsilon^4 + \mathcal{O}(\varepsilon^5)\,. \quad (3.65)$$

The fact that the first term in the ε expansion of γ is negative (note that we must take $\varepsilon > 0$ in order for our perturbative scheme to make sense) is a signal that our new geometries are RG unstable with respect to $SO(3)$ breaking perturbations. The question remains as to whether for larger values of the charge (or alternatively, larger values of ε) γ will become positive. In order to address this question we solve the problem numerically, and report our findings in Fig. 3.9. As a dashed red line we plot our perturbative result (3.65), while the exact numerical results are shown as blue disks. The agreement between the two at small charges is reassuring. The fact that γ remains *negative* for all values of the charge is the main result of this section and shows that our $SO(3)$ symmetric zero-temperature geometries are RG unstable to perturbations that break $SO(3)$. The endpoint of this $SO(3)$ breaking instability remains unknown and is under current investigation.

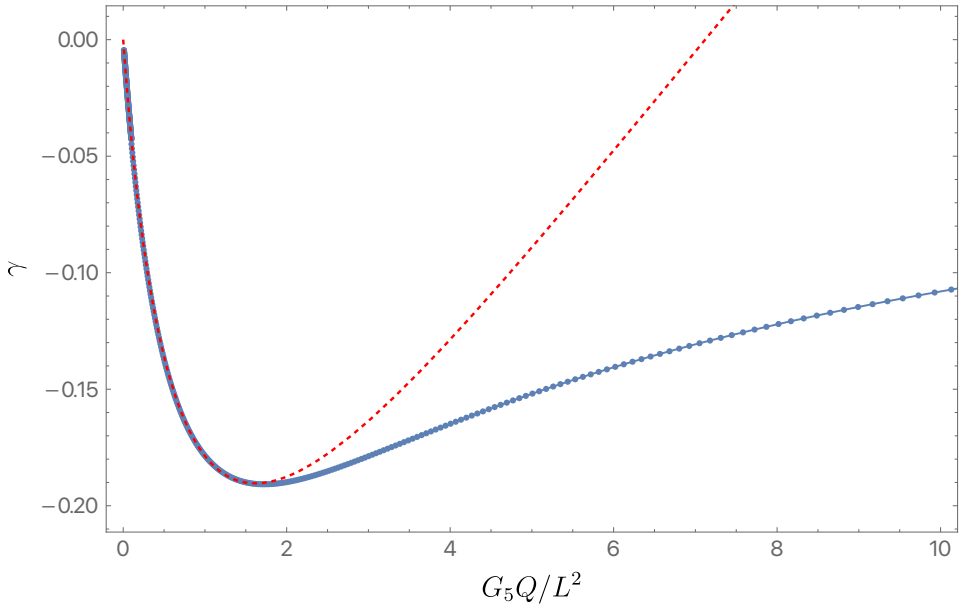

FIGURE 3.9: The lowest lying scaling exponent γ as a function of Q for $SO(3)$ breaking perturbations. The dashed red line is the perturbative result (3.65) whereas the blue disks label the exact numerical results. The agreement between the two at small charges is reassuring for both methods.

3.4 Toroidal black holes

We could repeat all the work performed in this Chapter also for the toroidal black holes. It may intuitively seem simpler since on the torus one works simply with periodic functions and does not need to worry about conical singularities. On the other hand, while spherical geometry is (up to scale) unique, the moduli space of three-dimensional torii is 6-dimensional. Indeed, a (flat) torus is $\mathbb{R}^3$ divided by discrete translations along three linearly independent vectors v_1, v_2, v_3. Up to rotations,

they are parameterized by their length and angles between them and thus we have a 6-dimensional family of geometries. As we will see, whether there are perturbative non-flat solutions nearby a given one depends not only on the scale but on all the details of the background geometry. Because discrete translations can be also thought of as generating a (crystal) lattice, we will use a crystallographic nomenclature when convenient.

Before diving into messy calculations, let us discuss what the picture that we should expect is. Based on Ch. 2, for very small torii, the scaling dimension γ may be very large and thus they are as smooth as needed. Then, there is a critical size at which they develop a null singularity ($0 < \gamma < 2$) along the lines of four-dimensional solutions. Finally, for even larger black holes we encounter RG instability ($\gamma < 0$). We are interested in the borderline case $\gamma = 0$. For the sake of brevity, we will work directly with the near-horizon geometry (it means we put $\gamma = 0$ from the very beginning). Let us start by describing the background. The metric reads

$$ds^2 = L^2 \left(\frac{1}{12} \left(-\rho^2 \mathrm{d}t^2 + \frac{\mathrm{d}\rho^2}{\rho^2} \right) + \mathring{q}_{ij} \mathrm{d}x^i \mathrm{d}x^j \right), \tag{3.66}$$

where $\mathring{q}_{ij}$ is a flat metric on $\mathbb{T}^3$. We normalize our toroidal coordinates in such a way that

$$x^i \sim x^i + 2\pi. \tag{3.67}$$

The potential is

$$A = -\frac{\sqrt{6}}{12} \rho \mathrm{d}t. \tag{3.68}$$

The charge inside clearly depends only on the volume of $\mathring{q}$. The general ansatz for this section is on the other hand:

$$ds^2 = L^2 \left(B(x^i) \left(-\rho^2 \mathrm{d}t^2 + \frac{\mathrm{d}\rho^2}{\rho^2} \right) + q_{ij} \mathrm{d}x^i \mathrm{d}x^j \right) \tag{3.69}$$

and

$$A = -q_{IR} \rho \mathrm{d}t. \tag{3.70}$$

We assume a perturbative expansion:

$$B = \frac{1}{12} + \sum_{I=1} B^{(I)}(x^i) \epsilon^I, \tag{3.71a}$$

$$q_{ij}(x^k) = \mathring{q}_{ij} + \sum_{I=1} q_{ij}^{(I)}(x^k) \epsilon^I \tag{3.71b}$$

and

$$q_{IR} = \frac{\sqrt{6}}{12} + \sum_{I=1} q_{IR}^{(I)} \epsilon^I \tag{3.71c}$$

We will now consider a simple example to illustrate the main difficulties we may encounter. Let

$$\mathring{q} = L_1^2 dx^2 + L_2^2 dy^2 + L_3^2 dy^2, \tag{3.72}$$

where $L_1 > L_2 > L_2$. Expanding Einstein-Maxwell equations in ϵ, we first find $q_{IR}^{(1)} = 0$. Then tt component of EOMs gives

$$B^{(1)} + \frac{1}{8L_1^2} \partial_{xx} B^{(1)} + \frac{1}{8L_2^2} \partial_{yy} B^{(1)} + \frac{1}{8L_3^2} \partial_{zz} B^{(1)} = 0. \tag{3.73}$$

Expanding $B^{(1)}$ into Fourier modes

$$B^{(1)}(x,y,z) = \sum_{\vec{k}\in\mathbb{Z}^3} (a_{\vec{k}}\cos(k_i x^i) + b_{\vec{k}}\sin(k_i x^i) \tag{3.74}$$

we see that solutions exist only if

$$\frac{k_x^2}{L_1^2} + \frac{k_y^2}{L_2^2} + \frac{k_z^2}{L_3^2} = 8. \tag{3.75}$$

Since we are interested in the lowest k, we have to choose $\vec{k} = (1,0,0)$ and $L_1 = \frac{1}{2\sqrt{2}}$. Thus[1],

$$B^{(1)} = \sin(x) \tag{3.76}$$

L_2, L_3 are arbitrary but smaller than L_1. Having found $B^{(1)}$, we may (upon a suitable gauge fixing) also determine $q^{(1)}$. It reads

$$q_{ij}^{(1)} = A_{ij} + B_{ij}\sin(x), \tag{3.77a}$$

where

$$B_{yy} = -24L_2^2 \tag{3.77b}$$

and

$$B_{zz} = -24L_3^2, \tag{3.77c}$$

and all other components of B_{ij} are zero. A_{ij} are completely arbitrary and they describe zero tensor modes that may become fixed by equations of higher order in ϵ.

Going to the next order is not any harder. It should be clear that we can expand all unknown functions in $1, \sin(x), \cos(x), \sin(2x), \cos(2x)$. Unfortunately, a direct calculation shows that the resulting equations are inconsistent. Thus, our linear perturbation cannot be lifted to a non-linear solution. The reason for this is a small symmetry of the underlying lattice. If we had, $L_1 = L_2 = L_3$, we could have simply written

$$B^{(1)} = \alpha_x\sin(x) + \alpha_y\sin(y) + \alpha_z\sin(z) \tag{3.78}$$

and then treat higher-order equations as constraints for $\alpha_x, \alpha_y, \alpha_z$. One could do the same with $L_1 = L_2 \neq L_3$ but then one would find still more constraints than free parameters. Examples will be presented shortly.

Before that, let us think for a moment about what these results suggest for the bulk. What if we started with a toroidal RN AdS_5 (of appropriate metric on the horizon) and then perturb boundary conditions by $\delta\mu \sim \sin(x)$? We still expect ∂_y, ∂_z to be Killing vector fields so we cannot expect just mentioned near-horizon geometries that perturbatively start with (3.78) to pop out. There is a different possibility though. It could happen that non-linearities drastically deform the horizon's geometry but in such a way that q_{ij} is still flat. Then, if q_{xx} is sufficiently small, we would not notice any problems at all. If this is the case, the toroidal black holes would be very boring. I do not know how to exclude that scenario a priori. However, a direct numerical calculation shows that it does not occur. Unfortunately, our accuracy is too small to conclude unambiguously what exactly happens. It seems relatively likely that in the limit $T \to 0$, the horizon could break into two pieces. Such infrared geometry (or rather: infrared geometries) would be of great interest from the

[1] We may always choose $\sin(x)$ instead of $\cos(x)$ by shifting x. In the same spirit, the coefficient can be chosen to be one by rescaling ϵ

holographic perspective. In particular, it *could* describe an insulating phase of the boundary[2]. I believe that this direction deserves much more attention than what I could have offered it so far.

3.4.1 Simple cubic torus

Having expressed all those comments, we will now construct a new geometry. Our starting point is a simple cubic torus[3]:

$$\mathring{q} = \frac{1}{8}\begin{pmatrix} 1 & 0 & 0 \\ 0 & 1 & 0 \\ 0 & 0 & 1 \end{pmatrix}. \tag{3.79}$$

We perturb it by[4]

$$B^{(1)} = \sin(x) + \sin(y) + \sin(z) \tag{3.80}$$

In general, we demand that

$$\int_{\mathbb{T}^3} B(x,y,z)\cos(x) = \int_{\mathbb{T}^3} B(x,y,z)\cos(y) = \int_{\mathbb{T}^3} B(x,y,z)\cos(z) = 0 \tag{3.81}$$

This is just a choice of a constant phase for (x,y,z). Additionally, we impose[5]

$$\int_{\mathbb{T}^3} B(x,y,z)\sin(x) = 4\pi^3\epsilon. \tag{3.82}$$

This is just a normalization condition for ϵ. Perturbative form of the metric (up to ϵ^2)[6] that starts with that seed is presented in Appendix B. It is an easy exercise to check that this geometry is still unstable – one of the zero modes obtains a scaling dimension γ that is negative and of order $O(\epsilon^2)$.

3.4.2 Graphene-like torus

The simple cubic perturbations have a discrete symmetry

$$\begin{aligned} \epsilon &\mapsto -\epsilon \\ (x,y,z) &\mapsto (x+\pi, y+\pi, z+\pi). \end{aligned} \tag{3.83}$$

As a result, any measurable quantity (like the total charge or scaling dimensions) must be an even function of ϵ. In this section, we shall consider a different background, for which perturbations with positive and negative ϵ are physically distinct. To this end, we wish to find a lattice on which $k = (1,0,0), (0,1,0), (1,1,0)$ have the

[2] It is a well-known result in AdS/CMT that *a single* black hole always corresponds to the conducting phase.

[3] The scale is of course chosen in such a way that there is a marginal perturbation.

[4] The equality (up to phase) between different Fourier modes is needed to ensure that the solution in the next order exists.

[5] One may be surprised that we do not impose this condition also on $\sin(y)$ and $\sin(z)$. Unfortunately, our further gauge choice is not symmetric with respect to permutations of (x,y,z), and at the third order in ϵ this would lead to inconsistencies.

[6] One should keep in my mind that at each order certain coefficients are left unknown and they become fixed in higher orders. To actually know unambiguously perturbation up to ϵ^2, we had to solve equations of motion up to the fourth order.

same length[7]. The most symmetric starting point is

$$\mathring{q} = \frac{1}{24}\begin{pmatrix} 4 & 2 & 0 \\ 2 & 4 & 0 \\ 0 & 0 & 3 \end{pmatrix}. \tag{3.84}$$

$z = const.$ surfaces have symmetries of a honeycomb. Thus one can imagine the underlying lattice as layers of graphene. In the first order, we find:[8]

$$B^{(1)} = \cos(x+y) + \sin(x) + \sin(y) + \sqrt{\frac{3}{2}}\sin(z) \tag{3.85}$$

Clearly, for this mode $\epsilon \mapsto -\epsilon$ is not a symmetry. Perturbative form of the metric (up to ϵ^3)[9] that starts with that seed is presented in Appendix B.

This expansion is not very illuminating in its own right. The most important question is what happens with zero modes of the background. Do they develop a power-law behavior, and if they do, with what exponent? To answer this question we should consider a zero mode that is also generated by

$$k = (1,0,0), (0,1,0), (1,1,0), (0,0,1), \tag{3.86}$$

but is different than the one above. Then, we should calculate its scaling dimension in the first order in ϵ. Of course, a random combination of those covectors will mix (at the next order) different powers of γ. One can check that a good starting point is

$$\delta B = \left(-(\alpha+\beta)\cos(x+y) + \beta\sin(y) + \alpha\sin(x)\right)\rho^\gamma + O(\epsilon). \tag{3.87}$$

Of course, we must also specify tensor modes. Then, depending on that specification, we obtain

$$\gamma = \frac{12}{5}(3 \pm \sqrt{14})\epsilon + O(\epsilon^2). \tag{3.88}$$

What is important is the fact that the numerical coefficient is positive (for the plus sign) or negative (for the minus sign). Thus, no matter what is the sign of ϵ, there is always a mode with $\gamma < 0$. We (again) reach a sad conclusion that our new solutions are RG unstable (at least for small ϵ).

3.5 Time-dependent perturbations

Let us now go back to the spherical black holes but ask a different question: what about time-dependent boundary conditions? For concreteness, let us imagine that we start extremal RN AdS in the bulk, and then at $t = t_i$ we deform BCs very slowly by changing $\mu = \mu(t,x)$ in such a way that at all t the boundary conditions are such as in Sec. 3.3[10]. Moreover, we keep the charge fixed. Then, at time $t = t_f$, the evolution stops, which means $\mu(t > t_f, x) = \mu(t_f, x)$. It seems that by making the change in μ very slow and $t_f - t_i$ very large, we should be able to do it almost

[7] One should keep in mind that k is a covector, so its norm is calculated using the inverse metric

[8] The coefficients are chosen to ensure that the higher-order constraints are satisfied.

[9] One should keep in my mind that at each order certain coefficients are left unknown and they become fixed in higher orders. To actually know unambiguously perturbation up to ϵ^3, we had to solve equations of motion up to the fifth order.

[10] There is no point in considering more general boundary conditions since we do not know what the stationary bulk solutions would be!

adiabatically. Now, the natural question that raises is: what would the result of this evolution be? I should emphasize that this section is much more speculative than the rest of this dissertation and it deserves a much deeper (probably numerical) study. Nevertheless, I find this issue so important that I believe it would be wrong of me to ignore it entirely.

Having said that, let me start by pointing out a small oversimplification I performed in the previous paragraph. Since the horizon is compact, it is rather unlikely that we may just treat any perturbation adiabatically. Indeed, any change in the boundary conditions requires pumping energy into the system. Since we start at $T = 0$ (and the horizon is compact), this will immediately increase the temperature. Thus, to be on the safe side, we should start at a finite (albeit very small in comparison to the area-radius of the horizon) temperature.

The naive picture of time evolution is very simple. The horizon will get deformed and it should slowly become more and more deformed reaching asymptotically the endpoint described in Sec. 3.3 (albeit at a slightly larger temperature). This is the only possible scenario in which the black hole stabilizes and becomes again static as $t \to \infty$ (as we usually assume while discussing any process in an *asymptotically flat* spacetime). However, a quick glance at Fig. 3.4 convinces us that this would lead to a violation of the Generalized Second Law of thermodynamics (which obviously cannot be an acceptable answer). Let us consider are our ways out of this situation:

(i) RN AdS is in fact RG stable

That statement may seem to be in direct contradiction with everything else said in this Chapter so far. However, one should note that only the extremal RN AdS_5 is unstable. There is no reason to expect any instability at a finite temperature. Based on dimensional analysis[11], we may expect that as long as

$$\frac{\delta\mu}{\mu} \ll (r_+ T)^{-\gamma}, \tag{3.89}$$

the endpoint's horizon should be close to the spherical symmetry and will not look like our deformed solutions. Then, there is no point in looking at the entropies shown in Fig. 3.4. However, it seems that (by making $t_f - t_i$ sufficiently long), we should be able to make $\delta\mu$ arbitrarily large still within the adiabatic approximation so this cannot be the full answer.

(ii) The assumption of adiabaticity is not valid

If this is the case, no matter how slowly we would change the boundary conditions, the rise in the temperature would be significant. It does not seem valid if we start at finite T. As discussed above, for very small $\delta\mu$, there is no way to observe the instability. Thus, the problems should arise at some finite deformation – we would need more and more energy to change μ, even extremely slowly. However, there is nothing to suggest that this is the case. (Of course, the final resolution must be based on the actual calculations, not just on simple observations or lack thereof!)

(iii) There is no stationary endpoint

If this statement is correct, we again do not need to worry about Fig. 3.4. However, it does not truly answer the question. Generalized Second Law still must

[11] To give perhaps a few more details, we expect (properly normalized) perturbations to behave close to the horizon as $\frac{\delta\mu}{\mu}(r_+ T)^\gamma$. If this quantity is small, we should be able to trust perturbation theory and not expect any large deviations from the spherical symmetry.

be satisfied and thus (now time-dependent) horizon's entropy will grow either way. Assuming it does not blow up[12], at least the horizon must settle down[13] so there is still a question of what is it actually.

(iv) RN AdS is actually a highly excited state

Since (again, at $T = 0$) RN AdS_5 is RG unstable, we may expect (based on the thermodynamical intuitions) that it is actually a local maximum of the (ADM) energy. Thus, it has more energy than the solutions of Sec. 3.3 and it actually evolves to their highly excited (and thus highly heated) counterpart. This may be seen as a more detailed version of the idea (ii).

This idea, though it may seem physically sound, possesses two drawbacks. First of all, we know that static solutions are always energy's minimizers (see [105] for the proof in the asymptotically flat context, I believe a similar claim is also true in AdS). Moreover, these two black holes exist for different boundary conditions[14] and thus they have different notions of ADM mass and there is no meaningful way to compare them. In particular, we could modify our action by any boundary functional of μ. At fixed μ that only shifts all the energy levels by a constant (and thus is not physical) but that would not be the case here, obviously. This shows that the whole discussion based on the ideas of energy is not rigorous.

Despite the hand-wavy nature of the last argument, I find it the most convincing. If this is correct, we should be not able to reach a small-temperature 'pancaked' horizon starting from the RN AdS. Of course, one should be open to the possibility that the proper numerical results will surprise us (again!)

3.6 Discussion

We have seen that the extremal Reissner-Nordström AdS solution does not provide a good dual description of the generic IR behavior of four (or higher) dimensional holographic theories. This is because its near-horizon geometry, $AdS_2 \times S^3$, is unstable to static perturbations that break $SO(4)$. We have constructed a new family of near-horizon geometries, labeled by the charge Q, and shown that they are stable to $SO(3)$-invariant linearized perturbations. Moreover, they are stable to nonlinear perturbations in this class, since they arise in the $T \to 0$ limit of an open family of $SO(3)$-invariant AdS black holes. Thus, following the usual holographic dictionary, under this reduced symmetry they represent stable IR fixed points of a dual RG flow.

Although our new IR geometries have the property that perturbations go to zero at the horizon, they are not generically completely smooth. As shown in Fig. 3.8, they go to zero like a power law with a power γ that is much less than one. This means that if we take two derivatives to compute the curvature, certain components will diverge. In other words, infalling observers experience diverging tidal forces at the horizon. For the solutions constructed in Sec. 4 that approach our new IR geometries, we have computed certain components of the Weyl tensor on the horizon

[12] That would be a surprising conclusion – an infinite shift of entropy generated by the finite energy inflow!

[13] This would be a solution similar to the well-known black resonators [36], for which the spacetime is not stationary but the horizon is still a Killing horizon

[14] At least at finite temperature, it would be interesting to understand what happens with the deformed solutions in the limit $\mu(x) \to const$.

as a function of T. We find that they diverge as $T \to 0$ in a way consistent with the perturbative argument in Sec. 3.3.

This is exactly analogous to the singularities described in Chapter 2. The main difference is that in four bulk dimensions, the horizon geometry remains $AdS_2 \times S^2$ and does not get distorted. As we have seen, all curvature scalars remain finite at the horizon, so if one analytically continues the solution to obtain a Euclidean black hole, it is completely smooth. The same will be true for the five-dimensional solutions constructed here. These singularities are only a feature of the Lorentzian solution, although they can affect thermodynamic quantities like the specific heat.

An important open problem is to find the generic stable IR geometry. In [66] another large class of $SO(3)$-invariant near-horizon geometries were constructed. They are associated with $\ell > 2$ instabilities of $AdS_2 \times S^3$ that only arise at large enough Q. However, all of them have at least one unstable $SO(3)$-invariant mode, so they are not stable RG fixed points, even under this reduced symmetry. Also, a very large class of near-horizon geometries without any rotational symmetry was constructed in that paper. These solutions exist close to $AdS_2 \times S^3$ when the S^3 is large enough. However, we expect these solutions will also be unstable since the unstable mode of $AdS_2 \times S^3$ should persist for the new solutions, via continuity.

We have also studied what happens for toroidal black holes. Similarly to the previous Chapter, small ones are as smooth as one wants them to be. Then, at some size, they become singular ($\gamma < 2$). If we further increase their volume, they become RG unstable ($\gamma < 0$). We constructed perturbatively new solutions that bifurcate from the RN AdS_5. The fundamental difference between spherical and toroidal BHs is that the moduli space of flat torii is 6-dimensional. Only for carefully chosen points from that space, do the bifurcating solutions exist. Otherwise, the linear perturbation (with $\gamma = 0$) does not satisfy additional quadratic constraints at higher orders in perturbation theory. All new solutions are RG unstable so also in this case the question for the endpoint is open.

In the previous Chapter we commented on the connections between our results and recent results in JT gravity (or rather its generalization obtained from the full dimensional reduction of a four-dimensional Einstein-Maxwell theory). We see that a higher-dimensional version of these calculations leads to even more radical effects. It seems sure that, if one tried to repeat the dimensional reduction to AdS_2 and then quantize Schwarzian, many problems would arise. Even without sources, since the KK modes are marginal (for $\Lambda = 0$) or relevant (for $\Lambda < 0$), their contribution to the partition function could compete with Schwarzian one. It would be exciting to see this story to unravel itself in more details in the future.

Chapter 4

Extremal black holes and UV physics

4.1 Motivation and introduction

In Chapter 2 we have seen that almost all extremal black holes in AdS_4 suffer from null singularities. These singularities affect not the infalling observers but also the black hole's thermodynamics. Thus, it seems rather discouraging that this interesting physics vanishes in the limit $\Lambda \to 0$. Nevertheless, let us emphasize that this is a result of a very unfortunate fine-tuning. The key geometrical ingredient, namely the scaling symmetry of the near-horizon limit, is still present. In particular, small charged black holes are generically singular for any $\Lambda \neq 0$. I could try to claim that since we live in a universe with a positive cosmological constant, these singularities are still present and we could observe them astrophysically. That would be a lie. Indeed, the cosmological constant is incredibly small and it is rather unlikely to observe highly charged black holes. Nevertheless, one could ask if there are different (so far neglected) corrections to the theory that make the scaling dimensions non-integer and lead to the effects larger than those based on the cosmological constant.

This is a perfect setting to use effective field theories. Instead of trying to come up with the corrected dynamics (and hope that this is a physically realized guess), we will consider all possible actions (up to a fixed number of derivatives) that are consistent with the symmetries of Einstein and Einstein-Maxwell theories. Unknown, small coefficients in front of the higher-derivative corrections should come from the UV degrees of freedom that we integrated out. As long as we will keep the coefficients arbitrary, we do not have to know too much about the UV completion[1]. As we will see in a moment, these corrections may be much larger than the cosmological constant.

4.1.1 A short introduction to gravitational EFTs

Let us start by considering a simple example of possible higher-derivative corrections to the Einstein-Hilbert action in four dimensions. This action contains two derivatives. The underlying theory is diffeomorphically invariant and we want to keep this symmetry. Thus, we may add to the Lagrangian only scalars built out of the metric, the Levi-Civita connection, and the Riemann tensor. It is not hard to check that there are no such terms with an odd number of derivatives. Thus, we should start with four derivative terms and there are five possible terms:

$$R^2, R_{\mu\nu}R^{\mu\nu}, R_{\mu\nu\alpha\beta}R^{\alpha\beta}, \nabla^\alpha\nabla_\alpha R, \nabla^\alpha\nabla^\beta R_{\alpha\beta}. \tag{4.1}$$

[1] In fact, there may be certain bounds on the coefficients to ensure that the theory is consistent. We will comment on them when we encounter such cases.

The last two are the full divergences and thus cannot affect equations of motion. (Besides, $\nabla^\alpha\nabla^\beta R_{\alpha\beta} = \frac{1}{2}\nabla^\alpha\nabla_\alpha R$, due to Bianchi identities.) Moreover, we have well-known Euler invariant

$$\mathcal{E} = \int_M \frac{\sqrt{-g}}{128\pi^2}\left(R_{\mu\nu\alpha\beta}R^{\alpha\beta} - 4R_{\mu\nu}R^{\mu\nu} + R^2\right) \tag{4.2}$$

Thus, only R^2 and $R_{\mu\nu}R^{\mu\nu}$ are independent. As a result, our effective action (up to four derivatives) reads[2]

$$S_{eff} = \frac{1}{2\kappa^2}\int d^4x\sqrt{-g}\left(R + 2d_1R^2 + 2d^2R_{\mu\nu}R^{\mu\nu}\right) \tag{4.3}$$

and we assume that c_1, c_2 are (in appropriate units to be specified later) small. S_{eff} may be further simplified. Indeed, let us consider a field redefinition

$$g_{\mu\nu} \mapsto g_{\mu\nu} + r_1R_{\mu\nu} + r_2Rg_{\mu\nu}, \tag{4.4}$$

where we again assume that r_1, r_2 are small. The change in the effective Lagrangian (to the first order in small parameters and ignoring the boundary terms) is simply

$$\delta\mathcal{L}_{eff} = -\frac{1}{2\kappa^2}\delta g_{\mu\nu}G^{\mu\mu}, \tag{4.5}$$

where $G_{\mu\nu} = R_{\mu\nu} - \frac{1}{2}Rg_{\mu\nu}$ is the Einstein tensor. As a result, the Wilson coefficients are changed:

$$d_1 \mapsto d_1 - \frac{1}{4}r_1 - \frac{1}{2}r_2 \tag{4.6a}$$

$$d_2 \mapsto d_2 + \frac{1}{2}r_1. \tag{4.6b}$$

Thus, we see that by an appropriate choice of r_1, r_2 we can make d_1, d_2 zero. Someone accustomed to thinking about the metric as a fundamental, somehow distinguished field may protest against those field redefinitions. However, the coefficients in the effective actions are usually derived in the context of the scattering and it is well-known fact that the $\mathcal{S}$ matrix is unchanged under them. Unfortunately, that means physically meaningful quantities (at, least in this approach) are only those that are invariant with respect to the field redefinitions. One can argue that the scaling dimensions satisfy that requirement. Indeed, we start with a smooth metric $\mathring{g}$ that describes the near-horizon region and smooth ($\mathring{\gamma} \in \mathbb{N}$) perturbations of that background. Field redefinitions (to leading order) are

$$g_{\mu\nu} \mapsto g_{\mu\nu} + h_{\mu\nu}[\mathring{g}], \tag{4.7}$$

where $h_{\mu\nu}$ is covariantly built out of $\mathring{g}$ (and $\mathring{F}$, if the Maxwell field is present) and thus is smooth (in particular, from the symmetry, it has the same $\mathring{\gamma}$). If g exhibit non-integer power law behavior with a scaling dimension γ, so must $g + h$ since the addition of something smooth cannot change the singular part of g. We will see this explicitly in the case of Reissner-Nordström.

Having checked that there are no non-trivial terms with four derivatives, let us discuss what happens with six or eight derivatives. One can check [20, 40] that

[2] Since it is important to keep track of the scales involved, we will restore units in this Chapter. In our conventions $\kappa = \sqrt{8\pi G}$.

modulo field redefinitions, the only possible terms are[3]

$$\mathcal{L} = \frac{1}{2\kappa^2}\left(R + \eta_e \kappa^4 \mathcal{R}^3 + \lambda_e \kappa^6 \mathcal{C}^2 + \tilde{\lambda}_e \kappa^6 \tilde{\mathcal{C}}^2\right), \tag{4.8}$$

where we define

$$\mathcal{R}^3 \equiv R_{ab}{}^{cd} R_{cd}{}^{ef} R_{ef}{}^{ab}, \tag{4.9a}$$

$$\mathcal{C} \equiv R_{abcd} R^{abcd} \tag{4.9b}$$

and

$$\tilde{\mathcal{C}} \equiv \tilde{R}_{abcd} R^{abcd}. \tag{4.9c}$$

with the dual tensor

$$\tilde{R}_{abcd} = \epsilon_{ab}{}^{pq} R_{pqcd}. \tag{4.9d}$$

In the above, η_e, λ_e, and $\tilde{\lambda}_e$ are dimensionless. We will discuss in detail the effect these operators have on the scaling dimensions in Sec. 4.3. Before that, let us state the equations of motion:

$$R_{ab} - \frac{1}{2} R g_{ab} = T^{\text{cubic}}_{ab} + T^{\text{quartic}}_{ab}, \tag{4.10}$$

where

$$T^{\text{cubic}}_{ab} = \eta_e \, \kappa^4 \left[3\, R_a{}^{cde} R_{de}{}^{gh} R_{ghcb} + \frac{1}{2} g_{ab} R_{gh}{}^{cd} R_{cd}{}^{ef} R_{ef}{}^{gh} - 6 \nabla^c \nabla^d \left(R_{acgh} R_{bd}{}^{gh}\right)\right] \tag{4.11a}$$

and

$$T^{\text{quartic}}_{ab} = -\lambda_e \, \kappa^6 \left(8 R_{acbd} \nabla^c \nabla^d \mathcal{C} + \frac{g_{ab}}{2} \mathcal{C}^2\right) - \tilde{\lambda}_e \, \kappa^6 \left(8 \tilde{R}_{acbd} \nabla^c \nabla^d \tilde{\mathcal{C}} + \frac{g_{ab}}{2} \tilde{\mathcal{C}}^2\right). \tag{4.11b}$$

We will also consider Einstein-Maxwell theory. The well-known Lagrangian is

$$\mathcal{L} = \frac{R}{2\kappa^2} - \frac{1}{4} F_{\mu\nu} F^{\mu\nu}, \tag{4.12}$$

where $F = dA$. Then, there exist non-trivial EFTs with four derivatives. Indeed, the most general (orientation-preserving) one is

$$\begin{aligned} \mathcal{L}_4 = {} & d_1 R^2 + d_2 R_{\mu\nu} R^{\mu\nu} + d_3 R_{\alpha\beta\gamma\delta} R^{\alpha\beta\gamma\delta} \\ & + \kappa^2 (d_4 R F^2 + d_5 R^{\mu\nu} F^2_{\mu\nu} + d_6 R^{\mu\nu\alpha\beta} F_{\mu\nu} F_{\alpha\beta}) \\ & + \kappa^4 (d_7 (F^2)^2 + d_8 F^2_{\mu\nu} F^{2\mu\nu}), \end{aligned} \tag{4.13}$$

The most general field redefinition is

$$g_{\mu\nu} \mapsto g_{\mu\nu} + r_1 R_{\mu\nu} + r_2 R g_{\mu\nu} + r_3 \kappa^2 F_{\mu\alpha} F_\nu{}^\alpha + r_4 \kappa^2 g_{\mu\nu} F_{\alpha\beta} F^{\alpha\beta}. \tag{4.14}$$

Then, only certain combinations of fields are invariant with respect to those redefinitions. These are:

$$d_0 := d_2 + 4 d_3 + d_5 + d_6 + 4 d_7 + 2 d_8, \tag{4.15a}$$

$$d_9 := d_2 + 4 d_3 + d_5 + 2 d_6 + d_8 \tag{4.15b}$$

and d_3, d_6. As we have discussed at the beginning, nothing can depend on d_3 since

[3] We omit parity-odd terms that cannot change the scaling dimensions in the leading order

we can reabsorb it into d_1, d_2 using the Euler invariant. Nevertheless, we will keep it to make contact with the literature. Moreover, in higher dimensions, (4.13) is still the most general Lagrangian we could have. The definitions of d_0, d_9 slightly change but d_3, d_6 remain invariant. With the κ^2 insertions we made, all d_i are dimensionless.

Before we proceed to the calculations we have in mind, let us explain the general logic guiding us here. If we had a UV completion of our theory (or at least if we knew which degrees of freedom from the full theory are relevant in the IR), we could calculate gravitons' and photons' scattering amplitudes (up to an appropriate number of loops). Then, we could ask what form of S_{eff} is needed to recover those results and in this way fix our coefficients. For now, we will skip this part and simply assume that they are small. Then, from S_{eff} we derive equations of motion. Then we solve them perturbatively in the higher-curvature coefficients up to the first order.

Let us emphasize that it would not be consistent to do it in the second order. To do so, we had to include in the action terms with even more derivatives (that can be now generated also through more loops). Notice that our calculations of the scaling dimensions will be affected at two stages. First of all, higher curvature corrections will modify the near-horizon background we consider. Let us emphasize that due to (4.14) the spacetime metric is not an invariant object. Then, on this background, we may consider linearized Einstein(-Maxwell) equations, also with additional corrections. Finally, we expand solutions to the linearized equations of motion with respect to d_i. In this way, a solution to the zeroth order (in other words: a solution to linearized Einstein-Maxwell equations without any EFT additions) serves as a source for the next order. From our previous discussions, it follows that stationary solutions may be decomposed into powers of the radial coordinate. This statement does not depend on the equations of motion but only on their geometric nature and the symmetries of the background. Since all near-horizon geometries are scale-invariant, this claim still holds.

4.2 Reissner-Nordström deformed

4.2.1 Four dimensions

Let us start with the Reissner-Nordström background. It is much easier than Kerr because we can stick with the four-derivative action (4.13) and use the spherical symmetry to reduce the problem to purely algebraic equations. We will repeat all the steps mentioned in the previous section to illustrate them. All equations used in this part were generated using the Mathematica suite of packages *xAct* (*xCoba* and *xPert*, to be more precise) [17]. The EOMs are rather lengthy and not especially illuminating so I will not write them down specifically.

Step 1: Deform the background

We start on the Berttoti-Robinson background:

$$ds^2 = r_+^2\left(-\frac{\mathrm{d}t^2}{z^2}+\frac{\mathrm{d}z^2}{z^2}+\mathrm{d}\theta^2+\sin^2\theta\mathrm{d}\phi^2\right) \tag{4.16a}$$

and

$$F^{tr} = -\frac{\sqrt{2}}{\kappa r_+^3}z^2. \tag{4.16b}$$

In the coordinates (t, z, θ, ϕ) the horizon is located at $z = \infty$. Our background has a lot of symmetries, namely $O(2,1) \times SO(3)$. We wish to find a solution

to the EFT equations of motion (up to terms linear in d_i) with the same symmetries. This is a simple exercise since the form of the metric is fixed by the symmetries uniquely and we only need to find (constant) coefficients. At the end of the day, we find[4]

$$g_{tt} = -\frac{1}{z^2}\left(r_+^2 - (4d_5 + 8d_6 + 32d_7 + 16d_8) + \Delta\right) \tag{4.17a}$$

$$g_{zz} = \frac{1}{z^2}\left(r_+^2 - (4d_5 + 8d_6 + 32d_7 + 16d_8)\right) \tag{4.17b}$$

$$F^{tz} = -\frac{\sqrt{2}}{\kappa r_+^3} z^2 \left(1 - \frac{4}{r_+^2}(d_4 + d_5 + 2d_6 + 6d_7 + 3d_8) - \frac{\Delta}{2r_+^2}\right). \tag{4.17c}$$

The presence of the constant Δ (that is supposed to be of order d_i) is a manifestation of the fact that the rescaling $t \mapsto \alpha t$ is not physically meaningful near the horizon. The proper normalization of ∂_t can be prescribed only in the asymptotically flat region. Nevertheless, because this rescaling is unphysical, no measurable result should depend on Δ. We may use it as an additional check of our calculations.

Step 2: Deform linearized EOMs
In the next step, we have to write down the deformed (again, up to terms linear in d_i) (linearized) equations of motions on the just-derived background. We may write them schematically as

$$E_0[\delta g, \delta F] + \sum_{i=1}^{8} d_i E_i[\delta g, \delta F] = 0, \tag{4.18}$$

where E_0 and E_i are linear operators. Note that E_i terms are built out of two different contributions. On one hand, they come from Einstein-Maxwell equations on the *deformed* background. On the other hand, $\mathcal{L}_4$ also modify linearized equations on the *undeformed* background. There is no need to distinguish between those two contributions. Because the equations are long, we shall not write them down explicitly. Everything was done in Mathematica anyway.

Step 3: Solve the resulting equations
The only thing that remains is to solve the resulting equations. We do it perturbatively, which means that we write

$$\delta g = \delta g_0 + \epsilon \delta g' \tag{4.19a}$$

and

$$\delta F = \delta F_0 + \epsilon \delta F', \tag{4.19b}$$

where $\epsilon = O(d_i)$ and

$$E_0[\delta g_0, \delta F_0] = 0. \tag{4.20}$$

[4] We will keep the radius r_+ fixed. This is not a physically proper way to do this because r_+ cannot be measured at infinity. Instead, we should rather keep the charge constant. Moreover, let me also point out that in the EFT, the horizon's area no longer has an interpretation of the entropy. Instead, one should use Wald's prescription [107]. In particular, this entropy is a well-defined quantity only as a function of charge and mass, not as a function of the radius. Nevertheless, because the scaling dimensions in the two-derivative theory do not depend on the size of a black hole, this cannot affect our results.

Then, we are left with:

$$\epsilon E_0[\delta g', \delta F'] = -\sum_{i=1}^{8} d_i E_i[\delta g_0, \delta F_0]. \tag{4.21}$$

In our case, we are interested only in static, scalar-derived perturbations. Thus, we may use the decomposition (2.37), only now coefficients f, h_L, h_T, h, q, w, z and the exponent γ are functions of ϵ. In this way, we may write (4.21) as a non-homogeneous matrix equation for $\frac{d}{d\epsilon}(f, h_L, h_T, h, q, w, z)|_{\epsilon=0}$. (The most interesting part, namely $\frac{d}{d\epsilon}\gamma|_{\epsilon=0} = \gamma_1$ does contribute actually as a source, on the RHS of the equation). This system in general is inconsistent unless γ_1 takes a particular value. To my bitter disappointment, that value happens to be $\gamma_1 = 0$. Thus, (the leading order) EFT corrections cannot make Reissner-Nordström horizon singular. The positive part of the answer is that it is definitely field-redefinitions invariant and does not depend on the unphysical parameter Δ. The same conclusion holds also for vector-derived perturbations.
It would interesting to understand whether this is just a numerical coincidence or maybe a result of some properties of RN. The fact that $\gamma_{\epsilon=0}$ is an integer may be understood on the grounds of dimensional analysis. The black hole has only one dimensionful parameter $Q = M$ so there is no way to create a dimensionless quantity and so γs must be Q-independent. However, this argument does not work in the EFT.

4.2.2 Five (and higher) dimensions

Not discouraged by this failure, we shall investigate what happens in higher dimensions. The procedure is analogous. The only (rather technical) difference is that we can have now zero modes. For such modes, $\delta g_0, \delta F_0$ are described by two free parameters h_L, h_T (while for all other modes, they are described by h_T only). However, h_L becomes fixed to zero when we go to the first order in ϵ. Since *xCoba* enforces one to work in a concrete dimension D, I had to derive γ_1 for each dimension D separately. I did it, up to $D = 11$. There is a very simple formula that describes the results in all those dimensions:

$$\gamma_1 = -d_0 \frac{8\kappa^2 (D-4)\ell(\ell+D-3)}{(D-3)^2(D-2)(2\ell-D+3)r_+^2}, \tag{4.22}$$

where

$$\begin{aligned} d_0 = {} & \frac{1}{4}(D-3)\left(2D^2-11D+16\right) d_2 + \frac{1}{2}\left(2D^3-16D^2+45D-44\right) d_3 \\ & + \frac{1}{4}(D-3)(D-4)^2 d_1 \frac{1}{2}(D-3)(D-2)(D-4) d_4 \\ & + \frac{1}{2}(D-3)^2(D-2)(d_5+d_6) + (D-3)(D-2)^2\left(d_7 + \frac{d_8}{2}\right) \end{aligned} \tag{4.23}$$

is an invariant combination of the Wilson coefficients. The obvious conjecture is that this result holds for any $D \geq 4$. A few remarks are in place:

- Weak Gravity Conjecture (WGC) implies that d_0 is positive. Thus, $\gamma_1 < 0$ for $\ell > \frac{D-3}{2}$.

- Since for $\ell = D-3 > \frac{D-3}{2}$, $\gamma_0 = 0$, it follows that the exponent becomes negative. As a result, a 5-dimensional extremal Reissner-Nordström black hole becomes RG unstable (in the nomenclature of the previous Chapter). For $D > 5$, it was already unstable but now there are more modes leading to that instability.
- Note that when $\gamma < 0$, the scalar quantities may actually diverge at the horizon. That would signalize the breakdown of the EFT approach, since $\mathcal{L}_4$ could be comparable to $\mathcal{L}_2$.
- In $D = 5$, $\ell = 3$ mode (without deformation) had $\gamma = \frac{1}{2}$ so it was on the threshold of being a weak solution. Since $\gamma_1 < 0$, it cannot be a weak solution in EFT[5].
- As a general rule, it seems that EFT corrections make black holes more singular. As we already mentioned, the only exceptions are $\ell < \frac{D-3}{2}$ modes. Nevertheless, for them $\gamma_0 < 0$ and so the perturbative treatment is not justified anyway.
- If we take $\ell \gg D$, the associated perturbation is as smooth as we want (at least if we ignore non-linearities that would produce all possible modes). Thus, a small change in the exponent could not be detected in any reasonable experiment.
- This γ_1 was calculated for modes $+-$ using the notation from the previous Chapters. The scaling dimensions for $++$ also depend only on d_0.
- A similar calculation can be performed also for vector and tensor modes. In $D = 4$, vector scaling dimensions are not changed (and there are no tensor ones). In higher dimensions, they are shifted. Although the shift is invariant, it does not have a positivity bound, as far as I know.

It seems rather peculiar that the change in the exponent is described by such a simple formula that depends only on d_0. Moreover, it is exactly d_0 that becomes constrained by the Weak Gravity Conjecture. In a sense, it seems that UV degrees of freedom (whatever they are) seem to destabilize extremal black holes in more than one way. Nevertheless, it is still an open question of what is the endpoint of the instability – a different geometry or maybe naked singularity in the bulk? As it is hopefully clear from the list of our remarks above, EFT is not necessarily to be trusted when $\gamma < 0$. Thus, in my opinion, this result is the most interesting in $D = 5$ where it signifies that *something qualitatively* changes when we introduce higher-curvature corrections.

4.3 Kerr deformed

We expand the metric as

$$g_{ab} = g^{(0)}_{ab} + \eta_e\, h^{(6)}_{ab} + \lambda_e\, h^{(8)}_{ab} + \tilde{\lambda}_e\, \tilde{h}^{(8)}_{ab}\,, \tag{4.24}$$

[5]Of course, since our EFT introduces higher derivatives, it is far from obvious that the notion of weak solutions remains the same. Nevertheless, our arguments regarding black hole thermodynamics for $\gamma < \frac{1}{2}$ could still hold

with $g^{(0)}$ satisfying the vacuum Einstein equation, and solve Eqs. (4.10) and (4.11) to linear order in the EFT coefficients $\{\eta_e, \lambda_e, \tilde{\lambda}_e\}$ [6]. To study tidal force singularities, we are interested in the leading behavior of the Weyl tensor associated with the EFT-corrected metric. The effects of interest to this paper only become important near the horizon of a nearly-extremal black hole, since they arise from unusual scaling in the near horizon region when the horizon becomes arbitrarily far away (in spacelike directions). For this reason, we can focus mainly on the near-horizon geometry. We do this in two steps: i) we EFT-correct the near-horizon extreme Kerr (NHEK) geometry [9], and ii) we then determine how metric perturbations fall off near the horizon by computing the so-called scaling dimensions γ.

We focus on extremal black hole solutions that are stationary and axisymmetric with respect to $k = \partial/\partial t$ and $m = \partial/\partial\phi$, respectively. Furthermore, we will impose the symmetry $(t, \phi) \to -(t, \phi)$. The most general ansatz compatible with the symmetries above can be written as

$$\begin{aligned} \mathrm{d}s^2 = 2\,J\,\Omega^2\Big[&-\rho^2\mathrm{d}t^2 + \frac{F_1}{\rho^2}\left(\mathrm{d}\rho + \rho\,F_2\,\mathrm{d}x\right)^2 \\ &+ \frac{\mathrm{d}x^2}{A} + B^2(\mathrm{d}\phi + \rho\,\omega\,\mathrm{d}t)^2\Big], \end{aligned} \tag{4.25}$$

where the factors of ρ are adjusted so that $\rho = 0$ is a Killing extremal horizon, $\phi \sim \phi + 2\pi$, and Ω, ω, A, B, F_1, and F_2 are functions of ρ and x, with $(\rho, x) \in \mathbb{R}^+ \times [-1, 1]$. To fix the gauge, we further impose $F_1 = 1$ and $F_2 = 0$. In the above, all coordinates are dimensionless, and in the case of the NHEK solution, J is simply the Kerr angular momentum (in geometric units of length squared given by the size of the black hole).

4.3.1 The EFT-corrected near horizon geometries

In order to find the near horizon geometry, we start by imposing $\mathrm{O}(2,1) \times \mathrm{U}(1)$ symmetry, in which case we take $\Omega = \Omega_{\mathrm{NH}}(x)$ and $B = B_{\mathrm{NH}}(x)$ in Eq. (4.25) to be functions of x only, as well as taking $A = A_{\mathrm{NH}} = (1 - x^2)/\Gamma_{\mathrm{NH}}^2$, with Γ_{NH} and $\omega = \omega_{\mathrm{NH}}$ constants. The resulting line element reads

$$\begin{aligned} \mathrm{d}s^2_{\mathrm{NH}} = 2\,J\,\Omega^2_{\mathrm{NH}}\Big[&-\rho^2\mathrm{d}t^2 + \frac{\mathrm{d}\rho^2}{\rho^2} + \frac{\Gamma^2_{\mathrm{NH}}\,\mathrm{d}x^2}{1 - x^2} \\ &+ B^2_{\mathrm{NH}}(\mathrm{d}\phi + \rho\,\omega_{\mathrm{NH}}\,\mathrm{d}t)^2\Big]. \end{aligned} \tag{4.26}$$

[6] We note that second-order perturbation $\delta h^{(6)}_{ab}$ from $\mathcal{R}^3$ at $O(\eta_e^2)$ is smaller than the linear-order quartic-Riemann perturbation $h^{(8)}_{ab}$ via the following reasoning. The linear perturbation from the cubic-Riemann term, by Eqs. (4.10) and (4.11), is given schematically by $\Box h^{(6)}_{ab} \sim \eta_e \mathcal{R}^3$, so $h^{(6)}_{ab} \sim \eta_e \kappa^4/J^2$. Then the $O(\eta_e^2)$ back-reaction effect is generated via the equation of motion as $\Box \delta h^{(6)}_{ab} \sim (\nabla h^{(6)}_{ab})^2 + \eta_e \mathcal{R}^2 \delta\mathcal{R} \sim \eta_e^2 \kappa^8/J^5$, so $\delta h^{(6)}_{ab} \sim \eta_e^2 \kappa^8/J^4$. In comparison, the linear-order metric perturbation $h^{(8)}_{ab}$ from the quartic-Riemann operator is generated schematically via $\Box h^{(8)}_{ab} \sim \lambda_e \mathcal{R}^4$, so $h^{(8)}_{ab} \sim \lambda_e \kappa^6/J^3$ and analogously for $\tilde{\lambda}_e$. Hence, $(\delta h^{(6)}_{ab})/(h^{(8)}_{ab}) \sim (\eta_e^2/\lambda_e)(\kappa^2/J)$, which we should be able to make arbitrarily small for sufficiently large black holes. Indeed, by the dispersion relation arguments of [21], one has $\eta_e^2/\lambda_e \lesssim 1/(\kappa^2 \Lambda_{\mathrm{UV}}^2)$, for Λ_{UV} the energy scale of new physics, so as long as the size of the black hole is larger than the Compton wavelength of the UV states generating the higher-dimension operators (which must be the case to apply the EFT in the first place), we indeed find that the $O(\eta_e^2)$ is negligible.

The first two terms in brackets correspond to the metric on a two-dimensional unit-radius AdS_2, with $\rho = 0$ being the location of the AdS_2 Poincaré horizon.

We expand all quantities appearing in Eq. (4.26) as

$$\begin{aligned}
\Omega_{\rm NH}&=\Omega^{(0)}(x)\left[1+\eta_e\Omega^{(6)}(x)+\lambda_e\Omega^{(8)}(x)+\tilde{\lambda}_e\tilde{\Omega}^{(8)}(x)\right]\\
B_{\rm NH}&=B^{(0)}(x)\left[1+\eta_e B^{(6)}(x)+\lambda_e B^{(8)}(x)+\tilde{\lambda}_e\tilde{B}^{(8)}(x)\right]\\
\Gamma_{\rm NH}&=\Gamma^{(0)}\left[1+\eta_e\Gamma^{(6)}+\lambda_e\Gamma^{(8)}+\tilde{\lambda}_e\tilde{\Gamma}^{(8)}\right]\\
\omega_{\rm NH}&=\omega^{(0)}\left[1+\eta_e\omega^{(6)}+\lambda_e\omega^{(8)}+\tilde{\lambda}_e\tilde{\omega}^{(8)}\right].
\end{aligned} \tag{4.27}$$

For $\eta_e = \lambda_e = \tilde{\lambda}_e = 0$ we recover the NHEK geometry, for which

$$\Omega^{(0)}(x)=\sqrt{\tfrac{1+x^2}{2}},\ B^{(0)}(x)=\tfrac{2\sqrt{1-x^2}}{1+x^2},\ \Gamma^{(0)}=\omega^{(0)}=1. \tag{4.28}$$

Proceeding to the next order, we determine the corresponding EFT corrections. For instance, we find

$$\begin{aligned}
\Gamma^{(6)} &= -\frac{15\kappa^4}{32\sqrt{2}J^2}, \qquad \omega^{(6)} = \frac{\kappa^4}{7J^2},\\
\Gamma^{(8)} &= -\frac{366435\,\kappa^6}{256\sqrt{2}J^3}, \quad \omega^{(8)} = \frac{(4864+1575\pi)\,\kappa^6}{20J^3},\\
\tilde{\Gamma}^{(8)} &= -\frac{368829\,\kappa^6}{64\sqrt{2}J^3}, \quad \tilde{\omega}^{(8)} = \frac{(4736+1575\pi)\,\kappa^6}{5J^3},
\end{aligned} \tag{4.29}$$

where some of these constants were chosen to ensure the absence of conical singularities near the poles $x = \pm 1$. Explicit expressions for $\Omega^{(I)}_{\rm NH}(x)$ and $B^{(I)}_{\rm NH}(x)$ can be found in the supplementary material (Sec. D.1).

4.3.2 Deforming the EFT-corrected NHEK geometries

Having found the new near-horizon geometries, we now study how they respond to external tidal deformations. These deformations are generated by simply having the near-horizon geometry connected to an asymptotically flat region. We expect such deformations to become arbitrarily small near the extremal horizon, and as such, we can use perturbation theory to study their properties.

We again start with Eq. (4.25) with $F_1 = 1$ and $F_2 = 0$, but now Ω, B, A and ω can be functions of both x and ρ. Since we are perturbing around an $O(2,1) \times U(1)$-symmetric solution and we are restricting our attention to stationary and axisymmetric perturbations, we decompose our perturbations in terms of harmonics on AdS_2 with dependence on ρ only. These turn out to be power-law solutions of the form ρ^γ. We thus set

$$\begin{aligned}
A(\rho,x) &= A_{\rm NH}(x)\left[1+\varepsilon\,\rho^\gamma\,Q_1(x)\right]\\
B(\rho,x) &= B_{\rm NH}(x)\left[1+\varepsilon\,\rho^\gamma\,Q_3(x)\right]\\
\Omega(\rho,x) &= \Omega_{\rm NH}(x)\left[1+\varepsilon\,\rho^\gamma\,Q_2(x)\right]\\
\omega(\rho,x) &= \omega_{\rm NH}\left[1+\varepsilon\,\rho^\gamma\,Q_4(x)\right],
\end{aligned} \tag{4.30}$$

with ε being a bookkeeping parameter we take to be infinitesimally small. All the Q_i, with $i = 1, 2, 3, 4$, and γ have an expansion in η_e, λ_e, and $\tilde{\lambda}_e$ of the form

$$\begin{aligned} Q_i(x) &= Q_i^{(0)}(x) + \eta_e Q_i^{(6)}(x) + \lambda_e Q_i^{(8)}(x) + \tilde{\lambda}_e \tilde{Q}_i^{(8)}(x) \\ \gamma &= \gamma^{(0)} + \eta_e \gamma^{(6)} + \lambda_e \gamma^{(8)} + \tilde{\lambda}_e \tilde{\gamma}^{(8)}. \end{aligned} \tag{4.31}$$

The main goal of this paper is to determine the corrections to the scaling dimension $\gamma^{(6)}$, $\gamma^{(8)}$, and $\tilde{\gamma}^{(8)}$, since these control the deviation from the standard Kerr result. At each order, we find that $Q_2^{(I)}$ and $Q_3^{(I)}$ can be expressed in terms of $Q_1^{(I)}$ and $Q_4^{(I)}$ and their first derivatives. We are thus left with two second-order differential equations for $Q_1^{(I)}$ and $Q_4^{(I)}$.

For $I = 0$, i.e., deviations away from NHEK, the equations for $Q_1^{(0)}$ and $Q_4^{(0)}$ are second-order homogeneous equations of the Sturm-Liouville type where $\gamma^{(0)}$ appears as an eigenvalue. These can be solved analytically in terms of standard Legendre polynomials P_ℓ of degree ℓ (see Sec. D.2 of the supplementary material). We find two classes of solutions, labeled by $\gamma_\pm^{(0)}$, with critical exponents given by [7]

$$\begin{aligned} \gamma_+^{(0)}(\ell) &= \ell \qquad \text{with} \quad \ell \in \mathbb{N} \geq 2, \\ \gamma_-^{(0)}(\ell) &= \ell + 1 \quad \text{with} \quad \ell \in \mathbb{N} \geq 1. \end{aligned} \tag{4.32}$$

Since the scaling exponents are positive integers, the perturbation decays and the horizon remains perfectly smooth. In other words, without higher-derivative corrections, the extremal Kerr horizon is unaffected by these deformations.

For fixed values of ℓ, there are two *distinct* values of $\gamma^{(0)}$, thus yielding a non-degenerate spectrum at fixed ℓ at zeroth order. We can thus proceed using standard perturbation theory. The resulting equations can again be solved analytically for each value of ℓ, and after some algebra one finds

$$\begin{aligned} \gamma_+^{(6)}(2) &= \gamma_-^{(6)}(1) = \frac{24\,\kappa^4}{7J^2} \\ \gamma_+^{(8)}(2) &= -\frac{21(32+45\pi)\kappa^6}{5J^3} \\ \gamma_-^{(8)}(1) &= -\frac{9(8576+3045\pi)\kappa^6}{20J^3} \\ \tilde{\gamma}_+^{(8)}(2) &= -\frac{12(736+315\pi)\kappa^6}{5J^3} \\ \tilde{\gamma}_-^{(8)}(1) &= -\frac{189(384+145\pi)\kappa^6}{5J^3}\,. \end{aligned} \tag{4.33}$$

At the moment we have no understanding of why $\gamma_-^{(6)}(1) = \gamma_+^{(6)}(2)$. Furthermore, $\gamma_-^{(I)}(\ell-1) \leq \gamma_+^{(I)}(\ell)$ for fixed values of ℓ.

Even though these are small corrections, the scaling exponent is no longer an integer, so when $\gamma < 2$ the curvature will diverge. The reader might worry that we have done this calculation using coordinates that are not regular at the extremal horizon. In the supplementary material in Sec. D.3, we give an explicit map between

[7] There is also an $\ell = 1$ mode for γ_+ that is not pure gauge, but it does not contribute to tidal forces. It is analogous to the $\ell = 0$ mode in spherically symmetric systems that changes M or Q.

the Kerr-like coordinates of Eq. (4.25) and Bondi-Sachs coordinates, which are manifestly regular at $\rho = 0$. It is in Bondi-Sachs coordinates that we compute the relevant components of the Weyl tensor and find diverging tidal force singularities at the future (and past) extremal event horizon so long as $\gamma < 2$.

Since the metric is C^1 but not C^2, Einstein's equations remain well defined in a distributional sense. However, since the event horizon is a Cauchy horizon for a constant-t hypersurface, the evolution is not unique.

4.4 Kerr-Newman black hole and RG stability

Let us consider yet another possibility for changing the theory. Instead of taking into account higher-curvature corrections, we may introduce additional matter fields. Thus, we will generalize the results of (2.2). We will replace a massless Klein–Gordon field with a charged, massive one. In the spirit of this Chapter, we shall put the cosmological constant to zero but allow for the rotations of the black hole. Thus, we consider a scalar field of mass m and charge q on the background of the extremal Kerr–Newman black hole[8]. We will work only close to the horizon, ignoring the question of the far-away asymptotics, sources for the scalar fields, and the way we shall avoid no-hair theorems.

In the Schwarzschild-like coordinates $(t, \rho, x\psi)$, the near-horizon geometry of the extremal Kerr-Newman black hole may be written down as

$$ds^2 = 2J_t\Omega(x)^2\left(-\rho^2 \mathrm{d}t^2 + \frac{\mathrm{d}\rho^2}{\rho^2} + \frac{\mathrm{d}x^2}{1-x^2} + \Lambda(x)^2(\mathrm{d}\psi + \rho\omega \mathrm{d}t)^2\right) \tag{4.34a}$$

and

$$A = \frac{Q_t\sqrt{J_t}}{2\Omega(x)^2}\left((1-(1-Q_t^2)x^2)\rho \mathrm{d}t + \sqrt{1-Q_t^2}(1-x^2)\mathrm{d}\psi\right), \tag{4.34b}$$

where

$$\Omega(x) = \frac{\sqrt{\left(1-Q_t^2\right)x^2+1}}{\sqrt{2}}, \tag{4.34c}$$

$$\Lambda(x) = \frac{\left(2-Q_t^2\right)\sqrt{1-x^2}}{\left(1-Q_t^2\right)x^2+1} \tag{4.34d}$$

and

$$\omega = \frac{2\sqrt{1-Q_t^2}}{2-Q_t^2}. \tag{4.34e}$$

As is usual in the spherical coordinates, $x \in [-1, 1]$ and ψ is a periodic function on $[0, 2\pi)$[9] J_t and Q_t are connected to the angular momentum J and charge Q as

$$J_t = \frac{J}{\sqrt{1-Q_t^2}} \tag{4.35a}$$

[8] Non-extremal black holes in AdS are known to develop scalar hairs – this is the key ingredient for the holographic superconductors. The fate of those condensates as $T \to 0$ may vary [67], in particular allowing for singular limits.

[9] The reason we use ψ instead of ϕ shall be clear soon.

and

$$Q_t = \frac{Q}{r_+}, \tag{4.35b}$$

where r_+ is the Boyer-Lindquist radius of the horizon.

On this background, we consider a field Ψ of charge q and mass m. It means, under gauge transformations

$$A \mapsto A + d\lambda, \tag{4.36}$$

it changes as

$$\Psi \mapsto e^{iq\lambda}\Psi. \tag{4.37}$$

The covariant (gauge-field) derivative acting Ψ gives

$$\mathcal{D}_a\Psi = \nabla_a\Psi - iqA_a\Psi, \tag{4.38}$$

and so under gauge transformations, we have

$$\mathcal{D}_a\Psi \mapsto e^{iq\lambda}\mathcal{D}_a\Psi. \tag{4.39}$$

Then, the equation of motion for the scalar field reads

$$g^{ab}\mathcal{D}_a\mathcal{D}_b\Psi - m^2\Psi = 0. \tag{4.40}$$

We will now try to solve Einstein-Maxwell-scalar equations perturbatively starting with the Kerr-Newman background. Since $\Psi = 0$ on the background, we must start simply with (4.40). Let us keep the axial symmetry. Since we are dealing with a linear equation, we may still use the symmetries of the background to decompose the perturbation with respect to the scaling dimensions. Thus, without a loss of generality, we take

$$\Psi(\rho, x) = \rho^\gamma P(x). \tag{4.41}$$

We will discuss how smoothness depends on ρ in a moment. (4.40) written in terms of P reads

$$\begin{aligned} 0 = {} & P(x)\left(Q_t^2-2\right)^2\left(\gamma^2+\gamma+\mu_t^2\left(\left(Q_t^2-1\right)x^2-1\right)\right) \\ & - P(x)q_t^2Q_t^2\left(Q_t^4-Q_t^2\left(x^2-1\right)+x^2-1\right)+\left(Q_t^2-2\right)^2\left(\left(x^2-1\right)P''(x)+2xP'(x)\right), \end{aligned} \tag{4.42}$$

where the rescaled parameters are

$$\mu_t = m\sqrt{J_t} \tag{4.43a}$$

and

$$q_t = q\sqrt{J_t}. \tag{4.43b}$$

Since the coefficient in front of $P(x)$ is just a linear combination of a constant and of x^2, a well-educated Reader immediately recognizes this as a Helmholtz equation written in the spheroidal coordinates:

$$(1-z^2)y'' - 2zy' + (\lambda + u^2(1-z))y = 0, \tag{4.44}$$

where λ is an eigenvalue and u measures the deviation from spherical symmetry (substitutions $u = 0$ recovers the well-known Legendre equation). Since it is a

Sturm-Liouville problem, there are countably many regular eigenfunctions[10] (ordered by their eigenvalues). We see that in our case

$$u = \sqrt{1-Q_t^2}\sqrt{\mu_t^2 - \frac{q_t^2 Q_t^2}{\left(2-Q_t^2\right)^2}}. \tag{4.45}$$

Taking $P(x)$ to be the ℓth eigenfunction, we get a quadratic equation for γ. Choosing (as in Sec. 2.2), a larger solution gives

$$\gamma = \frac{1}{2}\left(\sqrt{4\lambda_\ell - \frac{4q_t^2 Q_t^6}{\left(2-Q_t^2\right)^2} + 4\mu_t^2\left(2-Q_t^2\right)+1} - 1\right) \tag{4.46}$$

It may look rather implicit, so let us plot it. An example of γ behavior with respect to the parameters of the black hole is shown in Fig. 4.1. Interestingly enough, at some point, γ becomes negative which is a sign of instability – even a small (stationary) source for the scalar field far away will lead to extremely large values close to the extremal horizon. As a result, the perturbation theory breaks down and we may expect that the Kerr-Newman horizon hole is replaced either by a deformed horizon or by a singularity. In the latter case, one expects this singularity to be even more serious than the ones discussed in the Chapter 2 – those would correspond to the case $0 < \gamma < 1$.

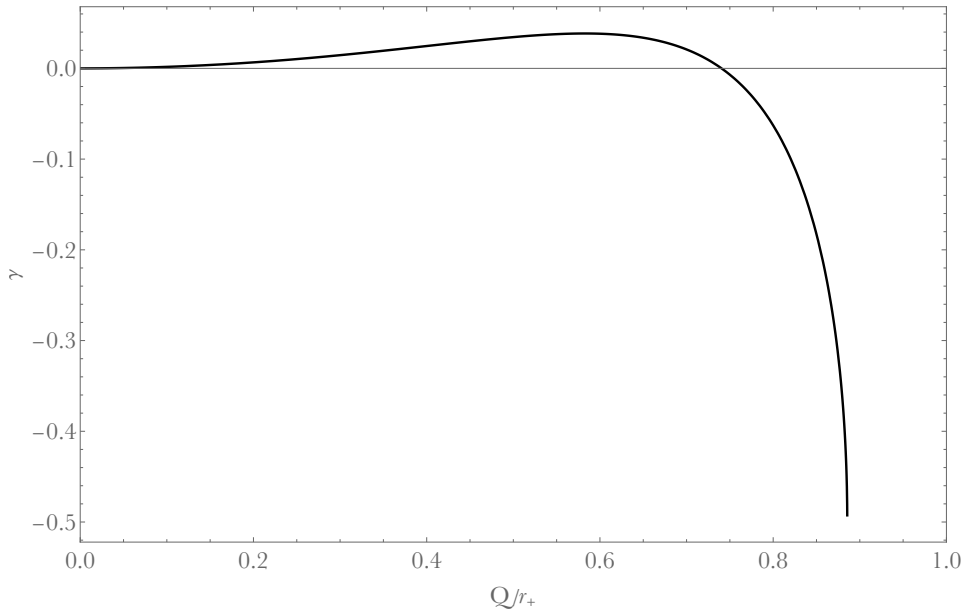

FIGURE 4.1: The scaling dimensions of the scalar field as a function of the black hole's parameter. In this example, $\ell = 0$, $\mu_t = 0$ and $q_t = 1$. For larger values of $\frac{Q}{r_+}$, the scaling dimension becomes complex.

The fact that we can get $\gamma < 0$ is not a result of a particularly bad choice of parameters. In fact, we find the instability (for sufficiently large $\frac{Q}{r_+}$) for any scalar field provided that $|q| \geq m$ (see Fig. 4.2 for an example). When the inequality is saturated, $\gamma = 0$ on the Reissner-Nordström background. Incidentally, the condition

[10] They are called the angular spheroidal functions of the first kind $P_{n,0}(u,z)$. In Mathematica, they are implemented as SpheroidalPS(n,0,u,z)

$|q| \geq m$ is the simplest version of the Weak Gravity Conjecture [55] stating that every consistent quantum theory incorporating gravity must have in its spectrum a particle for which the gravity is the weakest force. The primary motivations behind the WGC are exactly extremal black holes and possible channels of their decay. It is rather amusing to find out that it has such exciting implications even in the classical regime. We have encountered WGC a few times already in this story. Whether it is just a coincidence or a sign of a deeper connection between the two topics is yet to be understood.

Even more, there are parameters (below the orange line in the Fig. 4.2) such that $\gamma = -\frac{1}{2} \pm i\alpha$ for a non-zero (real) constant α. Such solutions are not only highly singular but also oscillate close to the horizon. A complex scaling dimension close to the AdS boundary would be seen as a violation of the Breitenlohner-Freedman (BF) bound. There is an analogous interpretation in the near-horizon region. Indeed, the NHG of Kerr-Newman is essentially a bundle of AdS_2 spaces over a non-homogeneous S^2. In a small patch on a sphere, we can treat the Maxwell field as effectively constant, and then our solution (locally) behaves like a neutral Klein–Gordon of a mass[11] $m^2 + q^2A^2$. It is a BF bound associated with those local AdS_2 and local effective masses that is violated here. Of course, due to the non-trivial bundle structure, AdS_2 spaces over different points of S^2 have different radii and would result in different BF bounds. Nevertheless, qualitatively, this is exactly what happens here.

4.4.1 The next order

Having found modes with $\gamma = 0$, one must feel tempted to go beyond the first order in the perturbation theory. There is a natural hope that maybe we could find a new near-horizon geometry. In the second order, we would have to solve Einstein and Maxwell equations sourced by Ψ. Let us start our discussion by calculating the $U(1)$ current. The standard formula is

$$j_a = i\left(\Psi^\star \mathcal{D}_a \Psi - \mathcal{D}_a \Psi^\star \Psi\right). \tag{4.47}$$

When $\gamma = 0$, Ψ is real and thus it simplifies:

$$j_a = qP(x)^2 A_a \tag{4.48}$$

From the current, we can read off the charge density, which is $\star j \sim \rho^{-1}$, and evidently diverges close to the horizon. This may seem rather surprising – why a smooth solution would lead to a non-regular charge distribution[12]?
To see how we should correct the The answer to this question lies in Eq. (4.34). Unfortunately, the Maxwell potential we used is not well-defined at the horizon. Thus, the smoothness of Ψ is just an artifact of the non-smoothness of A. We will proper solutions in a moment. Before that, let us notice that j_a is a gauge invariant quantity. As a result, Ψ written in a well-behaved gauge cannot be smooth.

To see what a smooth Maxwell potential looks like, let us start by changing coordinates to ones well-defined at the horizon. To this end, we write

$$t = v + \frac{1}{\rho} \tag{4.49a}$$

[11] Since the potential A is timelike, the second term in fact decreases the mass

[12] An attentive Reader will notice that not only the charge distribution is diverging, but also that the total charge stored close to the horizon is infinite

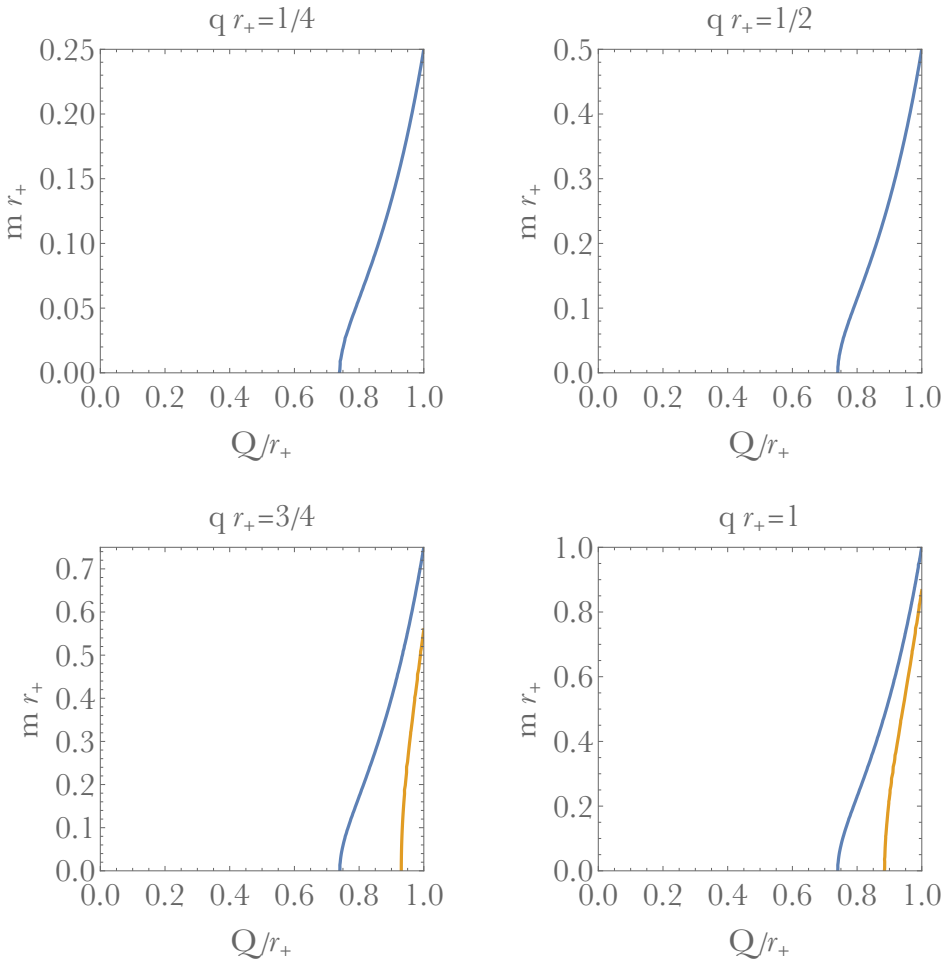

FIGURE 4.2: The scaling dimensions of the scalar field as a function of the black hole's parameter and its own mass. Below the blue line, γ is negative and thus the black hole is unstable. Below the orange one, $\mathrm{Re}\gamma = -\frac{1}{2}$ and $\mathrm{Im}\gamma \neq 0$. In this example, $\ell = 0$. We see that for fields with a small charge, BF bound is not violated (at least for positive mass squared).

and

$$\psi = \phi + \omega \log \frac{\rho}{r_+}. \tag{4.49b}$$

Clearly coordinates (v, ρ, x, ϕ) are well-defined at the horizon. Let us look at A:

$$\begin{aligned} A = &\frac{\mathrm{d}\rho \sqrt{J_t} Q_t^3}{\rho \left(Q_t^2 - 2\right)} + \frac{\mathrm{d}v \sqrt{J_t} \rho Q_t \left(-\left(\left(Q_t^2 - 1\right) x^2\right) - 1\right)}{\left(Q_t^2 - 1\right) x^2 - 1} \\ &+ \frac{\mathrm{d}\phi \sqrt{J_t} \sqrt{1 - Q_t^2} Q_t \left(x^2 - 1\right)}{\left(Q_t^2 - 1\right) x^2 - 1}. \end{aligned} \tag{4.50}$$

Since the coordinates are regular, clearly A is not due to the first term. However, the irregular part may be easily fixed by a simple (also singular) gauge transformation:

$$A \mapsto A - d\left(\frac{\sqrt{J_t} Q_t^3}{\left(Q_t^2 - 2\right)} \log \frac{\rho}{r_+}\right). \tag{4.51}$$

Under this gauge transformation, the scalar field becomes:

$$\Psi \mapsto e^{-iq\left(\frac{\sqrt{I_t}Q_t^3}{\left(Q_t^2-2\right)}\log\frac{\rho}{r_+}\right)}\Psi \sim \rho^{\gamma-iq\frac{\sqrt{I_t}Q_t^3}{\left(Q_t^2-2\right)}}P(x). \tag{4.52}$$

We thus see that the proper scaling dimensions are complex from the very beginning. In particular, if $\gamma = 0$, the scalar field is not even continuous at the horizon due to the oscillatory term. That explains why we found j_a to be singular as well.

Let us emphasize that from the discussion above it follows that any stationary solution cannot be smooth because $\mathrm{Im}\gamma \neq 0$. As a result, a single mode is of C^{k-1} class, where $k = \lfloor \mathrm{Re}\gamma \rfloor$.

4.4.2 Beyond the axial symmetry

For completeness, let us now discuss what happens if the perturbation is not axially symmetric. Since ∂_ϕ is a Killing vector of the background, we may decompose solutions into Fourier modes. In Schwarzschild-like coordinates, they will read

$$\Psi = e^{im\psi}\rho^\gamma P(x), \tag{4.53}$$

whereas in the global coordinates:

$$\tilde{\Psi} = e^{im\phi}\rho^{\tilde{\gamma}}P(x), \tag{4.54}$$

where

$$\tilde{\gamma} = \gamma - iq_t\frac{Q_t^3}{Q_t^2-2} + im\omega. \tag{4.55}$$

(We used Ψ and $\tilde{\Psi}$ to emphasize that those are the same object but written in a different gauge).

Either way, P satisfies an analogous equation as before but now with additional m-dependence. At the end of the day, the solutions are

$$P(x) = P_{n,m}(x,u), \tag{4.56}$$

where

$$u = \frac{\sqrt{\left(1-Q_t^2\right)\left(m^2\left(Q_t^2-1\right)-2mq_tQ_t\sqrt{1-Q_t^2}-q_t^2Q_t^2+\mu_t^2\left(Q_t^2-2\right)^2\right)}}{2-Q_t^2} \tag{4.57}$$

and analogously

$$\begin{aligned}\gamma = -\frac{1}{2Q_t^2-4}\Bigg[&-4\Big(2m^2\left(Q_t^4-5Q_t^2+4\right)+2mq_t\left(Q_t^2+2\right)\sqrt{1-Q_t^2}Q_t\\&+q_t^2Q_t^6-\lambda\left(Q_t^2-2\right)^2+\mu_t^2\left(Q_t^2-2\right)^3\Big)+Q_t^4-4Q_t^2+4\Bigg]^{\frac{1}{2}}-\frac{1}{2}\end{aligned} \tag{4.58}$$

In particular, we see that $m \mapsto -m$ is the same as $Q_t \mapsto -Q_t$. For this reason, we will restrict to $m \in \mathbb{N}$ and assume instead that $Q_t \in [-1,1]$.
For certain parameters we may obtain $\gamma < 0$ or $\gamma = -\frac{1}{2} + \alpha i, \alpha \in \mathbb{R}$ (see Fig. 4.3 below). In these aspects, the breaking of the axial symmetry does not change too

much. There is however one difference. If

$$q_t = m\omega \frac{Q_t^2 - 2}{Q_t^3} \tag{4.59}$$

$\tilde{\gamma}$ is going to be real (provided that γ is real). As a result, if $\gamma \in \mathbb{N}$, then also $\tilde{\gamma} \in \mathbb{N}$ and the mode is actually smooth. Unfortunately (after a numerical search) we found out that with this condition γ is bounded by 1 (see Fig. 4.4) The bound is saturated only by the Reissner-Nordström black hole and massless (yet charged!) scalar field. As a result, among smooth solutions there are no zero modes.

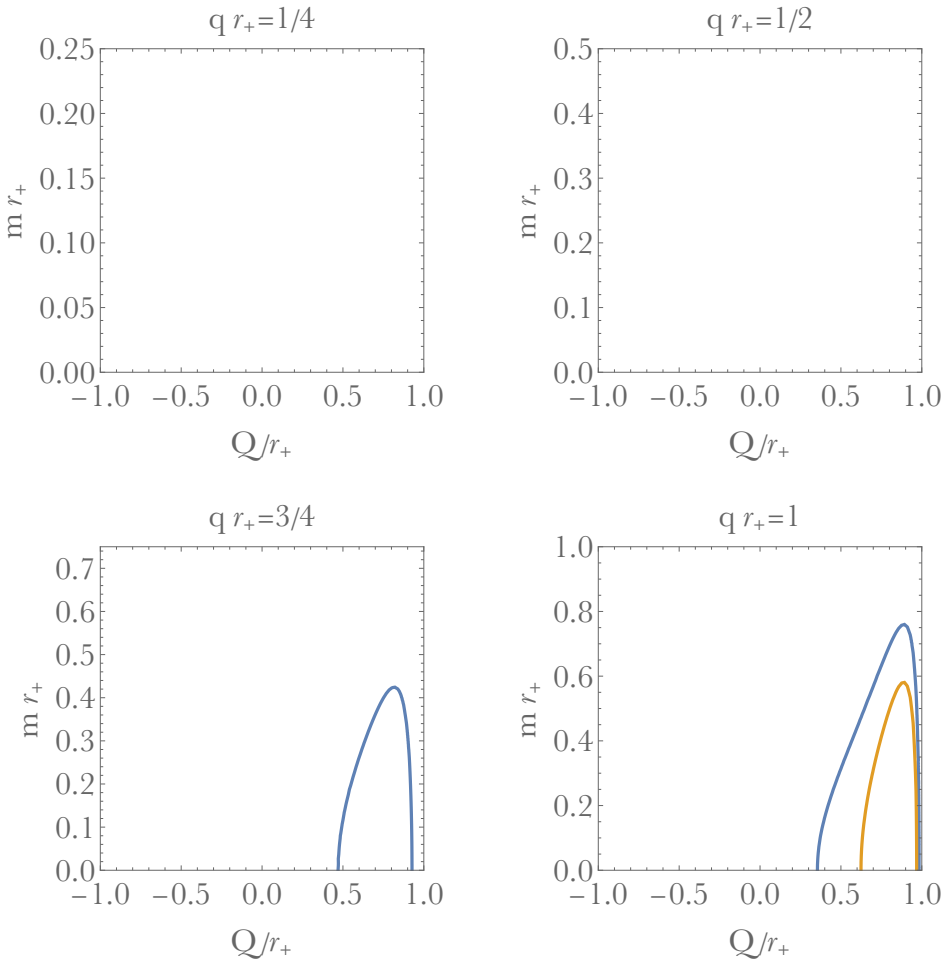

FIGURE 4.3: The scaling dimensions of the scalar field as a function of the black hole's parameter and its own mass. Below the blue line, γ is negative and thus the black hole is unstable. Below the orange one, Re$\gamma = -\frac{1}{2}$ and Im$\gamma \neq 0$. In this example, $\ell = 1, m = 1$. As one may see, for sufficiently small scalar's charges, the black hole is stable with respect to this mode (at least for non-negative m^2)

We shall not get discouraged by the fact that we found no interesting solutions so far and instead come back to our favorite $\Lambda < 0$ case (to be more precise: Kerr-Newman AdS). Then, finding γ requires actual (easy) numerics – one needs to find an eigenvalue of a simple ODE on an interval $[-1, 1]$. Instead of doing that (and producing not a very clear plot), let us just describe qualitatively what may happen.

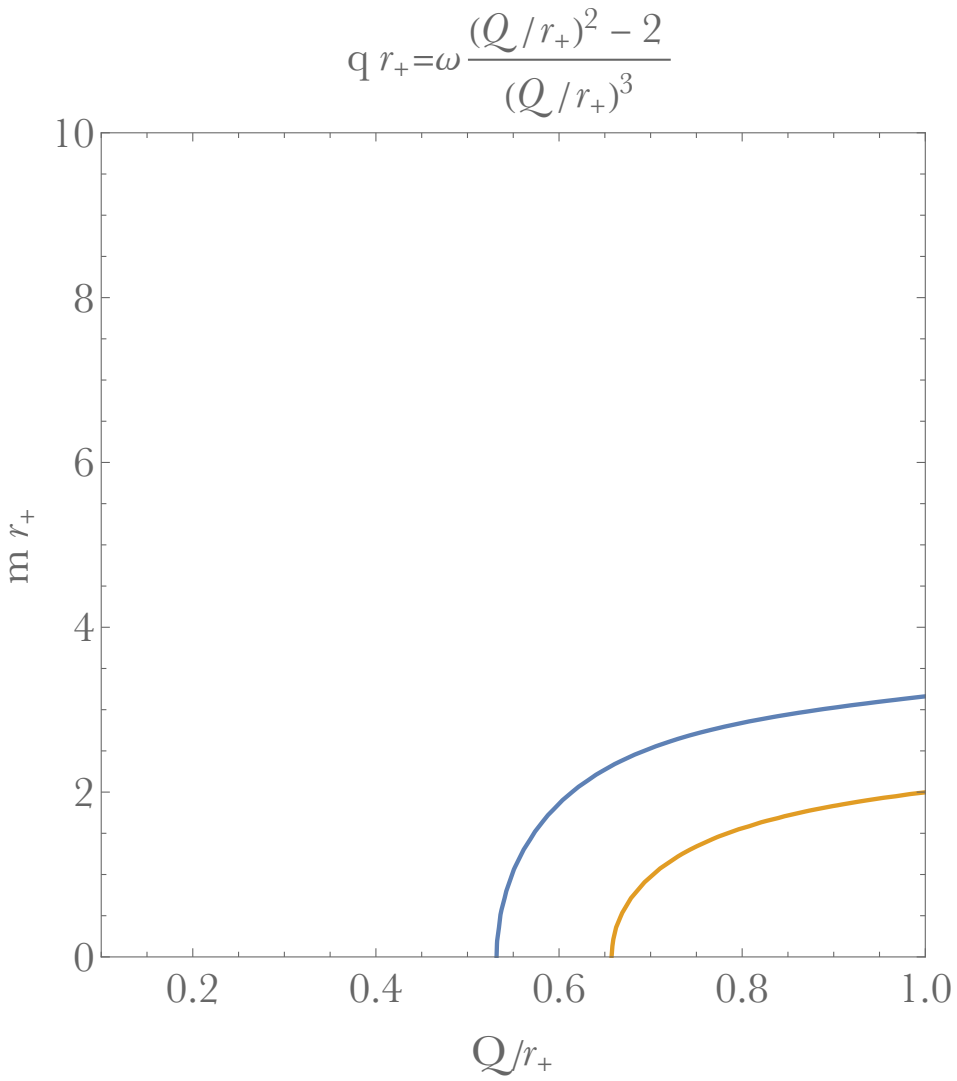

FIGURE 4.4: The scaling dimensions of the scalar field as a function of the black hole's parameter and its own mass. At the blue line $\gamma = 3$. At the orange one, $\gamma = 2$. In this example, $\ell = 1, m = 1$.

As before, we want to impose a condition that $\tilde{\gamma}$ is real. This condition reads

$$q_t \sim m\omega, \tag{4.60}$$

where the proportionality constant does not depend on the field. In particular, if we take the limit $\omega \to 0$, we have $q_t = 0$. Thus, on the background of RN AdS, only neutral scalar fields can have real scaling dimensions. In this case, we may find it exactly. It reads

$$\gamma_\pm = \frac{1}{2}\left[\pm\sqrt{1+\frac{4\left(\ell(\ell+1)+\mu^2 r_+^2\right)}{1+6\,r_+^2/L^2}}-1\right]. \tag{4.61}$$

Clearly, for $\mu^2 = -\frac{\ell(\ell+1)}{r_+^2}$, the exponent will vanish. Thus, we have a proper zero mode. Of course, as a result, we have to consider a field with negative mass squared. In AdS, this is not a problem as long as this mass is larger than the (four-dimensional)

BF bound:

$$\mu^2 \geq m_{BF}^2 = -\frac{9}{4L^2}. \tag{4.62}$$

Thus, such novel horizons could be embedded into AdS as long as

$$\frac{r_+^2}{L^2} > \frac{8}{9}. \tag{4.63}$$

We expect (and the aforementioned numerics confirms that) if we turn on a small rotation (while keeping its extremal) if we change the charge and mass accordingly, we may still find a zero-mode that is truly smooth. It would be a fun exercise to go beyond the first order in this calculation. It seems likely that this time we should not encounter any problems in the second order and the zero-mode could be uplifted to the full non-linear solution for a near-horizon geometry. At the same time, let us notice that this novel configuration is still RG unstable. $\ell = 0$ mode of Ψ is going to be badly divergent at the horizon. Unfortunately, that may limit any holographic usefulness of these solutions.

Let us quickly summarize the results of this Section. Scalar fields satisfying the Weak Gravity Conjecture $q > m$ may render sufficiently charged Kerr-Newman solutions unstable. There is no new solution bifurcating at the onset of the instability. Thus, one may only speculate what the endpoint of the instability is. Either way, it should be something very different in comparison to the Kerr-Newman solution (and its near-horizon limit). If we consider Kerr-Newman AdS instead, for sufficiently large black holes, there is a smooth zero mode (for a field with fine-tuned charge and mass above the BF bound) that we could uplift to a new non-linear solution for the near-horizon geometry. Unfortunately, the same charged field renders this configuration unstable due to badly divergent $\ell = 0$ mode.

4.5 Observations and discussions

The fate of the black hole horizon depends sensitively on the signs of the coefficients of the higher-dimension operators. From our calculation of the scaling dimensions, we see that extremal Kerr black hole horizons develop singularities if η_e is negative or if λ_e, or $\tilde{\lambda}_e$ are positive. Further, if $d_0 > 0$, then the extremal RN black hole in five dimensions develops a singular horizon [13]. The signs of the various Wilson coefficients in the EFT is therefore of paramount importance in determining the nature of the horizon.

Fortuitously, there exists an infrared consistency program of bounding the coefficients of EFTs from first principles using the tools of analytic dispersion relations in QFT, in a manner agnostic of the details of the UV theory [1]. Using either analyticity and unitarity of scattering amplitudes [11] or causality of graviton propagation [51], one can prove that, in any consistent theory of quantum gravity, the coefficients of the quartic Riemann operators λ_e and $\tilde{\lambda}_e$ must be positive. This is borne out in string theory [11], where calculations of the low-energy EFT yield $\lambda_e = \alpha'^3[13 + \zeta(3)]/8\kappa^6$ and $\tilde{\lambda}_e = \alpha'^3[1 + \zeta(3)]/32\kappa^6$ in the bosonic case [73, 74], $\lambda_e = 4\tilde{\lambda}_e = \alpha'^3\zeta(3)/8\kappa^6$ in the type II case [48, 49, 77], and $\lambda_e = 4\tilde{\lambda}_e = \alpha'^3[1 + 2\zeta(3)]/16\kappa^6$ in the heterotic [48, 77] (equivalently, type I [106]) case, respectively.

[13] The significance of the negative shift in γ, for $d_0 > 0$, for extremal charged black holes in $D \geq 6$ is less clear, since generic nonspherical perturbations blow up on the horizon already in the pure Einstein-Maxwell theory.

However, the Riemann-cubed operator is not amenable to such a general theory-independent bound on the basis of extant dispersion relations. While vanishing on general grounds in any supersymmetric theory [18], the η_e coefficients receives finite contributions at one loop [46] from massive states in the theory [14]:

$$\eta_e = \frac{1}{15120(4\pi)^2\kappa^2} \sum \left(\frac{1}{m_{\rm s}^2} - \frac{4}{m_{\rm f}^2} + \frac{3}{m_{\rm v}^2} \right), \tag{4.64}$$

where $m_{\rm s}$, $m_{\rm f}$, and $m_{\rm v}$ label the masses of the heavy real scalars, Dirac fermions, and vectors in the theory. As expected, this combination vanishes for supersymmetric theories. In the standard model, where all of the lightest states are fermions, we therefore will have $\eta_e < 0$, leading to singular horizons for rapidly-spinning Kerr black holes.

Further, the signs of Wilson coefficients in the Einstein-Maxwell EFT are of great importance for the Weak Gravity Conjecture (WGC) [4, 5, 24, 25, 76]. Let us remind the reader that the WGC is the statement that, when an Abelian gauge theory is consistently coupled to quantum gravity, there should always be a state in the spectrum for which $Q/M > 1$ in Planck units, with 1 corresponding to the charge-to-mass ratio of an extremal black hole [5]. In the presence of higher-dimension operators in the EFT, the black hole solutions are deformed, and thus the maximum allowed charge-to-mass ratio of black holes free of naked singularities is also shifted. For electric black holes, the particular combination d_0 defined in Eq. (4.23) dictates this shift, with $\Delta(Q/M) \propto d_0$ [25], so that $d_0 > 0$ allows the black holes themselves to satisfy the WGC. In this case, there are expected to be nonperturbative decay processes, i.e., a black hole version of Schwinger pair production, by which large extremal black holes decay to smaller ones with Q/M slightly > 1. Interestingly, the shift in the black hole entropy and on-shell action are also $\propto d_0$ [4, 25], and it was argued via black hole thermodynamics in Ref. [25] that $d_0 > 0$ in tree-level completions. It is interesting that for precisely this same situation $d_0 > 0$, we also find an instability toward singular extremal charged black holes in $D = 5$, and a negative shift in the associated scaling dimension for all $D \geq 5$. We leave the question of whether this effect is somehow connected with the WGC-mandated black hole decay to future work.

When the curvature diverges on the horizon of an extremal black hole, a near-extremal black hole has a curvature that diverges as one approaches extremality [66]. Since we observe rapidly spinning black holes in nature (see, e.g., Refs. [47, 101, 112]), one might wonder if the effect described here could be observable. That is possible, but detecting tidal forces much larger than the ambient curvature would require black holes much closer to extremality than have been observed to date. However, we take our results as proof of principle that black hole horizons can serve to amplify the effects of higher-derivative terms in the action. Since all the scalar quantities are bounded, we expect that the EFT approach should be still valid.

[14] At two loops, η_e is generated even in a purely gravitational theory, with a beta function that leads to positive η_e in the asymptotic infrared [12, 13], though this effect is too small to be physically relevant, even for astrophysical black holes.

Chapter 5

Conclusions

5.1 Summary

In this thesis, we tried to understand: what does the neighborhood of a *generic* degenerate black hole look like? From the astrophysical point of view, it is of no interest. After all, due to the third law of thermodynamics, we expect that there are no $T = 0$ black holes in our universe. However, extremal black holes are quite important for quantum gravity. They inspired deep conjectures like Weak Gravity Conjecture. Moreover, they allow enhanced control over the quantization which led to a series of beautiful results such as a non-perturbative calculation of the black hole entropy as $T \to 0$. Moreover, in AdS/CFT black holes are dual to thermal states of the boundary theory (usually with a non-vanishing chemical potential). In this context, the low-temperature regime is of obvious interest.

Of course, if we assume Einstein(-Maxwell) equations everywhere, asymptotic flatness, stationarity, and four dimensions, this is a void question because extremal black holes are completely classified in this setting. They must be in either Kerr-Newman or Majumdar–Papapetrou solution class. Thus, to talk about genericity, we had to include either a distant matter distribution or non-trivial boundary conditions (for example in AdS).

Chapter 2 was devoted to this very question in AdS_4 with symmetry-breaking boundary conditions. Somehow surprisingly, we found that generically the horizon is replaced by a null singularity. To be more precise, the Weyl tensor in the null-gaussian coordinates (v, ρ, x^A) reads

$$C_{\rho a \rho b} \sim (\gamma - 1)\rho^{\gamma - 2}. \tag{5.1}$$

Counter-intuitively, the larger the black hole the worse the singularity is (it means, the smaller the γ). We have a few different regions in the parameter space:

- $\gamma > 2$
  This happens only for small toroidal black holes. It means that the horizon is not singular (albeit probably still not smooth)

- $1 < \gamma < 2$
  In this case, the horizon is replaced by a singularity that is very mild. In particular, the tidal forces are integrable and thus would lead only to a finite deformation of an infalling test body.

- $\frac{1}{2} < \gamma < 1$
  When $\gamma < 1$, the tidal forces stop being integrable. An infalling test body would get destroyed.

- $0 < \gamma \leq \frac{1}{2}$
  The tidal forces are still not integrable. Moreover, the Einstein(-Maxwell) equations do not hold anymore on the horizon even in a distributional sense.

- $\gamma < 0$
  This happens only for large hyperbolic black holes. If this is the case, a 'small' perturbation diverges at the horizon, the perturbative expansion breaks down and the whole solution is RG unstable. We do not know what the endpoint of that instability is.

Despite the fact that solutions are singular[1], their analytic continuation to the Euclidean signature is perfectly smooth. Thus, it seems that, as long as $\gamma > 0$, those configurations can be prepared by the gravitational path integral and should not be ruled out as unphysical singularities (in contrast to a singularity at $r = 0$ for $M < 0$ Schwarzschild). Even more, because all curvature scalars remain small at the horizon, we do not expect higher-curvature corrections (of either stringy or quantum origin) to change that conclusion.

Although turning the temperature T up restores the smoothness, it still leaves significant observational imprints. In particular, the Weyl tensor at the horizon reads

$$C_{\rho a \rho b} \sim T^{\gamma - 2} \tag{5.2}$$

and thus may be arbitrarily large. Moreover, the second-order perturbation theory shows that the horizon's entropy increases by something proportional to $T^{2\gamma}$. As a result, the specific heat (say at a fixed charge) obtains an anomalous term

$$C_Q = C_1 T + \tilde{C} T^{2\gamma} + O(T^2, T^{4\gamma}) \tag{5.3}$$

that dominates at low temperatures assuming that $2\gamma < 1$. This seems to be a clear prediction for the boundary theory. It would be interesting to see a field-theoretic derivation of this scaling.

Let me also remind the Reader that we found that when a cosmological constant Λ vanishes, all γs become integers and the horizon is C^∞. For $\Lambda > 0$, the scaling dimensions grow with the black hole's size. Only small (in comparison with the Hubble radius), charged black holes remain singular albeit with $1 < \gamma$.

Having investigated four-dimensional black holes, we moved into higher dimensions. We found out that generic stationary perturbations of RN AdS_5 have $\gamma < 0$, and thus they lead to drastic changes in the horizon's geometry (we say it is RG unstable). This is rather an unexpected turn of events. Apparently, putting a (holographic) CFT_4 on a slightly deformed background leads to a drastically different infrared. It seems that a lot of work on the topic so far studied the IR fixed point that was unstable and there is still a lot to understand. Again, it would be interesting to see that RG flow also on the field theory side of the story. In particular, I would like to understand whether this is a property of only holographic CFTs or maybe a more robust behavior. If the theory is placed on a three-dimensional torus (instead of a three-sphere), then the phase diagram becomes even richer. For small torii (in comparison with the chemical potential), background deformations are irrelevant and they become more and more relevant as we increase the size. In particular, at the threshold of instability, one can check that the dc resistivity approaches a constant.

Several new near-horizon geometries (both spherical and toroidal) were constructed perturbatively and numerically. Unfortunately, all of them are RG unstable.

[1] Or, in the case $0 < \gamma < \frac{1}{2}$, are not even solutions

Thus, the proper IR fixed point remains elusive. Our numerical search suggests that at least for small (spherical) RN AdS, there is no stable near-horizon geometry. This suggests that maybe the endpoint of RG instability is not a black hole at all. This, in turn, allows one to conjecture what are the properties of the new phase. If it is not described by a single horizon, it does not have to be a conductor at all. Maybe we have a new holographic conductor/insulator phase transition? Either way, one should keep in mind that this is rather a speculative discussion.

We also showed that higher-curvature corrections may render extremal Kerr singular even without any additional sources. This should happen in particular for black holes of astrophysical sizes (assuming that neutrinos are the lightest massive particles). For supersymmetric theories it is a robust statement that does not depend on the black hole's size or the UV matter content. Unfortunately, scaling dimensions of RN_4 are unchanged (to leading order). This is no longer the case in higher dimensions. If the Weak Gravity Conjecture holds, it follows that RN_5 is RG unstable. Moreover, charged scalar field satisfying WGC also renders Kerr-Newman RG unstable. The appearance of WGC is perhaps not very surprising (since it started exactly with extremal black holes) but I think it would be worthwhile to actually understand the connection.

5.2 Further work

Essentially all the work done in this thesis was (in one sense or another) classical. I believe that the most important next step is trying to connect our results with very impressive statements regarding quantum extremal black holes. Most of them assume from the very start that all Kaluza–Klein modes are not sourced. In this thesis, we saw that when they are, they may significantly alter thermodynamics. The interaction (or at least competition) between the quantum effects and sources is something I would like to investigate further. The simplest way to do it would be to treat KK modes as small perturbations of Schwarzian theory. If this can be done consistently (it means, if their contribution to the effective action remains small), that would strongly suggest that quantum effects dominate as $T \to 0$. One should probably also understand better the interplay between Schwarzian physics and higher-curvature corrections.

Going back to the classical realm, we could ask about non-compact (say, planar) horizons and perturb the boundary conditions adiabatically in real time. Due to non-compactness, we may do this without changing the temperature. Then, we can expect that at late times, the curvature at the horizon would grow unboundedly. In this way, we could potentially create a new counterexample to the weak cosmic censorship in AdS_4. One may notice a similarity to [68]. The only practical difference is the fact that for our example we need only an infinitesimal perturbation of the boundary conditions because we now know to look for null tidal forces. I think it is important to understand whether the connection between the Weak Gravity Conjecture and Weak Cosmic Censorship will be still present – for now it seems to me that it would not have to be there.

Even more work is needed in higher dimensions. Due to RG instability, any source would drastically alter the horizon's geometry. The very first question would be: what is the endpoint? What kind of properties does it have and what is the correspondence IR for the boundary theory? One could also ask about the time-dependence boundary conditions at infinity that could trigger in some sense phase transition. On a more mathematical side, the problem of classifying near-horizon

geometries in five dimensions seems harder than ever. There is a plethora of new solutions that awaits a good idea of how to describe them all.

Our work on the higher-curvature corrections showed a connection between RG stability of extremal black holes and the Weak Gravity Conjecture. That does not seem to be a coincidence. Since WGC is exactly about making extremal black holes unstable (though in a particle physics sense), the fact that it leads to 'the destruction' of RN_5 horizon feels right. Getting a better understanding of the process from the point of view of UV could shed new light on WGC and swampland.

Let me finish my dissertation with this very Section. As one can see, certain results were obtained here but there is much more that we do not know. I hope to have a pleasure to work on these topics again in the future.

Appendix A

Anomalous scaling of the specific heat

In this Appendix, we provide some details of the calculation of the anomalous scaling of the specific heat with temperature. The final answer agrees with the scaling argument (2.30) given in Sec. 2.3.2. We will use second-order perturbation theory about the near-horizon geometry of an extreme RN AdS black hole.

Since our argument relies on second-order perturbation theory, our calculations will become less explicit and, for the sake of presentation, less general. We will focus on deformations of the near-horizon geometry that break $SO(3)$ but preserve a $U(1)_\phi$ symmetry. Additionally, we will impose the discrete symmetry $\phi \to -\phi$. We then write an Ansätze for the deformed metric and gauge field in Bondi-Sachs coordinates adapted to the extremal horizon:

$$\begin{aligned} \mathrm{d}s^2 = L^2 \Bigg\{ & - A(\rho,\theta)\,\rho^2 \frac{\mathrm{d}v^2}{L^2} + \frac{2\,\mathrm{d}v\,\mathrm{d}\rho}{L} \\ & + y_+^2\, H_L(\rho,\theta) \left[H_T(\rho,\theta) \left(\mathrm{d}\theta - \frac{U_\theta(\rho,\theta)\,\rho\,\mathrm{d}v}{L} \right)^2 + \frac{\sin^2\theta}{H_T(\rho,\theta)} \mathrm{d}\phi^2 \right] \Bigg\}, \end{aligned} \tag{A.1a}$$

and

$$A = \rho\, A_v(\rho,\theta)\,\mathrm{d}v + L\, A_\theta(\rho,\theta)\,\mathrm{d}\theta\,, \tag{A.1b}$$

with the extremal horizon being located at $\rho = 0$, as usual.

We now expand all metric and gauge field functions in terms of harmonics on the round S^2, by identifying how each transforms under diffeomorphism on a two-sphere. This will make contact with section 2.3.3. Essentially, A, H_L and A_v can be written as an infinite sum of scalar spherical harmonics and U_θ and A_θ as an infinite sum of gradients of spherical harmonics. H_T is slightly more subtle, but its transformations properties can be read from (2.36b). Note that no spherical vector harmonics appear in our expansion, since these would necessarily break the discrete symmetry $\phi \to -\phi$ that we want to preserve. To sum up, we have

$$A(\rho,\theta) = \sum_{\ell=0}^{+\infty} \mathbb{S}_\ell(\theta) a^\ell(\rho)\,, \tag{A.2a}$$

$$H_L(\rho,\theta) = \sum_{\ell=0}^{+\infty} \mathbb{S}_\ell(\theta) h_L^\ell(\rho)\,, \tag{A.2b}$$

$$A_v(\rho,\theta) = \sum_{\ell=0}^{+\infty} \mathbb{S}_\ell(\theta) a_v^\ell(\rho)\,, \tag{A.2c}$$

$$U_\theta(\rho,\theta) = \sum_{\ell=1}^{+\infty} \partial_\theta \mathrm{S}_\ell(\theta) u_\theta^\ell(\rho)\,, \tag{A.2d}$$

$$A_\theta(\rho,\theta) = \sum_{\ell=1}^{+\infty} \partial_\theta \mathrm{S}_\ell(\theta) a_\theta^\ell(\rho)\,, \tag{A.2e}$$

and

$$H_T(\rho,\theta) = \sum_{\ell=2}^{+\infty} \left[\ell(\ell+1)\mathrm{S}_\ell + 2\cot\theta\,\partial_\theta \mathrm{S}_\ell(\theta)\right] h_T^\ell(\rho)\,. \tag{A.2f}$$

So far we have not made any approximation. Indeed, we could have used this expansion to perform the full nonlinear numerical analysis of section (2.4.1), precisely in the spirit of Galerkin spectral methods.

We now introduce our approximation scheme. We expand each of the functions $\{a^\ell, h_L^\ell, a_v^\ell, u_\theta^\ell, a_\theta^\ell, h_T^\ell\}$ as a power series in a book keeping parameter ε which we take to be small

$$a^\ell(\rho) = \sum_{j=0}^{+\infty} \varepsilon^j a^\ell_{(j)}(\rho)\,, \tag{A.3a}$$

$$h_L^\ell(\rho) = \sum_{j=0}^{+\infty} \varepsilon^j h^\ell_{L\,(j)}(\rho)\,, \tag{A.3b}$$

$$a_v^\ell(\rho) = \sum_{j=0}^{+\infty} \varepsilon^j a^\ell_{v\,(j)}(\rho)\,, \tag{A.3c}$$

$$u_\theta^\ell(\rho) = \sum_{j=0}^{+\infty} \varepsilon^j u^\ell_{\theta\,(j)}(\rho)\,, \tag{A.3d}$$

$$a_\theta^\ell(\rho) = \sum_{j=0}^{+\infty} \varepsilon^j a^\ell_{\theta\,(j)}(\rho)\,, \tag{A.3e}$$

and

$$h_T^\ell(\rho) = \sum_{j=0}^{+\infty} \varepsilon^j h^\ell_{T\,(j)}(\rho)\,. \tag{A.3f}$$

We take the background, *i.e.* the order ε^0, to be given by an extreme RN AdS black hole, which amounts to taking

$$a^0_{(0)}(\rho) = 6 + \frac{1}{y_+^2}\,, \quad h^0_{L\,(0)} = 1 \quad \text{and} \quad a^0_{v\,(0)} = \frac{\sqrt{1+3y_+^2}}{y_+}\,. \tag{A.4}$$

with all the remaining coefficients in (A.3) set to zero.

At linear order, *i.e.* ε^1, we impose an $\ell = 2$ deformation. If we imagine that these near-horizon deformations arise from a boundary deformation of a generic profile, the $\ell = 2$ perturbation is the one that decays the slowest as we approach the horizon, and as such provides the leading effect we want to study. In order to only keep a $\ell = 2$ deformation, we take $a^2_{(1)}(\rho)$, $u^2_{\theta\,(1)}(\rho)$, $h^2_{L\,(1)}(\rho)$, $h^2_{T\,(1)}(\rho)$, $a^2_{v\,(1)}(\rho)$ and $a^2_{\theta\,(1)}(\rho)$ to be non-vanishing, but keep all the remaining coefficients with $\ell > 2$ zero. Solving

the linear Einstein-Maxwell equations yields

$$a^2_{(1)}(\rho) = \rho^\gamma\,, \tag{A.5a}$$

$$u^2_{\theta\,(1)}(\rho) = \frac{1}{\left(1+6y_+^2\right)(\gamma-1)}\,\rho^\gamma\,, \tag{A.5b}$$

$$h^2_{L\,(1)}(\rho) = 0\,, \tag{A.5c}$$

$$h^2_{T\,(1)}(\rho) = \frac{y_+^2(\gamma+1)}{4\left(1+6y_+^2\right)}\,\frac{\gamma^2+\gamma-10+6y_+^2\left(\gamma^2+\gamma-2\right)}{6+\gamma\left[\gamma^2-7+6y_+^2\left(\gamma^2-1\right)\right]}\,\rho^\gamma\,, \tag{A.5d}$$

$$a^2_{v\,(1)}(\rho) = \frac{6y_+}{1+6y_+^2}\,\frac{\sqrt{1+3y_+^2}}{6+\gamma\left[\gamma^2-7+6y_+^2\left(\gamma^2-1\right)\right]}\,\rho^\gamma\,, \tag{A.5e}$$

$$a^2_{\theta\,(1)}(\rho) = \frac{y_+^3}{1+6y_+^2}\,\frac{\sqrt{1+3y_+^2}}{6+\gamma\left[\gamma^2-7+6y_+^2\left(\gamma^2-1\right)\right]}\,\rho^\gamma\,, \tag{A.5f}$$

where the first equation defines what we mean by ε. The exponent γ can again take four distinct values. Two are negative, and we ignore those via boundary conditions, and we are interested in the smallest of the two that are positive. This yields

$$\gamma = \frac{1}{2}\left[\sqrt{5+\frac{24}{1+6y_+^2}-4\sqrt{1+\frac{24\left(1+3y_+^2\right)}{\left(1+6y_+^2\right)^2}}}-1\right]\,, \tag{A.5g}$$

which matches γ_{+-} in Eq. (2.39a) with $\ell = 2$, as it should. Note that $h^2_{L\,(1)}$ vanishes via the equations of motion.

One can now proceed to second order in ε. At quadratic order, modes with $\ell = 0, 2, 4$ are generated in the expansion. The final expression for each of the coefficients is rather complicated and not very illuminating. However, in order to make the argument we want, we only need to focus on H_L. The reason for this is that the area of a surface of constant v and $\rho = \rho_0$ is simply given by

$$A(\rho_0) = 2\pi L^2\, y_+^2 \int_0^\pi H_L(\rho_0,\theta)\,\sin\theta\,\mathrm{d}\theta = 4\pi L^2\, y_+^2 h_L^0(\rho_0)\,, \tag{A.6}$$

where we used that spherical harmonics have vanishing integral over the sphere. Note that the above expression is exact. From this expression, it is clear that we can only get contributions to the area coming from the $\ell = 0$ harmonic. This justifies why we need to go to second order in ε to see the effect we want.

After some algebra, one finds

$$h^0_{L\,(2)}(\rho) = C_2(\gamma)\,\rho^{2\gamma} + C_0 + C_1\,\rho\,, \tag{A.7a}$$

with

$$C_2(\gamma) = \frac{(\gamma+1)(\gamma+2)}{5760(1-2\gamma)(1-\gamma)\left(\gamma^2+\gamma+6\right)}\left[48+12\gamma-4\gamma^2-35\gamma^3-25\gamma^4-9\gamma^5\right.$$
$$\left.-3\gamma^6+\frac{72-22\gamma-27\gamma^2-10\gamma^3-5\gamma^4}{\sqrt{3}}\sqrt{\gamma(\gamma+1)\left(\gamma^2+\gamma+4\right)}\right] \tag{A.7b}$$

where we regard y_+ as a function of γ by inverting (A.5g), *i.e.*

$$y_+ = \frac{1}{\sqrt{6}} \frac{1}{\sqrt{(1-\gamma)(\gamma+2)}} \sqrt{\gamma(\gamma+1) - 8 + 2\sqrt{3 + \frac{12}{\gamma(\gamma+1)}}}\,. \tag{A.8}$$

In the above, C_0 and C_1 are integration constants. We set $C_0 = 0$, which essentially defines y_+. C_1, on the other hand, *cannot* be set to zero.

The exact form of Eq. (A.7) is largely unimportant, except for a few of points. The most important point is that it turns out to be non-zero, unlike at first order in ε. The second important point is that in the range $0 < \gamma < 1/2$, the leading contribution to $h^0_{L\,(2)}(\rho)$ is proportional to $\rho^{2\gamma}$. Furthermore, its coefficient, $C_2(\gamma)$, turns out to be positive definite (see Fig. A.1 below).

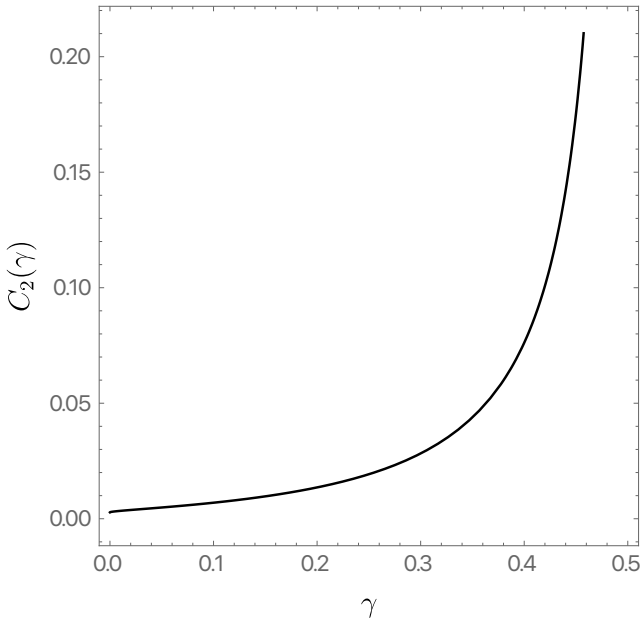

FIGURE A.1: $C_2(\gamma)$ as a function of γ in the range $0 < \gamma < 1/2$.

The apparent singularity at $\gamma = 1/2$ reflects the fact that, for that value of γ, $h^0_{L\,(2)}(\rho)$ is no longer given as in (A.7a), but instead

$$h^0_{L\,(2)} = C_0 + C_1\rho + \frac{997 + 281\sqrt{19}}{110592}\rho\,\log\left(\frac{1}{\rho}\right)\,, \tag{A.9}$$

where again we can set $C_0 = 0$, but not C_1. The leading behaviour near $\rho = 0$ is then given by $\rho\log(1/\rho)$, again with a positive coefficient.

We can now apply the same scaling argument we used in section 2.3.2 to the black hole entropy. Indeed, if we use (A.6), we have just shown that a surface of constant v and $\rho = \rho_0$, to leading order in $\rho_0 \ll 1$, has an area given by

$$A(\rho_0) = 4\pi L^2 y_+^2 \left[1 + C_2(\gamma)\,\rho_0^{2\gamma}\right]\,, \tag{A.10}$$

in the range $0 < \gamma < 1/2$, which yields an entropy of the black hole horizon scaling as

$$S \approx S_0 + S_2\,T^{2\gamma} \tag{A.11}$$

where S_0 and S_2 are suitable constants. Using similar arguments, applied for $\gamma = 1/2$, we find instead

$$S \approx \tilde{S}_0 + \tilde{S}_2\, T\, \log T + \tilde{S}_3 T\,, \tag{A.12}$$

for suitable constants $\tilde{S}_0$, $\tilde{S}_2$ and $\tilde{S}_3$. Note that γ is ultimately fixed by the total charge Q (or alternatively y_+). Using standard thermodynamic relations, we predict the scaling of the specific heat at constant charge Q, at sufficiently small temperatures, to be given by

$$C_Q \approx 2\gamma \tilde{S}_2 T^{2\gamma} \tag{A.13}$$

in the range $0 < \gamma < 1/2$ and

$$C_Q \approx T\left(\tilde{S}_2 + \tilde{S}_3\right) + \tilde{S}_2 T \log T\,, \tag{A.14}$$

for $\gamma = 1/2$. Note that the fact that $C_2(\gamma)$ is positive is paramount to argue that the near-horizon geometry we found is thermodynamically locally stable since $\tilde{S}_2$ turns out to be proportional to $C_2(\gamma)$, which makes C_Q in (A.13) also positive.

Though we have deduced this anomalous scaling for Einstein-Mawell, we predict this will be true for a variety of systems that suffer from tidal force-type singularities. For instance, in section 2.5.2 we show that our finite temperature scalar model exhibits a scaling of the form (A.13).

Appendix B

Expressions for the equations governing the IR perturbations in Sec. 3.3.3

$$\alpha_0 \equiv \frac{8\rho_{\rm IR}^2 Y_+^2 H^2}{9B^2B'}\left[3B(1-4B)-4\rho_{\rm IR}^2\right], \tag{B.1a}$$

$$\alpha_1 \equiv \frac{8\rho_{\rm IR}^2 Y_+^2 \sin\theta H^3}{9B^2B'}\Big\{4Y_+^2\left[3B(1-4B)-4\rho_{\rm IR}^2\right]\left[\rho_{\rm IR}^2-B(1-6B)\right]H^2 - 9B(1-12B)B'^2\Big\}+\frac{48\rho_{\rm IR}^2H^4B'}{\sin\theta}, \tag{B.1b}$$

$$\alpha_2 \equiv \frac{16\rho_{\rm IR}^2 Y_+^2 \sin\theta H^3}{9BB'}\left\{2Y_+^2\left[4\rho_{\rm IR}^2-3B(1-4B)\right]H^2+9B'^2\right\}, \tag{B.1c}$$

$$\beta_0 \equiv \frac{4Y_+^2H^2}{3B^2}\left(7\rho_{\rm IR}^2-3B\right) \tag{B.1d}$$

$$\beta_1 \equiv -\frac{2Y_+^2\left(2\rho_{\rm IR}^2-B\right)\sin\theta H^3}{3B^2}\left[4Y_+^2\left(5\rho_{\rm IR}^2-3B+6B^2\right)H^2+9B'^2\right], \tag{B.1e}$$

$$\beta_2 \equiv \frac{H^2Y_+^2}{3B}\Big\{9HB'\left(8B\cos\theta+\sin\theta B'\right)-36B\sin\theta B'H' - 4H^3\sin\theta\, Y_+^2\left[23\rho_{\rm IR}^2-3B(5-14B)\right]\Big\}, \tag{B.1f}$$

$$\beta_3 \equiv 4Y_+^4\sin\theta H^5, \tag{B.1g}$$

$$\kappa_0 \equiv -\frac{28\rho_{\rm IR}^2Y_+^2H^2}{3B^2}, \tag{B.1h}$$

$$\kappa_1 \equiv \frac{4\rho_{\rm IR}^2Y_+^2\sin\theta H^3}{3B^2}\left\{4Y_+^2\left[5\rho_{\rm IR}^2-3B(1-2B)\right]H^2+9B'^2\right\}, \tag{B.1i}$$

and

$$\kappa_2 = \frac{16\rho_{\rm IR}^2Y_+^4\sin\theta H^5}{B}. \tag{B.1j}$$

Appendix C

Deformed toroidal horizons – perturbative expansions

In this Appendix, we shall present in more detail perturbatively constructed near-horizon geometries that are topologically torii. All the results were essentially obtained by first expanding in ϵ and then into appropriate Fourier modes. In this way, the periodicity of the coordinates is automatically enforced. We shall follow the notation of 3.4.

C.1 Simple cubic

The following expansion is up to order ϵ^2. One may keep in mind that higher-order equations of motion lead also to constraints for lower terms. Thus, to obtain an unambiguous solution up to the second order, we had to solve EoMs up to the fourth one. Our starting point is a three-dimensional metric

$$\mathring{q} = \frac{1}{8}\begin{pmatrix} 1 & 0 & 0 \\ 0 & 1 & 0 \\ 0 & 0 & 1 \end{pmatrix}. \tag{C.1}$$

As a seed in the first order, we find:[1]

$$B^{(1)} = \sin(x) + \sin(y) + \sin(z). \tag{C.2}$$

The parameter q_{IR} reads

$$q_{IR} = \frac{1}{2\sqrt{6}} - 6\sqrt{6}\epsilon^2 + O(\epsilon^4). \tag{C.3}$$

Note that because the solution has a symmetry $\epsilon \to -\epsilon$, there cannot be ϵ^3 term in q_{IR}.

Then, all the remaining functions are

$$B^{(1)} = \sin(x) + \sin(y) + \sin(z) \tag{C.4a}$$

$$B^{(2)} = -48(2\sin(x)(\sin(y) + \sin(z)) + 2\sin(y)\sin(z) - 1) \tag{C.4b}$$

$$q^{(1)}_{xx} = -3(\sin(y) + \sin(z)) \tag{C.4c}$$

$$q^{(2)}_{xx} = -\frac{9}{4}\left(-152\sin(y)\sin(z) + 9\cos(2y) - 9\sin^2(z) + 9\cos^2(z) + 557\right) \tag{C.4d}$$

[1] The coefficients are chosen to ensure that the higher-order constraints are satisfied.

$$q^{(1)}_{yy} = -3(\sin(x) + \sin(z)) \tag{C.4e}$$

$$\begin{aligned} q^{(2)}_{yy} = -\frac{9}{4}\Big(&- 264\sin(x)\sin(y) - 152\sin(x)\sin(z) - 9\sin^2(x) + 9\cos^2(x) \\ &- 9\sin^2(z) + 9\cos^2(z) + 557\Big) \end{aligned} \tag{C.4f}$$

$$q^{(1)}_{zz} = -3(\sin(x) + \sin(y)) \tag{C.4g}$$

$$\begin{aligned} q^{(2)}_{zz} = -\frac{9}{4}\Big(&- 152\sin(x)\sin(y) - 264\sin(x)\sin(z) - 9\sin^2(x) + 9\cos^2(x) \\ &- 264\sin(y)\sin(z) - 9\sin^2(y) + 9\cos^2(y) + 557\Big). \end{aligned} \tag{C.4h}$$

All the other coefficients vanish.

C.2 Graphene-like torus

The following expansion is up to order ϵ^3. One may keep in mind that higher-order equations of motion lead also to constraints for lower terms. Thus, to obtain an unambiguous solution up to the third order, we had to solve EoMs up to the fifth one.

Our starting point is a three-dimensional metric

$$\mathring{q} = \frac{1}{24}\begin{pmatrix} 4 & 2 & 0 \\ 2 & 4 & 0 \\ 0 & 0 & 3 \end{pmatrix}. \tag{C.5}$$

As a seed in the first order, we find:[2]

$$B^{(1)} = \cos(x+y) + \sin(x) + \sin(y) + \sqrt{\frac{3}{2}}\sin(z). \tag{C.6}$$

Notice that (in contrast to the simple cubic case) $\epsilon \mapsto -\epsilon$ is not a symmetry. The parameter q_{IR} reads

$$q_{IR} = \frac{1}{2\sqrt{6}} - 9\sqrt{6}\epsilon^2 - 576\sqrt{6}\epsilon^3 + O(\epsilon^4) \tag{C.7}$$

Then, all the remaining functions are

$$B^{(1)} = \cos(x+y) + \sin(x) + \sin(y) + \sqrt{\frac{3}{2}}\sin(z) \tag{C.8a}$$

$$\begin{aligned} B^{(2)} = &-24\sqrt{6}\sin(x+y+z) + 24\sqrt{6}\sin(x+y-z) - 5\sin(2x+y) \\ &- 17\sin(x+2y) - 29\cos(x-y) - 2\cos(2(x+y)) - 24\sqrt{6}\cos(x-z) \\ &+ 24\sqrt{6}\cos(x+z) + 12\sin(x) + 2\cos(2x) - 24\sqrt{6}\cos(y-z) \\ &+ 24\sqrt{6}\cos(y+z) + 24\sin(y) + 2\cos(2y) + 41\sqrt{\frac{3}{2}}\sin(z) + 78 \end{aligned} \tag{C.8b}$$

[2]The coefficients are chosen to ensure that the higher-order constraints are satisfied.

$$
\begin{aligned}
16B^{(3)} = &-23712\sqrt{6}\sin(x-y-z) - 2658\sqrt{6}\sin(2x+2y-z)\\
&- 45984\sqrt{6}\sin(x+y+z) + 45984\sqrt{6}\sin(x+y-z)\\
&+ 23712\sqrt{6}\sin(x-y+z) + 2658\sqrt{6}\sin(2x+2y+z)\\
&- 5856\sqrt{6}\cos(2x+y+z) - 14784\sqrt{6}\cos(x+2y+z)\\
&- 19926\cos(x+y+2z) - 19926\cos(x+y-2z)\\
&+ 5856\sqrt{6}\cos(2x+y-z) + 14784\sqrt{6}\cos(x+2y-z)\\
&+ 4772\sin(2x-y) + 6248\sin(2x+y) + 5888\sin(x+2y)\\
&+ 228\sin(3x+2y) + 4004\sin(2x+3y) - 10372\sin(x-2y)\\
&+ 1688\cos(x-y) - 2336\cos(2(x+y)) + 72\cos(3(x+y))\\
&- 228\cos(3x+y) - 6268\cos(x+3y) - 2658\sqrt{6}\sin(2x+z)\\
&- 19926\sin(x+2z) - 19926\sin(x-2z) + 2658\sqrt{6}\sin(2x-z)\\
&- 54912\sqrt{6}\cos(x-z)54912\sqrt{6}\cos(x+z) + 96\sin(x) - 72\sin(3x)\\
&+ 4256\cos(2x) - 2658\sqrt{6}\sin(2y+z) - 19926\sin(y+2z)\\
&- 19926\sin(y-2z) + 2658\sqrt{6}\sin(2y-z) - 63840\sqrt{6}\cos(y-z)\\
&+ 63840\sqrt{6}\cos(y+z) + 2280\sin(y) - 72\sin(3y) + 26816\cos(2y)\\
&- 29642\sqrt{6}\sin(z) - 81\sqrt{6}\sin(3z) + 66816
\end{aligned}
\tag{C.8c}
$$

$$
q_{xx}^{(1)} = -4\sin(y) - 2\sqrt{6}\sin(z) - 9 \tag{C.8d}
$$

$$
\begin{aligned}
2q_{xx}^{(2)} = &\, 456\sqrt{6}\sin(y)\sin(z) + 70\sin^2(y) + 292\sin(y) - 70\cos^2(y)\\
&+ 81\sin^2(z) + 52\sqrt{6}\sin(z) - 81\cos^2(z) - 2474
\end{aligned}
\tag{C.8e}
$$

$$
\begin{aligned}
4q_{xx}^{(3)} = &-8202\sqrt{6}\sin(2y-z) + 36126\sin(y+2z) + 36126\sin(y-2z)\\
&+ 8202\sqrt{6}\sin(2y+z) - 38376\sqrt{6}\cos(y+z) + 38376\sqrt{6}\cos(y-z)\\
&+ 134344\sin(y) + 1080\sin(3y) - 15460\cos(2y) + 117602\sqrt{6}\sin(z)\\
&+ 513\sqrt{6}\sin(3z) - 4536\cos(2z) - 939388,
\end{aligned}
\tag{C.8f}
$$

$$
q_{xy}^{(1)} = -\sqrt{6}\sin(z) - \frac{9}{2}, \tag{C.8g}
$$

$$
q_{xy}^{(2)} = \frac{1}{4}\left(52\sqrt{6}\sin(z) - 81\cos(2z) - 2570\right), \tag{C.8h}
$$

$$
q_{xy}^{(3)} = \frac{1}{8}\left(137186\sqrt{6}\sin(z) + 513\sqrt{6}\sin(3z) - 4536\cos(2z) - 935740\right), \tag{C.8i}
$$

$$
q_{xz}^{(1)} = 0, \tag{C.8j}
$$

$$
q_{xz}^{(2)} = 90\sqrt{6}\cos(y)\cos(z), \tag{C.8k}
$$

$$
q_{xz}^{(3)} = -\frac{9}{2}\cos(y)\cos(z)\left(409\sqrt{6}\sin(y) + 6156\sin(z) - 2108\sqrt{6}\right) \tag{C.8l}
$$

$$q_{zz}^{(1)} = -3(\cos(x+y)+\sin(x)+\sin(y)) \tag{C.8m}$$

$$\begin{aligned}-\frac{4}{3}q_{zz}^{(2)} = &-456\sqrt{6}\sin(x+y+z)+456\sqrt{6}\sin(x+y-z)-136\sin(2x+y)\\ &-232\sin(x+2y)-328\cos(x-y)-70\cos(2(x+y))+5061\\ &-456\sqrt{6}\cos(x-z)+456\sqrt{6}\cos(x+z)+96\sin(x)+70\cos(2x)\\ &-456\sqrt{6}\cos(y-z)+456\sqrt{6}\cos(y+z)+192\sin(y)+70\cos(2y)\end{aligned} \tag{C.8n}$$

$$\begin{aligned}-\frac{8}{3}q_{zz}^{(3)} = &-38456\sqrt{6}\sin(x-y-z)-6480\sqrt{6}\sin(2x+2y-z)\\ &-48312\sqrt{6}\sin(x+y+z)+48312\sqrt{6}\sin(x+y-z)\\ &+38456\sqrt{6}\sin(x-y+z)+6480\sqrt{6}\sin(2x+2y+z)\\ &-13172\sqrt{6}\cos(2x+y+z)-30824\sqrt{6}\cos(x+2y+z)\\ &-83403\cos(x+y+2z)-83403\cos(x+y-2z)\\ &+13172\sqrt{6}\cos(2x+y-z)+30824\sqrt{6}\cos(x+2y-z)\\ &+6346\sin(2x-y)+1300\sin(2x+y)+1120\sin(x+2y)\\ &+1626\sin(3x+2y)+4666\sin(2x+3y)-9146\sin(x-2y)\\ &-980\cos(x-y)-106848\cos(x+y)-3220\cos(2(x+y))\\ &+540\cos(3(x+y))-1626\cos(3x+y)-5942\cos(x+3y)\\ &-6480\sqrt{6}\sin(2x+z)-83403\sin(x+2z)-83403\sin(x-2z)\\ &+6480\sqrt{6}\sin(2x-z)-55944\sqrt{6}\cos(x-z)+55944\sqrt{6}\cos(x+z)\\ &-107952\sin(x)-540\sin(3x)+6484\cos(2x)-6480\sqrt{6}\sin(2y+z)\\ &-83403\sin(y+2z)-83403\sin(y-2z)+6480\sqrt{6}\sin(2y-z)\\ &-69336\sqrt{6}\cos(y-z)+69336\sqrt{6}\cos(y+z)-108012\sin(y)\\ &-540\sin(3y)+20068\cos(2y)+743274\end{aligned} \tag{C.8o}$$

From the symmetry, it follows that $q_{xx}(x,y,z) = q_{yy}(y,x,z)$ and $q_{xz}(x,y,z) = q_{yz}(y,x,z)$.

Appendix D

EFT-corrected solutions

D.1 The EFT-corrected near-horizon geometries

Let $C^{(6)}$, $C^{(8)}$, and $\tilde{C}^{(8)}$ be integration constants, and define

$$K(x) \equiv \arcsin\left(\frac{\sqrt{2}x}{\sqrt{1+x^2}}\right) - \arcsin x. \tag{D.1}$$

$I = 6$

For the six-derivative corrections, we find

$$B^{(6)}(x) = \frac{\kappa^4}{J^2}\left[\frac{2656 - 42885x^2 + 45895x^4 - 8130x^6 - 1218x^8 + 183x^{10} + 139x^{12}}{224(1+x^2)^6} - \frac{15\sqrt{2}x(3-x^2)}{32(1+x^2)\sqrt{1-x^2}}K(x)\right] \tag{D.2}$$

and

$$\Omega^{(6)}(x) = \frac{\kappa^4}{J^2}\left[C^{(6)} - \frac{3285 - 55449x^2 + 54210x^4 - 7058x^6 - 1527x^8 - 309x^{10}}{224(1+x^2)^6} + \frac{15x\sqrt{2}\sqrt{1-x^2}}{64(1+x^2)}K(x)\right]. \tag{D.3}$$

$I = 8$

For the eight-derivative corrections, there are two families of solutions:

$$B^{(8)}(x) = \frac{\kappa^6}{J^3}\left[\frac{3(277663 - 33600\pi)}{1280} - \frac{407005 + 32887800x^2 + 38302380x^4 + 227158536x^6}{1280(1+x^2)^9} - \frac{244951182x^8 + 207667400x^{10} + 108083820x^{12} + 31954360x^{14} + 4114685x^{16}}{1280(1+x^2)^9} + \frac{1612800x}{2560(1+x^2)}\arctan x - \frac{366435x(3-x^2)}{256\sqrt{2}\sqrt{1-x^2}(1+x^2)}K(x)\right], \tag{D.4}$$

$$\omega^{(8)}(x) = \frac{\kappa^6}{J^3}\Bigg[C^{(8)} + \frac{783837 + 16684758x^2 + 33602022x^4 + 119986542x^6}{1280(1+x^2)^9} + \frac{138199680x^8 + 115247810x^{10} + 59401850x^{12} + 17424890x^{14} + 2229315x^{16}}{1280(1+x^2)^9} - \frac{315x}{1+x^2}\arctan x + \frac{366435x\sqrt{1-x^2}}{256\sqrt{2}(1+x^2)}K(x)\Bigg], \quad \text{(D.5)}$$

$$\tilde{B}^{(8)}(x) = \frac{\kappa^6}{J^3}\Bigg[\frac{3}{320}(282113 - 33600\pi) - \frac{368829x(3-x^2)}{64\sqrt{2}\sqrt{1-x^2}(1+x^2)}K(x) - \frac{1149443 + 5618952x^2 + 136013268x^4 + 154320120x^6 + 254641842x^8}{320(1+x^2)^9} - \frac{208733752x^{10} + 108674580x^{12} + 32136008x^{14} + 4138723x^{16}}{320(1+x^2)^9} + \frac{2520x}{1+x^2}\arctan x\Bigg], \quad \text{(D.6)}$$

and

$$\tilde{\omega}^{(8)}(x) = \frac{\kappa^6}{J^3}\Bigg[\tilde{C}^{(8)} - \frac{368829x\sqrt{1-x^2}}{64\sqrt{2}(1+x^2)}K(x) + \frac{1018371 + 7724394x^2 + 67516506x^4 + 96062418x^6 + 141833088x^8}{320(1+x^2)^9} + \frac{115923454x^{10} + 59757382x^{12} + 17530822x^{14} + 2243037x^{16}}{320(1+x^2)^9} - \frac{1260x}{1+x^2}\arctan x\Bigg]. \quad \text{(D.7)}$$

D.2 The approach to the near horizon geometry

We find two families of modes for stationary and axisymmetric deformations of the near horizon limit of the extremal Kerr black hole.

For the + family, we find

$$\begin{aligned}
\gamma_+^{(0)}(\ell) &= \ell \\
Q_1^{(0)}{}_+(x) &= P'_\ell(x) \\
Q_2^{(0)}{}_+(x) &= \frac{1}{2(1+x^2)}\Big[\ell(\ell+1)\,x\,P_\ell(x) + (1-x^2)P'_\ell(x)\Big] \\
Q_3^{(0)}{}_+(x) &= -\frac{1}{2(1+x^2)}\Big[2\ell(\ell+1)\,x\,P_\ell(x) + (1-3x^2)P'_\ell(x)\Big] \\
Q_4^{(0)}{}_+(x) &= \frac{1}{2}\Big[\ell\,x\,P_\ell(x) + \frac{(1-x^2)(\ell^2+\ell+2)}{2(\ell+1)}P'_\ell(x)\Big],
\end{aligned} \quad \text{(D.8)}$$

where $'$ denotes differentiation with respect to x. Modes with $\ell = 0$ vanish, while modes with $\ell = 1$ are special[1], so that in the $+$ family we take $\ell \geq 2$.

For the $-$ family, we find

$$\begin{aligned}
\gamma_-^{(0)}(\ell) &= \ell + 1 \\
{Q_1^{(0)}}_-(x) &= 0 \\
{Q_2^{(0)}}_-(x) &= -\frac{1}{2}\frac{1-x^2}{1+x^2}\left\{\ell(\ell+1)\,x\,P_\ell(x) - \left[2+(1-x^2)\ell\right]P'_\ell(x)\right\} \\
{Q_3^{(0)}}_-(x) &= \frac{1-x^2}{1+x^2}\left\{\ell(\ell+1)\,x\,P_\ell(x) - \left[2+(1-x^2)\ell\right]P'_\ell(x)\right\} \\
{Q_4^{(0)}}_-(x) &= \ell(\ell+1)\,x\,P_\ell(x) + (1+x^2\ell)\,P'_\ell(x),
\end{aligned} \tag{D.9}$$

where modes with $\ell = 0$ vanish, so that for the $-$ family we take $\ell \geq 1$.

D.2.1 Two examples of EFT corrected deformations

We normalize perturbations so that, for each value of ℓ,

$$\int_{-1}^{1} {Q_1}_+(x)^2 \mathrm{d}x = \ell(\ell+1) \quad \text{and} \quad \int_{-1}^{1} \frac{(1-x^2)^2}{x^2} {Q_4'}_-(x)^2 \mathrm{d}x = \frac{2\ell(\ell+1)^3(\ell+2)(\ell+3)}{2\ell+3}\,. \tag{D.10}$$

We give examples of EFT corrections in the $+$ family, with $\ell = 2$. For the six-derivative correction, we find

$$\begin{aligned}
{Q_1^{(6)}}_+(x) = \frac{\kappa^4}{J^2}\frac{3x}{224}\Bigg\{ & 35\sqrt{2} - 1675 - \frac{36372480}{(1+x^2)^7} + \frac{72826880}{(1+x^2)^6} - \frac{50065408}{(1+x^2)^5} + \frac{13659904}{(1+x^2)^4} - \frac{1148992}{(1+x^2)^3} \\
& - \frac{136}{(1+x^2)^2} - \frac{374}{1+x^2} + 384\log\left[\frac{1}{2}(1+x^2)\right] + \frac{105\sqrt{1-x^2}}{\sqrt{2}}\frac{K(x)}{x}\Bigg\},
\end{aligned} \tag{D.11}$$

while for one of the eight-derivative corrections, we have

$$\begin{aligned}
{Q_1^{(8)}}_+(x) = \frac{\kappa^6}{J^3}\frac{9x}{20}\Bigg\{ & \frac{203230547 - 2721885065x^2 + 10948541740x^4 - 13485253140x^6 + 8456364570x^8}{480(1+x^2)^{10}} \\
& - \frac{729506558x^{10} - 621146940x^{12} - 217212700x^{14} - 50262315x^{16} - 5216895x^{18}}{480(1+x^2)^{10}} \\
& + \frac{420\pi}{1-x^2} - \frac{4462619}{320} + \frac{203575}{32\sqrt{2}} + 2520C - 2985\pi + \frac{610725\sqrt{1-x^2}}{64\sqrt{2}}\frac{K(x)}{x} \\
& + \frac{1680(2-3x^2)}{(1-x^2)}\frac{\arctan x}{x} - 5040\arctan x\,\mathrm{arctanh}x - 448\log\left(\frac{1+x^2}{2}\right) \\
& - 630\pi\log\left(\frac{1-x^2}{4}\right) - 2520\,D\left[\left(\frac{1+i}{2}\right)(1-x)\right] - 2520\,D\left[\left(\frac{1+i}{2}\right)(1+x)\right]\Bigg\},
\end{aligned} \tag{D.12}$$

where $D(z)$ is the Bloch-Wigner dilogarithm function defined as

$$D(z) = \mathrm{Im}(\mathrm{Li}_2(z)) + \arg(1-z)\,\log|z|\,, \tag{D.13}$$

[1] See a footnote on p. 80 for the explanation

$\mathrm{Li}_2(z)$ is the dilogarithm function, and $-\pi \leq \arg z < \pi$. Note that $D(z)$ is a real analytic on $\mathbb{C}$ except at the two points $z = 0$ and $z = 1$, where it is continuous but not differentiable (with singularities of the form $|z| \log |z|$ and $|1-z| \log |1-z|$, respectively). Finally, $C = \sum_{n=0}^{\infty} (-1)^n/(2n+1)^2 \approx 0.915966$ is Catalan's constant.

D.3 Map between perturbations in Kerr-like coordinates, and Bondi-Sachs

One might worry that the coordinates we used to determine the behavior of near-horizon deformations away from the EFT-corrected near-horizon geometries are not regular at the event horizon. Indeed, this is the case even for the Kerr-like coordinates used in Eq. (4.26). In this section, we show that a simple map exists between the Kerr-like coordinates of Eq. (4.25) (with $F_1 = 1$ and $F_2 = 0$) and standard Bondi-Sachs coordinates. This map was worked out as an expansion in ε.

Recall that Bondi-Sachs coordinates take the following general form:

$$\mathrm{d}s^2 = (-V \mathrm{d}v^2 + 2\,\mathrm{d}v\,\mathrm{d}\rho) e^{2\beta} + e^{2\chi} h_{\dot{p}\dot{q}} (\mathrm{d}y^{\dot{p}} + U^{\dot{p}} \mathrm{d}v)(\mathrm{d}y^{\dot{q}} + U^{\dot{q}} \mathrm{d}v)\,. \tag{D.14}$$

with $\dot{p}, \dot{q} = 1, 2$. Consider the following coordinate transformation:

$$\begin{aligned} t &= v + \frac{1}{\rho} \\ \phi &= \varphi + \log \rho + \lambda(\rho, x). \end{aligned} \tag{D.15}$$

One finds that Eq. (4.25) takes the same form as (D.14) with $V = \rho^2$, $y^{\dot{p}} = \{x, \varphi\}$, $e^{2\beta} = e^{2\chi} = 2J\Omega^2$, and

$$\begin{aligned} h_{\dot{p}\dot{q}} &= \begin{bmatrix} \dfrac{1}{A} + B^2 \left(\dfrac{\partial \lambda}{\partial x}\right)^2 & -B^2 \left(\dfrac{\partial \lambda}{\partial x}\right) \\ -B^2 \left(\dfrac{\partial \lambda}{\partial x}\right) & B^2 \end{bmatrix} \\ U^{\dot{p}} &= \begin{bmatrix} 0 & \rho\,\omega \end{bmatrix}, \end{aligned} \tag{D.16}$$

so long as

$$\frac{\partial \lambda}{\partial \rho} = \frac{1-\omega}{\rho}\,. \tag{D.17}$$

The last equation is a first-order equation in ρ and can be readily solved for any ω.

Since $V = \rho^2$, in Bondi-Sachs coordinates, the future extremal event horizon is the null hypersurface $\rho = 0$. So long as $\gamma > 0$, these coordinates are regular at the horizon and can be used to extend the deformations of the EFT near-horizon geometries to a new region with $\rho < 0$. Since for extremal black holes, the (past and future) event horizons are also Cauchy surfaces for initial data on constant-t hypersurfaces, the extension beyond $\rho = 0$ into the new region with $\rho < 0$ is not *unique*.

It is now a simple exercise to show that, to linear order in ε, the Weyl tensor satisfies

$$C_{\rho\dot{p}\rho\dot{q}} = J\,(1-\gamma)\,\rho^{\gamma-2}\,\varepsilon \begin{bmatrix} -\dfrac{\gamma\,\Gamma_{\rm NH}^2(Q_1+2Q_3)\Omega_{\rm NH}^2}{2(1-x^2)} & B_{\rm NH}^2\Omega_{\rm NH}^2 Q_4' \\ \\ B_{\rm NH}^2\Omega_{\rm NH}^2 Q_4' & -\dfrac{\gamma\,B_{\rm NH}^2(Q_1+2Q_3)\Omega_{\rm NH}^2}{2} \end{bmatrix}. \tag{D.18}$$

For Kerr, the smallest scaling exponent that contributes to the above quantity has $\gamma = 2$, rendering $C_{\rho\dot{p}\rho\dot{q}}$ finite. But when higher derivative corrections are included, $\gamma < 2$ and the curvature diverges, resulting in infinite tidal forces.

Bibliography

[1] Allan Adams et al. "Causality, analyticity and an IR obstruction to UV completion". In: *JHEP* 10 (2006), p. 014. DOI: 10.1088/1126-6708/2006/10/014. arXiv: hep-th/0602178.

[2] Spyros Alexakis, Alexandru D Ionescu, and Sergiu Klainerman. "Hawking's local rigidity theorem without analyticity". In: *Geometric and Functional Analysis* 20.4 (2010), pp. 845–869.

[3] Stefanos Aretakis. "Stability and Instability of Extreme Reissner-Nordström Black Hole Spacetimes for Linear Scalar Perturbations I". In: *Commun. Math. Phys.* 307 (2011), pp. 17–63. DOI: 10.1007/s00220-011-1254-5. arXiv: 1110.2007 [gr-qc].

[4] Nima Arkani-Hamed et al. "Causality, unitarity, and the weak gravity conjecture". In: *JHEP* 03 (2022), p. 083. DOI: 10.1007/JHEP03(2022)083. arXiv: 2109.13937 [hep-th].

[5] Nima Arkani-Hamed et al. "The String landscape, black holes and gravity as the weakest force". In: *JHEP* 06 (2007), p. 060. DOI: 10.1088/1126-6708/2007/06/060. arXiv: hep-th/0601001.

[6] Abhay Ashtekar, Stephen Fairhurst, and Badri Krishnan. "Isolated horizons: Hamiltonian evolution and the first law". In: *Phys. Rev. D* 62 (2000), p. 104025. DOI: 10.1103/PhysRevD.62.104025. arXiv: gr-qc/0005083.

[7] Abhay Ashtekar and Badri Krishnan. "Isolated and dynamical horizons and their applications". In: *Living Reviews in Relativity* 7.1 (2004), pp. 1–91.

[8] James M. Bardeen, B. Carter, and S. W. Hawking. "The Four laws of black hole mechanics". In: *Commun. Math. Phys.* 31 (1973), pp. 161–170. DOI: 10.1007/BF01645742.

[9] James M. Bardeen and Gary T. Horowitz. "The Extreme Kerr throat geometry: A Vacuum analog of AdS(2) x S**2". In: *Phys. Rev. D* 60 (1999), p. 104030. DOI: 10.1103/PhysRevD.60.104030. arXiv: hep-th/9905099.

[10] Jacob D. Bekenstein. "Black holes and entropy". In: *Phys. Rev. D* 7 (1973), pp. 2333–2346. DOI: 10.1103/PhysRevD.7.2333.

[11] Brando Bellazzini, Clifford Cheung, and Grant N. Remmen. "Quantum Gravity Constraints from Unitarity and Analyticity". In: *Phys. Rev. D* 93 (2016), p. 064076. DOI: 10.1103/PhysRevD.93.064076. arXiv: 1509.00851 [hep-th].

[12] Zvi Bern et al. "Evanescent Effects Can Alter Ultraviolet Divergences in Quantum Gravity without Physical Consequences". In: *Phys. Rev. Lett.* 115 (2015), p. 211301. DOI: 10.1103/PhysRevLett.115.211301. arXiv: 1507.06118 [hep-th].

[13] Zvi Bern et al. "Two-Loop Renormalization of Quantum Gravity Simplified". In: *Phys. Rev. D* 95 (2017), p. 046013. DOI: 10.1103/PhysRevD.95.046013. arXiv: 1701.02422 [hep-th].

[14] William D. Biggs and Jorge E. Santos. "Black Tunnels and Hammocks". In: (July 2022). arXiv: 2207.14306 [hep-th].

[15] James Bonifacio. "Bootstrapping closed hyperbolic surfaces". In: *JHEP* 03 (2022), p. 093. DOI: 10.1007/JHEP03(2022)093. arXiv: 2111.13215 [hep-th].

[16] Jan Boruch et al. "BPS and near-BPS black holes in AdS_5 and their spectrum in $\mathcal{N} = 4$ SYM". In: (Mar. 2022). arXiv: 2203.01331 [hep-th].

[17] David Brizuela, Jose M. Martin-Garcia, and Guillermo A. Mena Marugan. "xPert: Computer algebra for metric perturbation theory". In: *Gen. Rel. Grav.* 41 (2009), pp. 2415–2431. DOI: 10.1007/s10714-009-0773-2. arXiv: 0807.0824 [gr-qc].

[18] Xian O. Camanho et al. "Causality Constraints on Corrections to the Graviton Three-Point Coupling". In: *JHEP* 02 (2016), p. 020. DOI: 10.1007/JHEP02(2016)020. arXiv: 1407.5597 [hep-th].

[19] Graeme N. Candlish and Harvey S. Reall. "On the smoothness of static multi-black hole solutions of higher-dimensional Einstein-Maxwell theory". In: *Class. Quant. Grav.* 24 (2007), pp. 6025–6040. DOI: 10.1088/0264-9381/24/23/022. arXiv: 0707.4420 [gr-qc].

[20] Pablo A. Cano and Alejandro Ruipérez. "Leading higher-derivative corrections to Kerr geometry". In: *JHEP* 05 (2019). [Erratum: JHEP 03, 187 (2020)], p. 189. DOI: 10.1007/JHEP05(2019)189. arXiv: 1901.01315 [gr-qc].

[21] Simon Caron-Huot et al. "Causality constraints on corrections to Einstein gravity". In: (Jan. 2022). arXiv: 2201.06602 [hep-th].

[22] Alejandra Castro and Evita Verheijden. "Near-AdS2 Spectroscopy: Classifying the Spectrum of Operators and Interactions in N=2 4D Supergravity". In: *Universe* 7.12 (2021), p. 475. DOI: 10.3390/universe7120475. arXiv: 2110.04208 [hep-th].

[23] Paul Chesler, Andrew Lucas, and Subir Sachdev. "Conformal field theories in a periodic potential: results from holography and field theory". In: *Phys. Rev. D* 89.2 (2014), p. 026005. DOI: 10.1103/PhysRevD.89.026005. arXiv: 1308.0329 [hep-th].

[24] Clifford Cheung, Junyu Liu, and Grant N. Remmen. "Entropy Bounds on Effective Field Theory from Rotating Dyonic Black Holes". In: *Phys. Rev. D* 100 (2019), p. 046003. DOI: 10.1103/PhysRevD.100.046003. arXiv: 1903.09156 [hep-th].

[25] Clifford Cheung, Junyu Liu, and Grant N. Remmen. "Proof of the Weak Gravity Conjecture from Black Hole Entropy". In: *JHEP* 10 (2018), p. 004. DOI: 10.1007/JHEP10(2018)004. arXiv: 1801.08546 [hep-th].

[26] P. T. Chrusciel. "On the global structure of Robinson-Trautman space-times". In: *Proc. Roy. Soc. Lond. A* 436 (1992), pp. 299–316. DOI: 10.1098/rspa.1992.0019.

[27] Piotr Chrusciel. *Geometry of Black Holes*. International Series of Monographs on Physics. Oxford University Press, Aug. 2020. ISBN: 978-0-19-885541-5.

[28] Piotr T. Chrusciel and Luc Nguyen. "A uniqueness theorem for degenerate Kerr-Newman black holes". In: *Annales Henri Poincare* 11 (2010), pp. 585–609. DOI: 10.1007/s00023-010-0038-3. arXiv: 1002.1737 [gr-qc].

[29] Piotr T. Chruściel, Sebastian J. Szybka, and Paul Tod. "Towards a classification of vacuum near-horizons geometries". In: *Class. Quant. Grav.* 35.1 (2018), p. 015002. DOI: 10.1088/1361-6382/aa90e7. arXiv: 1707.01118 [gr-qc].

[30] Piotr T. Chrusciel and Paul Tod. "The Classification of static electro-vacuum space-times containing an asymptotically flat spacelike hypersurface with compact interior". In: *Commun. Math. Phys.* 271 (2007), pp. 577–589. DOI: 10.1007/s00220-007-0191-9. arXiv: gr-qc/0512043.

[31] Eric D'Hoker and Daniel Z. Freedman. "Supersymmetric gauge theories and the AdS / CFT correspondence". In: *Theoretical Advanced Study Institute in Elementary Particle Physics (TASI 2001): Strings, Branes and EXTRA Dimensions*. Jan. 2002, pp. 3–158. arXiv: hep-th/0201253.

[32] Oscar J. C. Dias, Gary T. Horowitz, and Jorge E. Santos. "Black holes with only one Killing field". In: *JHEP* 07 (2011), p. 115. DOI: 10.1007/JHEP07(2011)115. arXiv: 1105.4167 [hep-th].

[33] Oscar J. C. Dias, Gary T. Horowitz, and Jorge E. Santos. "Extremal black holes that are not extremal: maximal warm holes". In: *JHEP* 01 (2022), p. 064. DOI: 10.1007/JHEP01(2022)064. arXiv: 2109.14633 [hep-th].

[34] Óscar J. C. Dias and Ramon Masachs. "Hairy black holes and the endpoint of AdS_4 charged superradiance". In: *JHEP* 02 (2017), p. 128. DOI: 10.1007/JHEP02(2017)128. arXiv: 1610.03496 [hep-th].

[35] Oscar J. C. Dias, Jorge E. Santos, and Maren Stein. "Kerr-AdS and its Near-horizon Geometry: Perturbations and the Kerr/CFT Correspondence". In: *JHEP* 10 (2012), p. 182. DOI: 10.1007/JHEP10(2012)182. arXiv: 1208.3322 [hep-th].

[36] Óscar J. C. Dias, Jorge E. Santos, and Benson Way. "Black holes with a single Killing vector field: black resonators". In: *JHEP* 12 (2015), p. 171. DOI: 10.1007/JHEP12(2015)171. arXiv: 1505.04793 [hep-th].

[37] Óscar J. C. Dias, Jorge E. Santos, and Benson Way. "Numerical Methods for Finding Stationary Gravitational Solutions". In: *Class. Quant. Grav.* 33.13 (2016), p. 133001. DOI: 10.1088/0264-9381/33/13/133001. arXiv: 1510.02804 [hep-th].

[38] Denis Dobkowski-Ryłko et al. "The Near Horizon Geometry equation on compact 2-manifolds including the general solution for $g > 0$". In: *Phys. Lett. B* 785 (2018), pp. 381–385. DOI: 10.1016/j.physletb.2018.08.048. arXiv: 1807.05934 [gr-qc].

[39] Ahmad El Soufi and Saıd Ilias. "Le volume conforme et ses applications d'après Li et Yau". In: *Séminaire de théorie spectrale et géométrie* 2 (1983), pp. 1–15.

[40] Solomon Endlich et al. "An effective formalism for testing extensions to General Relativity with gravitational waves". In: *JHEP* 09 (2017), p. 122. DOI: 10.1007/JHEP09(2017)122. arXiv: 1704.01590 [gr-qc].

[41] Netta Engelhardt and Åsmund Folkestad. "Holography abhors visible trapped surfaces". In: *JHEP* 07 (2021), p. 066. DOI: 10.1007/JHEP07(2021)066. arXiv: 2012.11445 [hep-th].

[42] Netta Engelhardt and Aron C. Wall. "Decoding the Apparent Horizon: Coarse-Grained Holographic Entropy". In: *Phys. Rev. Lett.* 121.21 (2018), p. 211301. DOI: 10.1103/PhysRevLett.121.211301. arXiv: 1706.02038 [hep-th].

[43] Thomas Faulkner, Hong Liu, and Mukund Rangamani. "Integrating out geometry: Holographic Wilsonian RG and the membrane paradigm". In: *JHEP* 08 (2011), p. 051. DOI: 10.1007/JHEP08(2011)051. arXiv: 1010.4036 [hep-th].

[44] A. Fontanella and J. B. Gutowski. "Moduli Spaces of Transverse Deformations of Near-Horizon Geometries". In: *J. Phys. A* 50.21 (2017), p. 215202. DOI: 10.1088/1751-8121/aa6cbf. arXiv: 1610.09949 [hep-th].

[45] Robert Geroch. "Limits of spacetimes". In: *Communications in Mathematical Physics* 13.3 (1969), pp. 180–193.

[46] Garrett Goon. "Heavy Fields and Gravity". In: *JHEP* 01 (2017). [Erratum: *JHEP* **03** (2017) 161], p. 045. DOI: 10.1007/JHEP01(2017)045. arXiv: 1611.02705 [hep-th].

[47] Lijun Gou et al. "The Extreme Spin of the Black Hole in Cygnus X-1". In: *Astrophys. J.* 742 (2011), p. 85. DOI: 10.1088/0004-637X/742/2/85. arXiv: 1106.3690 [astro-ph.HE].

[48] David J. Gross and John H. Sloan. "The quartic effective action for the heterotic string". In: *Nucl. Phys. B* 291 (1987), p. 41. DOI: 10.1016/0550-3213(87)90465-2.

[49] David J. Gross and Edward Witten. "Superstring modifications of Einstein's equations". In: *Nucl. Phys. B* 277 (1986), p. 1. DOI: https://doi.org/10.1016/0550-3213(86)90429-3.

[50] J. Grover, J. B. Gutowski, and W. A. Sabra. "Non-existence of supersymmetric AdS_5 black rings". In: *JHEP* 11 (2014), p. 027. DOI: 10.1007/JHEP11(2014)027. arXiv: 1306.0017 [hep-th].

[51] A. Gruzinov and M. Kleban. "Causality Constrains Higher Curvature Corrections to Gravity". In: *Class. Quant. Grav.* 24 (2007), pp. 3521–3524. DOI: 10.1088/0264-9381/24/13/N02. arXiv: hep-th/0612015.

[52] S. S. Gubser, Igor R. Klebanov, and Alexander M. Polyakov. "Gauge theory correlators from noncritical string theory". In: *Phys. Lett. B* 428 (1998), pp. 105–114. DOI: 10.1016/S0370-2693(98)00377-3. arXiv: hep-th/9802109.

[53] Steven S. Gubser. "Curvature singularities: The Good, the bad, and the naked". In: *Adv. Theor. Math. Phys.* 4 (2000), pp. 679–745. DOI: 10.4310/ATMP.2000.v4.n3.a6. arXiv: hep-th/0002160.

[54] Jan B. Gutowski and Harvey S. Reall. "Supersymmetric AdS(5) black holes". In: *JHEP* 02 (2004), p. 006. DOI: 10.1088/1126-6708/2004/02/006. arXiv: hep-th/0401042.

[55] Daniel Harlow et al. "The Weak Gravity Conjecture: A Review". In: (Jan. 2022). arXiv: 2201.08380 [hep-th].

[56] Sean A. Hartnoll. "Horizons, holography and condensed matter". In: *Black holes in higher dimensions*. Ed. by Gary T. Horowitz. Cambridge, UK: Cambridge Univ. Pr., 2012, pp. 387–419. ISBN: 978-1-107-01345-2. arXiv: 1106.4324 [hep-th].

[57] Sean A. Hartnoll and Diego M. Hofman. "Locally Critical Resistivities from Umklapp Scattering". In: *Phys. Rev. Lett.* 108 (2012), p. 241601. DOI: 10.1103/PhysRevLett.108.241601. arXiv: 1201.3917 [hep-th].

[58] Sean A. Hartnoll, Andrew Lucas, and Subir Sachdev. "Holographic quantum matter". In: (Dec. 2016). arXiv: 1612.07324 [hep-th].

[59] S. W. Hawking. "Particle Creation by Black Holes". In: *Commun. Math. Phys.* 43 (1975). Ed. by G. W. Gibbons and S. W. Hawking. [Erratum: Commun.Math.Phys. 46, 206 (1976)], pp. 199–220. DOI: 10.1007/BF02345020.

[60] S. W. Hawking and G. F. R. Ellis. *The Large Scale Structure of Space-Time*. Cambridge Monographs on Mathematical Physics. Cambridge University Press, Feb. 2011. ISBN: 978-0-521-20016-5, 978-0-521-09906-6, 978-0-511-82630-6, 978-0-521-09906-6. DOI: 10.1017/CBO9780511524646.

[61] Idse Heemskerk and Joseph Polchinski. "Holographic and Wilsonian Renormalization Groups". In: *JHEP* 06 (2011), p. 031. DOI: 10.1007/JHEP06(2011)031. arXiv: 1010.1264 [hep-th].

[62] Ben Heidenreich, Matthew Reece, and Tom Rudelius. "Sharpening the Weak Gravity Conjecture with Dimensional Reduction". In: *JHEP* 02 (2016), p. 140. DOI: 10.1007/JHEP02(2016)140. arXiv: 1509.06374 [hep-th].

[63] Andrew Hickling. "Bulk Duals for Generic Static, Scale-Invariant Holographic CFT States". In: *Class. Quant. Grav.* 32.17 (2015), p. 175011. DOI: 10.1088/0264-9381/32/17/175011. arXiv: 1504.03723 [hep-th].

[64] Stefan Hollands, Akihiro Ishibashi, and Robert M. Wald. "A Higher dimensional stationary rotating black hole must be axisymmetric". In: *Commun. Math. Phys.* 271 (2007), pp. 699–722. DOI: 10.1007/s00220-007-0216-4. arXiv: gr-qc/0605106.

[65] Gary T. Horowitz, Maciej Kolanowski, and Jorge E. Santos. "A deformed IR: a new IR fixed point for four-dimensional holographic theories". In: *JHEP* 02 (2023), p. 152. DOI: 10.1007/JHEP02(2023)152. arXiv: 2211.01385 [hep-th].

[66] Gary T. Horowitz, Maciej Kolanowski, and Jorge E. Santos. "Almost all extremal black holes in AdS are singular". In: *JHEP* 01 (2023), p. 162. DOI: 10.1007/JHEP01(2023)162. arXiv: 2210.02473 [hep-th].

[67] Gary T. Horowitz and Matthew M. Roberts. "Zero Temperature Limit of Holographic Superconductors". In: *JHEP* 11 (2009), p. 015. DOI: 10.1088/1126-6708/2009/11/015. arXiv: 0908.3677 [hep-th].

[68] Gary T. Horowitz, Jorge E. Santos, and Benson Way. "Evidence for an Electrifying Violation of Cosmic Censorship". In: *Class. Quant. Grav.* 33.19 (2016), p. 195007. DOI: 10.1088/0264-9381/33/19/195007. arXiv: 1604.06465 [hep-th].

[69] Gary T. Horowitz et al. "Extremal Kerr black holes as amplifiers of UV physics". In: *to appear* (Mar. 2023).

[70] Gary T. Horowitz et al. "Hovering Black Holes from Charged Defects". In: *Class. Quant. Grav.* 32 (2015), p. 105001. DOI: 10.1088/0264-9381/32/10/105001. arXiv: 1412.1830 [hep-th].

[71] Norihiro Iizuka, Akihiro Ishibashi, and Kengo Maeda. "Flows of extremal attractor black holes". In: *JHEP* 09 (2022), p. 093. DOI: 10.1007/JHEP09(2022)093. arXiv: 2206.04845 [hep-th].

[72] Luca V. Iliesiu and Gustavo J. Turiaci. "The statistical mechanics of near-extremal black holes". In: *JHEP* 05 (2021), p. 145. DOI: 10.1007/JHEP05(2021)145. arXiv: 2003.02860 [hep-th].

[73] I. Jack, D. R. T. Jones, and N. Mohammedi. "A four-loop calculation of the metric β-function for the bosonic σ-model and the string effective action". In: *Nucl. Phys. B* 322 (1989), p. 431. DOI: 10.1016/0550-3213(89)90422-7.

[74] I. Jack, D. R. T. Jones, and N. Mohammedi. "The four-loop metric β-function for the bosonic σ-model". In: *Phys. Lett. B* 220 (1989), p. 171. DOI: 10.1016/0370-2693(89)90031-2.

[75] Jacek Jezierski and Bartek Kaminski. "Towards uniqueness of degenerate axially symmetric Killing horizon". In: *Gen. Rel. Grav.* 45 (2013), pp. 987–1004. DOI: 10.1007/s10714-013-1506-0. arXiv: 1206.5136 [gr-qc].

[76] Yevgeny Kats, Lubos Motl, and Megha Padi. "Higher-order corrections to mass-charge relation of extremal black holes". In: *JHEP* 12 (2007), p. 068. DOI: 10.1088/1126-6708/2007/12/068. arXiv: hep-th/0606100.

[77] Y. Kikuchi, C. Marzban, and Y. J. Ng. "Heterotic string modifications of Einstein's and Yang-Mills' actions". In: *Phys. Lett. B* 176 (1986), p. 57. DOI: 10.1016/0370-2693(86)90924-X.

[78] Hideo Kodama and Akihiro Ishibashi. "Master equations for perturbations of generalized static black holes with charge in higher dimensions". In: *Prog. Theor. Phys.* 111 (2004), pp. 29–73. DOI: 10.1143/PTP.111.29. arXiv: hep-th/0308128.

[79] Maciej Kolanowski. "Towards the black hole uniqueness: transverse deformations of the extremal Reissner-Nordström-(A)dS horizon". In: *JHEP* 01 (2022), p. 042. DOI: 10.1007/JHEP01(2022)042. arXiv: 2111.00806 [gr-qc].

[80] Maciej Kolanowski, Jerzy Lewandowski, and Adam Szereszewski. "Extremal horizons stationary to the second order: new constraints". In: *Phys. Rev. D* 100.10 (2019), p. 104057. DOI: 10.1103/PhysRevD.100.104057. arXiv: 1907.00955 [gr-qc].

[81] Petr Kravchuk, Dalimil Mazac, and Sridip Pal. "Automorphic Spectra and the Conformal Bootstrap". In: (Nov. 2021). arXiv: 2111.12716 [hep-th].

[82] Hari K. Kunduri and James Lucietti. "Classification of near-horizon geometries of extremal black holes". In: *Living Rev. Rel.* 16 (2013), p. 8. DOI: 10.12942/lrr-2013-8. arXiv: 1306.2517 [hep-th].

[83] Hari K. Kunduri and James Lucietti. "Static near-horizon geometries in five dimensions". In: *Class. Quant. Grav.* 26 (2009), p. 245010. DOI: 10.1088/0264-9381/26/24/245010. arXiv: 0907.0410 [hep-th].

[84] Hari K. Kunduri and James Lucietti. "Uniqueness of near-horizon geometries of rotating extremal AdS(4) black holes". In: *Class. Quant. Grav.* 26 (2009), p. 055019. DOI: 10.1088/0264-9381/26/5/055019. arXiv: 0812.1576 [hep-th].

[85] Hari K. Kunduri, James Lucietti, and Harvey S. Reall. "Do supersymmetric anti-de Sitter black rings exist?" In: *JHEP* 02 (2007), p. 026. DOI: 10.1088/1126-6708/2007/02/026. arXiv: hep-th/0611351.

[86] Hari K. Kunduri, James Lucietti, and Harvey S. Reall. "Near-horizon symmetries of extremal black holes". In: *Class. Quant. Grav.* 24 (2007), pp. 4169–4190. DOI: 10.1088/0264-9381/24/16/012. arXiv: 0705.4214 [hep-th].

[87] Jerzy Lewandowski and Tomasz Pawlowski. "Extremal isolated horizons: A Local uniqueness theorem". In: *Class. Quant. Grav.* 20 (2003), pp. 587–606. DOI: 10.1088/0264-9381/20/4/303. arXiv: gr-qc/0208032.

[88] Jerzy Lewandowski and Tomasz Pawlowski. "Quasi-local rotating black holes in higher dimension: Geometry". In: *Class. Quant. Grav.* 22 (2005), pp. 1573–1598. DOI: 10.1088/0264-9381/22/9/007. arXiv: gr-qc/0410146.

[89] Carmen Li and James Lucietti. "Electrovacuum spacetime near an extreme horizon". In: *Adv. Theor. Math. Phys.* 23 (2019), pp. 1903–1950. DOI: 10.4310/ATMP.2019.v23.n7.a5. arXiv: 1809.08164 [gr-qc].

[90] Carmen Li and James Lucietti. "Transverse deformations of extreme horizons". In: *Class. Quant. Grav.* 33.7 (2016), p. 075015. DOI: 10.1088/0264-9381/33/7/075015. arXiv: 1509.03469 [gr-qc].

[91] Henry W. Lin et al. "Looking at supersymmetric black holes for a very long time". In: (July 2022). arXiv: 2207.00408 [hep-th].

[92] Kengo Maeda, Takashi Okamura, and Jun-ichirou Koga. "Inhomogeneous charged black hole solutions in asymptotically anti-de Sitter spacetime". In: *Phys. Rev. D* 85 (2012), p. 066003. DOI: 10.1103/PhysRevD.85.066003. arXiv: 1107.3677 [gr-qc].

[93] Juan Martin Maldacena. "The Large N limit of superconformal field theories and supergravity". In: *Adv. Theor. Math. Phys.* 2 (1998), pp. 231–252. DOI: 10.1023/A:1026654312961. arXiv: hep-th/9711200.

[94] Julija Markeviciute and Jorge E. Santos. "Evidence for the existence of a novel class of supersymmetric black holes with $AdS_5 \times S^5$ asymptotics". In: *Class. Quant. Grav.* 36.2 (2019), 02LT01. DOI: 10.1088/1361-6382/aaf680. arXiv: 1806.01849 [hep-th].

[95] Donald Marolf. "States and boundary terms: Subtleties of Lorentzian AdS / CFT". In: *JHEP* 05 (2005), p. 042. DOI: 10.1088/1126-6708/2005/05/042. arXiv: hep-th/0412032.

[96] Vincent Moncrief and James Isenberg. "Symmetries of cosmological Cauchy horizons". In: *Commun. Math. Phys.* 89.3 (1983), pp. 387–413. DOI: 10.1007/BF01214662.

[97] Amanda W. Peet and Joseph Polchinski. "UV / IR relations in AdS dynamics". In: *Phys. Rev. D* 59 (1999), p. 065011. DOI: 10.1103/PhysRevD.59.065011. arXiv: hep-th/9809022.

[98] Amanda W. Peet and Simon F. Ross. "Microcanonical phases of string theory on $AdS_m \times S^n$". In: *JHEP* 12 (1998), p. 020. DOI: 10.1088/1126-6708/1998/12/020. arXiv: hep-th/9810200 [hep-th].

[99] Roger Penrose. "Gravitational collapse and space-time singularities". In: *Physical Review Letters* 14.3 (1965), p. 57.

[100] Adam G. Riess et al. "Observational evidence from supernovae for an accelerating universe and a cosmological constant". In: *Astron. J.* 116 (1998), pp. 1009–1038. DOI: 10.1086/300499. arXiv: astro-ph/9805201.

[101] G. Risaliti et al. "A rapidly spinning supermassive black hole at the centre of NGC 1365". In: *Nature* 494 (2013), p. 449. DOI: 10.1038/nature11938. arXiv: 1302.7002 [astro-ph.HE].

[102] Shinsei Ryu and Tadashi Takayanagi. "Holographic derivation of entanglement entropy from AdS/CFT". In: *Phys. Rev. Lett.* 96 (2006), p. 181602. DOI: 10.1103/PhysRevLett.96.181602. arXiv: hep-th/0603001.

[103] Larry Smarr. "Surface Geometry of Charged Rotating Black Holes". In: *Phys. Rev. D* 7 (1973), pp. 289–295. DOI: 10.1103/PhysRevD.7.289.

[104] Andrew Strominger and Cumrun Vafa. "Microscopic origin of the Bekenstein-Hawking entropy". In: *Phys. Lett. B* 379 (1996), pp. 99–104. DOI: 10.1016/0370-2693(96)00345-0. arXiv: hep-th/9601029.

[105] D. Sudarsky and Robert M. Wald. "Extrema of mass, stationarity, and staticity, and solutions to the Einstein Yang-Mills equations". In: *Phys. Rev. D* 46 (1992), pp. 1453–1474. DOI: 10.1103/PhysRevD.46.1453.

[106] Arkady A. Tseytlin. "Heterotic – type I superstring duality and low-energy effective actions". In: *Nucl. Phys. B* 467 (1996), p. 383. DOI: 10.1016/0550-3213(96)00080-6. arXiv: hep-th/9512081.

[107] Robert M. Wald. "Black hole entropy is the Noether charge". In: *Phys. Rev. D* 48.8 (1993), R3427–R3431. DOI: 10.1103/PhysRevD.48.R3427. arXiv: gr-qc/9307038.

[108] Robert M. Wald. *General Relativity*. Chicago, USA: Chicago Univ. Pr., 1984. DOI: 10.7208/chicago/9780226870373.001.0001.

[109] Dean L. Welch. "On the smoothness of the horizons of multi - black hole solutions". In: *Phys. Rev. D* 52 (1995), pp. 985–991. DOI: 10.1103/PhysRevD.52.985. arXiv: hep-th/9502146.

[110] Edward Witten. "Anti-de Sitter space and holography". In: *Adv. Theor. Math. Phys.* 2 (1998), pp. 253–291. DOI: 10.4310/ATMP.1998.v2.n2.a2. arXiv: hep-th/9802150.

[111] Paul C Yang and Shing-Tung Yau. "Eigenvalues of the Laplacian of compact Riemann surfaces and minimal submanifolds". In: *Annali della Scuola Normale Superiore di Pisa-Classe di Scienze* 7.1 (1980), pp. 55–63.

[112] Barak Zackay et al. "Highly spinning and aligned binary black hole merger in the Advanced LIGO first observing run". In: *Phys. Rev. D* 100 (2019), p. 023007. DOI: 10.1103/PhysRevD.100.023007. arXiv: 1902.10331 [astro-ph.HE].